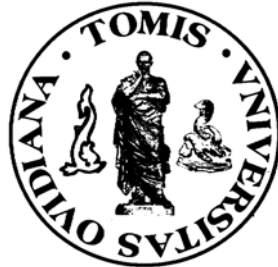


**“OVIDIUS” UNIVERSITY OF CONSTANTZA
UNIVERSITATEA „OVIDIUS” CONSTANȚA**



**“OVIDIUS” UNIVERSITY ANNALS -
CONSTANTZA
Year XIII – Issue 13
(2011)**

Series: CIVIL ENGINEERING

**ANALELE UNIVERSITĂȚII
„OVIDIUS” CONSTANȚA
ANUL XIII – Nr 13
(2011)**

Seria: CONSTRUCȚII

**Ovidius University Press
2011**

“OVIDIUS” UNIVERSITY ANNALS - CONSTANTZA
SERIES: CIVIL ENGINEERING
ANALELE UNIVERSITĂȚII „OVIDIUS” CONSTANȚA
SERIA: CONSTRUCȚII

EDITOR IN CHIEF:

Lucica ROȘU, PhD, Eng., “OVIDIUS” University, Faculty of Civil Engineering,
124, Mamaia Blvd., 900527, RO., Constantza, Romania, phone +40-241-545093,
fax +40-241-612300 lucirosu@yahoo.fr

EXECUTIVE EDITOR:

Carmen MAFTEI, PhD, Eng., “OVIDIUS” University, Faculty of Civil Engineering,
124, Mamaia Blvd., 900527, RO., Constantza, Romania, phone +40-241-545093,
fax +40-241-612300 cmaftei@univ-ovidius.ro
Anca CONSTANTIN, PhD, Eng, University, Faculty of Civil Engineering,
124, Mamaia Blvd., 900527, RO., Constantza, phone +40-241-545093,
fax +40-241-612300 Romania, anca.constantin@ymail.com

EDITORIAL BOARD

Haydar ACKA, Ph.D., Dumitru Ion ARSENIU, Ph.D. Eng.,	Abu Dhabi University, United Arab Emirates, Faculty of Civil Engineering “OVIDIUS” University of Constantza, Romania;
Roumen ARSOV, Ph.D. Eng.,	University of Architecture, Civil Engineering & Geodesy, Sofia, Bulgaria
Khalidou M. BA, PhD Alina BARBULESCU, PhD Iosif BARTHA, Ph.D. Eng., Alex Horia BĂRBAT, Ph.D. Eng., Petru BOERIU, PhD Virgil BREABĂN, Ph.D. Eng., Alin CARȘTEANU, PhD, Meri CVETKOVSKA, Ph.D.	Faculty of Engineering, UAE, Mexico “OVIDIUS” University of Constantza, Romania; “GH. ASACHI”, Technical University, Iassy, Romania; Technical University of Catalonia, Spain; UNESCO-IHE Delft, Netherlands “OVIDIUS” University of Constantza, Romania; ESFM – National Polytechnic Institute, Mexico Faculty of Civil Engineering, University Sts. Cyril and Methodius, Skopje, Macedonia, SAKARYA University, Turkey
Mehmet DURMAN, Ph.D. Eng., Petar I FILKOV, PhD.	Faculty of Hydraulic Engineering , University of Architecture, Civil Engineering and Geodesy, Sofia, Bulgaria “GH. ASACHI”, Technical University, Iassy, Romania;
Ion GIURMA, Ph.D. Eng., Pierre HUBERT, PhD., Axinte IONIȚĂ, Ph.D., Eng., Jacek KATZER, PhD., S.D. (Saskia) KEESSTRA, PhD Teodor Eugen MAN, Ph.D. Eng, Maria MAVROVA-GIRGINOVA, Ph.D lawyer Turan ÖZTURAN, Ph.D. Eng., Ioana POPESCU, PhD Andrej ŠOLTÉS, Ph.D.	IAHS, England Tennessee University, U.S.A. Koszalin University of Technology, Poland Wageningen University, Netherlands “Politehnica” University of Timisoara, Romania University of Architecture, Civil Engineering and Geodesy Sofia, Bulgaria BOGAZICI University, Istanbul, Turkey; UNESCO-IHE Institute for Water Education, Netherlands Faculty of Civil Engineering, Slovak University of Technology in Bratislava, Slovakia
Dan STEMATIU, Ph.D. Eng.,	Technical University of Civil Engineering of Bucharest, Romania;

DESK EDITORS

Constantin BUTA, Cristina SERBAN, "OVIDIUS" University, Faculty of Civil Engineering,
124, Mamaia Blvd., 900527, RO., Constantza, Romania

Number of Copies: 100

PUBLISHED BY: OVIDIUS UNIVERSITY PRESS, 126, Mamaia Blvd., 900527, RO.,
Constantza, Romania, Phone/Fax +40-241606421, library@bcuovidius.ro, Contact
Person: Ioan Popisteanu

FREQUENCY: Yearly

COVERED BY: INDEX COPERNICUS, IC VALUES IN 2010 3.26
<http://journals.indexcopernicus.com/karta.php?action=masterlist&id=5000>

REMIT OF JOURNAL:

Journal can be free downloaded from the site: <http://www.univ-ovidius.ro/revista-constructii/>; the authors receive a copy of their paper.

ORDERING INFORMATION

The printed version of the journal may be obtained by ordering at the "OVIDIUS"
University Press, or on exchange basis with similar Romanian or foreign institutions.

The price for a single volume is 40 euros plus postal charges.

126, Mamaia Blvd., 900527, RO., Constantza, Romania

© 2000 Ovidius University Press. All rights reserved.

For subscriptions and submission of papers, please use the e-mail address:
serban.cristina@univ-ovidius.ro or costi_buta@yahoo.com or postal address 22B Unirii
str., 900524 RO, Constantza, Romania

Instructions for authors can be found at: <http://www.univ-ovidius.ro/revista-constructii/>

ISSN 1584-5990

© 2000 Ovidius University Press. All rights reserved.

“OVIDIUS” UNIVERSITY ANNALS – CONSTANTZA
Series: CIVIL ENGINEERING
Year XII (2010)

TABLE OF CONTENTS

	Pag
Committees	3
Operation Improvement of an Irrigation Water Supply Floating Pumping Station in Constantza County	7
1 <i>Anca Constantin, Claudiu Nițecu, Mădălina Stănescu, Lucica Roșu</i>	
Pump Selection for Extending Drip Irrigation Systems	13
2 <i>Petar I. Filkov, Rossitza A. Meranzova</i>	
Sewer System by SeWaCAD	21
3 <i>Ștefan Stanko</i>	
Cracking Moment in Steel Fibre Reinforced Concrete Beams Based on Waste Sand	29
4 <i>Jacek Domski</i>	
Impact of the Grain-Size Distribution of the Fine Aggregate Cement Composites on the Rebound Hammer Test	35
5 <i>Jacek Katzer</i>	
The Response of Maritime Structures with Vertical Walls at Braking Wave Forces in Terms of Duration of the Impact	41
6 <i>Mirela Popa, Gabriela Drăghici, Cosmin Filip</i>	
Seismic Assessment of the Faculty of Land Reclamation and Environmental Engineering, Bucharest according to norm P 100-3/2008	51
7 <i>Camelia Slave</i>	
The Quantification of Potential and Actual Evapotranspiration in the Process of Soil Draught Creation	57
8 <i>Milan Gomboš, Branislav Kandra</i>	
The Impact of Groundwater Level Position on the Actual Evapotranspiration in Heavy Soils in Eastern-Slovakian Lowland	65
9 <i>Milan Gomboš, Dana Pavelková</i>	
Trends of Extreme Precipitation Events in Dobrudja	73
10 <i>Judicaël Deguenon, Alina Bărbulescu</i>	

	Statistical Analysis of Precipitation Variability in Dobrudja Region	
11	<i>Carmen Maștei, Alina Bărbulescu, Cristina Serban (Gherghina), Iulia Ilie</i>	81
12	Mathematical Models for Extreme Monthly Precipitation <i>Alina Bărbulescu, Judicaël Deguenon</i>	93

Operation Improvement of an Irrigation Water Supply Floating Pumping Station in Constantza County

Anca Constantin, Claudiu Nițescu, Mădălina Stănescu, Lucica Roșu

Abstract – The irrigation water supply floating pumping station *SPA Lipnita* has to be modernized. The station has a geodetic head of 83,3 m that exceeds the new limit of 70 m imposed for the total pumping head in the hilly regions. The experts involved in the engineering design conceived two variants for the rehabilitation. One of them proposes the replacement of the station with two ones in series, in order to avoid a total pumping head over the upper limit. The second takes into consideration pumps with a better inner hydraulics, but with the same pumping head as the old station. The two variants are presented in an energetic perspective and compared.

Keywords – energetic efficiency, irrigation system, pumping station.

1. INTRODUCTION

Rational and efficient use of water resources becomes more and more important over time. Therefore, aside from the new constructions made in our country, the old Romanian irrigation systems have to be modernised, in order to improve efficiency and diminish their operation costs.

The performance of many irrigation systems in Romania is lower than their potential, due to both design/execution issues and their management. We might mention:

- shortcomings of the initial projects, or improper operation specifications;
- distribution system is not suitable to the land management system (farm size, location);
- poor management of irrigation systems.

Romania reviewed the national drainage and irrigation sector, with financial assistance provided by the World Bank and technical support of consultants from *Binnie & Partners and Hunting Technical Services Ltd. and ISPIF S.A. Bucharest*. The objective of this study was to provide the Ministry of Agriculture and Food an investment strategy for the rehabilitation and modernization of irrigation and drainage systems. For the 20 irrigation systems selected as pilot schemes, it was concluded that, economically, surface irrigation in hilly regions, with multi-stage pumping systems, should be limited to maximal pumping head of 70 m.

2. IRRIGATION WATER SUPPLY FLOATING PUMPING STATION SPA LIPNITA

Irrigation water supply floating pumping station *SPA Lipnita* is part of the Irrigation System *Babusa*, Constanta County”. The total arranged area is of 1432.09 ha, from which 1299.59 ha are the net area and belong to the stakeholders from O.U.A.I. „Ostov Babusa”, Constanta County.

Manuscript received October 1st, 2011 and accepted November 10, 2011.

A. Constantin Author is with Ovidius University of Constanta, Bd. Mamaia nr. 124, 900356-Constanta, Romania e-mail: aconstantina@univ-ovidius.com.

C. Nițescu Author is with Ovidius University of Constanta, Bd. Mamaia nr. 124, 900356-Constanta, Romania (e-mail: claudiu.nitescu@univ-ovidius.com).

M. Stănescu Author is with Ovidius University of Constanta, Bd. Mamaia nr. 124, 900356-Constanta, Romania (e-mail: mada_x_dobre@yahoo.com).

L. Roșu Author is with Ovidius University of Constanta, Bd. Mamaia nr. 124, 900356-Constanta, Romania (e-mail: lucirosu@yahoo.com)

SPA Lipnita was engineering designed in 1970 and put to operation in 1972. Such a long duration of operation resulted in a low energetic efficiency and a high level of damage risk, as the pumps, the pipelines and their mechanical equipments are internally worn and the auxiliary installations are unreliable.

Frequent and expensive repairs were needed in the last decade.

The electropumps, dating from 1971 are not only worn but also old type; therefore they are considerable electric energy consumers. Moreover the internally corroded ducts and fittings lead to additional losses of hydraulic energy and consequently to a higher electric energy consumption. The station was proposed to be renewed.

SPA Lipnita takes water from the Danube and discharges it in a storage reservoir of 800 m³, placed 1500 m away from the Danube riverbank, at +87mrBS terrain level. From there on, the water is taken by the following pumping stage, *SRPA Castelu*. The old station was built to serve a larger area, thus its installed flow rate was of 6400 m³/h. In fact *SPA Lipnita* consists of a floating ship equipped with cu 4 electropumps type 14 NDS. They are centrifugal double flux pumps with horizontally mounted shaft. Their initial pump parameters were: discharge, $Q_p = 1600 \text{ m}^3/\text{h}$; total head $H = 90 \text{ m}$, power $P = 630 \text{ kW}$; rotation speed $n = 1500 \text{ rot/min}$; and voltage $U = 3 \text{ kV}$.

The ship is also equipped with two other auxiliary electropumps, Lotru 125, for bilge and ballast. Their parameters were: discharge $Q_a = 180 \text{ m}^3/\text{h}$, head $H_a = 40 \text{ m}$, power $P = 30 \text{ kW}$, rotation speed $n = 3000 \text{ rot/min}$, voltage $U = 0,4 \text{ KV}$.

Each pump has its own metal made pedestal inside the ship.

The pumps have individual suction ducts, equipped with isolation valves. The discharge is common, through a 1000 mm in diameter metal duct that transports water to the 800 m³ discharge reservoir.

SPA-Lipnita is also equipped with a priming installation consisting of a water ring vacuum pump MIL 60 and a tank for the water ring supply.

As the pumps deteriorated, the operation and maintenance costs became unacceptable. Pump efficiencies declined over time due to wear (e.g. increasing clearances as impellers reduce in size). Thus the pumping station ought to be re-equipped with new pumps, piping system and hydraulic equipment.

The ship needed no repairs, thus only the pumping installation had to be rehabilitated.



Fig. 1 SPA Lipnita – View toward the ship from the discharge pipeline

The pumping station has a high geodetic head, of 83,3m, which only itself is over the total admitted pumping head. The experts enrolled in the engineering design conceived two variants for the rehabilitation. One of them proposed the replacement of the station with two ones, in order to avoid a total pumping head over 70m. The second takes into consideration pumps with a better inner hydraulics, but with the same pumping head as the old station. The two variants are presented and compared below.

3. REHABILITATION VARIANTS

3.1. First Variant

The first variant, with two pumping stages is to be adopted, because the total pumping head for each stage is under the upper limit of 70m and the construction will be funded. The first pumping stage is to be on the

existing floating ship. An additional reservoir is to be built at the terrain level of 65 m rBS. In the valves chamber, inside this reservoir, another pumping group-the second pumping stage-will be mounted. As it may be seen in Table 1, the head will be 69m for the first stage and 43,5 m for the second one.

Table 1. Floating SPA –LIPNIȚA-I

First stage					
ELECTROPUMPS: LS 350-450 S1NL1 4004 cu Φ 460mm left side					
No. of Pumps	Power P kW	Rotation speed n rot/min	Voltage U kV	Total head H m	Discharge Q m ³ /h
5	400	1489	3	69	1360
Efficiency: 77,6%					
Second stage					
ELECTROPUMPS: LC350-450 S2NL14004, with an impeller's diameter of Φ410mm, standard					
No. of Pumps	Power P kW	Rotation speed n rot/min	Voltage U kV	Total head H m	Discharge Q m ³ /h
3	400	1475	6	43,5	2048
Efficiency: 86%					

This construction solution is very expensive. The high cost is caused by the big number of main pumps in the two pumping installations and by the additional reservoir.

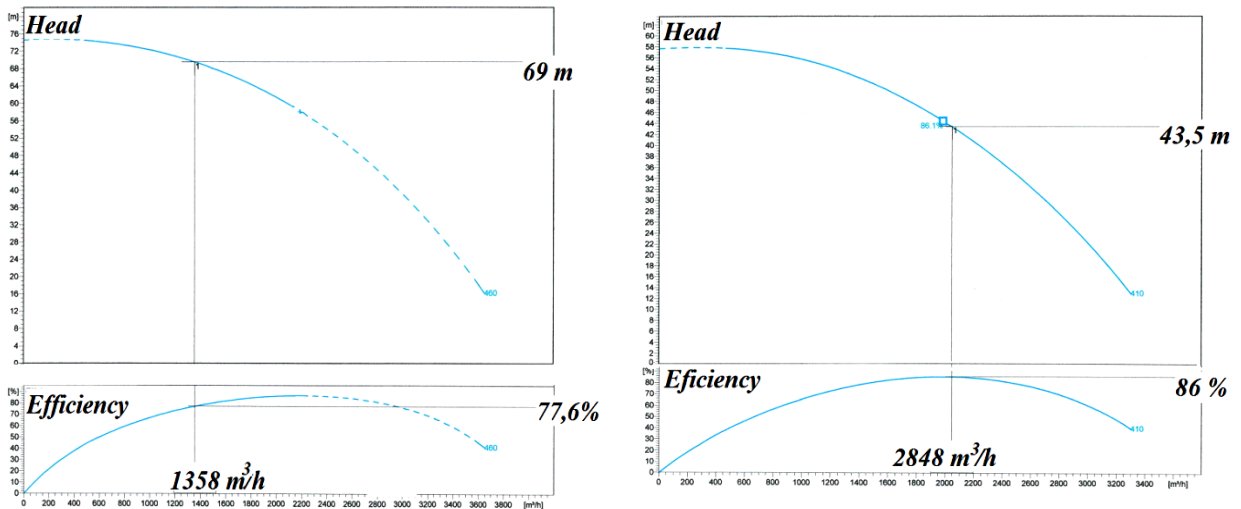


Fig. 2 Performance map of the pump used in the first (two pumping stages) variant

3.2. Second Variant

The second variant consists of replacing the pumps with new ones, of higher performance. The operation parameters are gathered into Table 2.

Table 2. Floating SPA –LIPNIȚA-II

ELECTROPUMP: LS-300-500-S1NN1-45004 with an impeller's diameter of $\Phi 533$, left side discharge					
No. of Pumps	Power P kW	Rotation speed n Rot/min	Voltage U kV	Total head H m	Discharge Q m ³ /h
5 buc.	450	1475	3	90	1198
Efficiency: 85%					

The overall performance map of the chosen pump is given in Fig.2.

Along with the pumps, the fittings will be also replaced. In Fig.3 it may be seen a pumping unit and its hydraulic equipment, inside the floating ship. Butterfly type check valves will be mounted due to their reduced head loss coefficient.

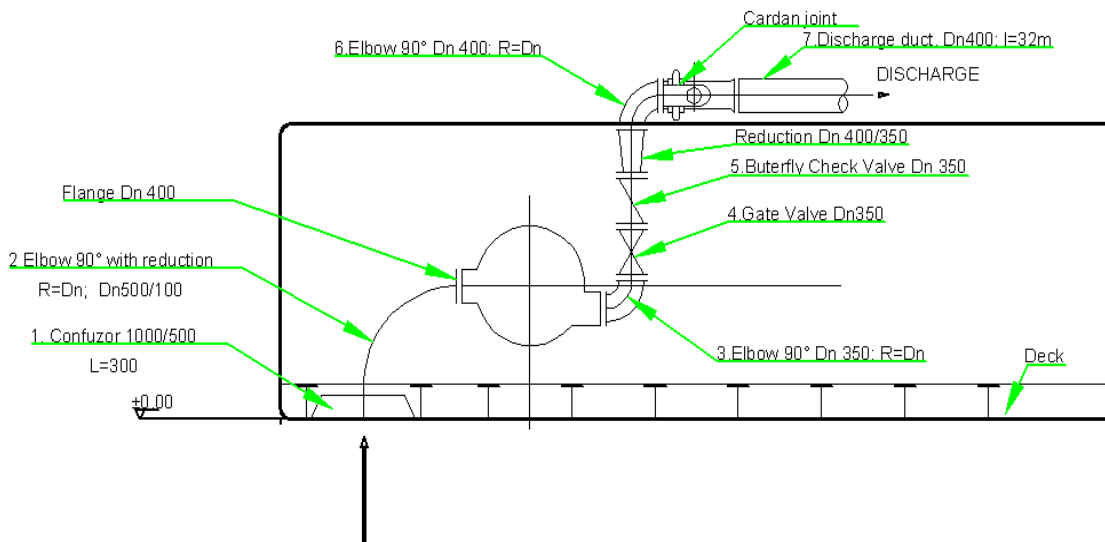


Fig. 3 SPA Lipnita – Draft of the pump and its hydraulic equipment

Two of the pumps will be provided with frequency converters, in order to operate also at small discharge flow rates.

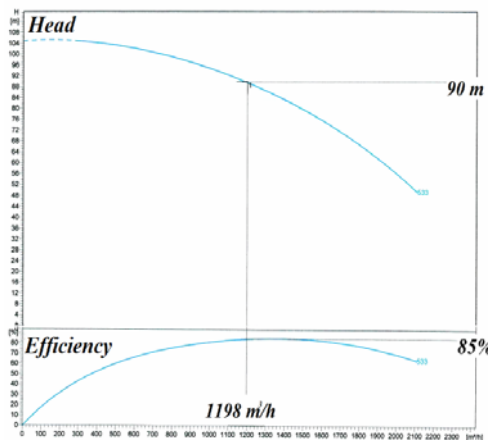


Fig. 4 Performance map of the pump used in the second (one pumping stage) variant

4. ENERGETIC PERSPECTIVE OVER THE TWO VARIANTS

The head losses have a small weight on the total pumping head, due to an appropriate engineering design of the pipelines, thus the participating discharge of a pump is almost the same, no matter the number of parallel operating pumps. And this statement is true for the both variants. Consequently, we may consider the duty points registered in the Tables 1 and 2 as best operation points. We may use these points to assess the energetic consumption for a 1000 m³ of pumped water, in both variants and to compare them.

It is well known that the consumed power for an electrically driven pump is:

$$P = \frac{\gamma QH}{3600 \cdot \eta_p \cdot \eta_m} \quad [W] \quad (1)$$

where

- Q- discharge, [m³/h];
- H-total pumping head, [m];
- η_p – pump's efficiency, [-];
- η_e – electrical motor's efficiency, [-];
- γ – specific weight of the pumped liquid, [N/m³]

Starting from the relationship (1) we obtain the most relevant amount, which is the specific energy coefficient, c. It expresses the energy consumed to pump 1000 m³ at the specified pumping head:

$$c = 2.723 \frac{H}{\eta} \quad [kWh/1000 m^3] \quad (2)$$

where

η -overall efficiency of the electropump, $\eta = \eta_p \cdot \eta_m$.

The values for this coefficient, in both variants, are:

$$c_I = 380 \text{ kWh}/1000 \text{ m}^3$$

$$c_{II} = 290 \text{ kWh}/1000 \text{ m}^3$$

It is obvious that in operation, the second variant is more cost effective than the first one, with approximately 30%.

5. CONCLUSION

The *replacement of the old pumps* results in an increasing energy efficiency of the pumping units for all the operation points. Moreover, a more appropriate operation of pumps was obtained, all over the pumping head range, due to the improved inner hydraulics of the new types of pumps. We make reference to the better NPSH of the new pumps. This replacement involves consistent investments, but it lowers the operation costs.

Another source of operation cost savings is the possibility of two pumps, equipped with frequency converters, to operate at **variable rotational speed**. Thus they will be able to deliver small discharge values, often required in irrigation system operation.

The main advantages offered by the rehabilitation consist of:

- **reduction of energy losses** by the renewing of old pumps, pipelines and fittings;
- **lower operation costs** due the new possibility of discharge adjustment;
- savings made by the **elimination of repair needs**;
- savings due to **automation and monitoring** of the pumps operation.

In spite of these general advantages, the best variant to adopt for rehabilitation has to be rigorously analysed, from both technical and economic viewpoint. **Decision and restrictions imposed on the basis of a general study, should be reconsidered in cases where better alternative might be chosen.** It is obvious that the replacement of the floating pumping station with a series of two pumping stages is not only expensive, but also leads to higher energy consumption and implicitly higher costs of the future pumped water.

6. REFERENCES

- [1].Brennen C.E, *Hydraulics of Pumps*, Cambridge University Press, 1985.
- [2].Constantin Anca, *Guidlines for pumping station engineering design*, Ed. Ovidius University Press, Constanța, 2004.
- [3].Georgescu C. *Calculation and Operation of Hydraulic Systems and their Electropumps*, Ed. MATRIX ROM, Bucharest, 2006.
- [4].Giușcă R. I., *Contribution to the optimization of the pumping stations used in the land improvement systems*, doctoral thesis, IANB, Faculty of Land Improvement, Bucharest, 1990.
- [5].Hâncu S., Marin G., *Hydraulics. Theory and practice*, Vol. I, Editura Cartea Universitară, Bucharest, 2007.
- [6].] Popescu, M., Arsenie, D.I., Vlase, P., *Applied Hydraulic Transients for Hydropower Plants and Pumping Stations*, Balkema Publishers, Lisse, Abington, Tokyo, 2003, 2004.

Pump Selection for Extending Drip Irrigation Systems

Petar I. Filkov, Rossitza A. Meranzova

Abstract – In the past few years in Bulgaria some farmers have extended their arable area and their drip irrigation systems. The same water source and existing pipe network are often used, as the system is developed in stages. In some cases, at the last stage of the extension the irrigated area or the needed discharge is increased more than twice. Usually such extension is not taken into account at the original design of the system, so the pump replacement and reconstruction of a part of the network are necessary. Variants for the selection of new pump equipment for extended systems and corresponding constraints for their application are considered in the article. In case of design of new drip irrigation systems recommendations for pump selection are given based on adequate pump use both for the design stage and for possible future expanding of the system. A practical example is also presented in the article.

Keywords – drip irrigation, extension, pump selection, variable speed pumps.

1. INTRODUCTION

Recently lots of drip irrigation systems in Bulgaria have been enlarged. Depending on the way the enlargement is done two general cases can be distinguished. The first one consists of building a new pipeline network fed by the same or other water source. The new network is not connected and has no interaction with the old, existing network. The second case is when the existing network is developed and additional pipelines are built, so the same water source is used. The systems transformed this way can be called for short *extended network systems* and they are the subject of this paper.

Lots of drip irrigation systems use their own water source – surface water (from rivers or dam lakes) or groundwater (from wells or drillings). As a practice the small farms use only one pump to deliver water into the field. The extended network systems are usually developed by a few stages and the level of the extension is limited by the capacity of the water source, since the irrigated area, i.e. the water demand is increased. Such expansion of the irrigation system is not preliminarily taken into account in the original design project, so at some stage the pump replacement and reconstruction of a part of the network are necessary.

During the development of the extended network systems the increase of the discharge leads to the raise of the required total head at the point of intake (p.o.i). A few options are available to meet the increased demand. Option **A (Fig. 1a)** is to select a new pump, as the second option **B (Fig. 1b)** is to place an additional pump in series with the original one, or, in case of an existing multistage pump, to install additional stage or stages. Option **C (Fig. 1c)** is to mount an addition pump in parallel.

The first option **A** is the easiest, but the most expensive decision. It is applicable in all cases – small or big increase of the discharge and/or required total head; surface water or groundwater source, submersible or end suction pumps. When the discharge and/or the required total head are not increased significantly it is

Manuscript received October 1st, 2011 and accepted November 10, 2011.

Petar Ivanov Filkov is with the University of Architecture, Civil Engineering and Geodesy, 1, Hristo Smirnovsky Boulevard, 1046-Sofia, Bulgaria (e-mail: filkov_fhe@uacg.bg; pifilkov@yahoo.com).

Rossitza A. Meranzova is with Agricultural University of Plovdiv, 12, Mendelev Boulevard, 4000-Plovdiv, Bulgaria (e-mail: rossi7bg@gmail.com).

recommended to consider other alternatives. Taking into account the specifics of the pump performance curves $Q-H$ and $\eta-Q$ [1] option **B** is suitable for small discharge increases (20÷30%) causing relatively high raisings of the required total head. This option cannot be applied if the original pump is selected to run near the end of its performance $Q-H$ curve. Option **C** can be applied in case of bigger discharge increases (more than 30%) regardless of the head raise, but it is not suitable for groundwater sources with submersible borehole pumps.

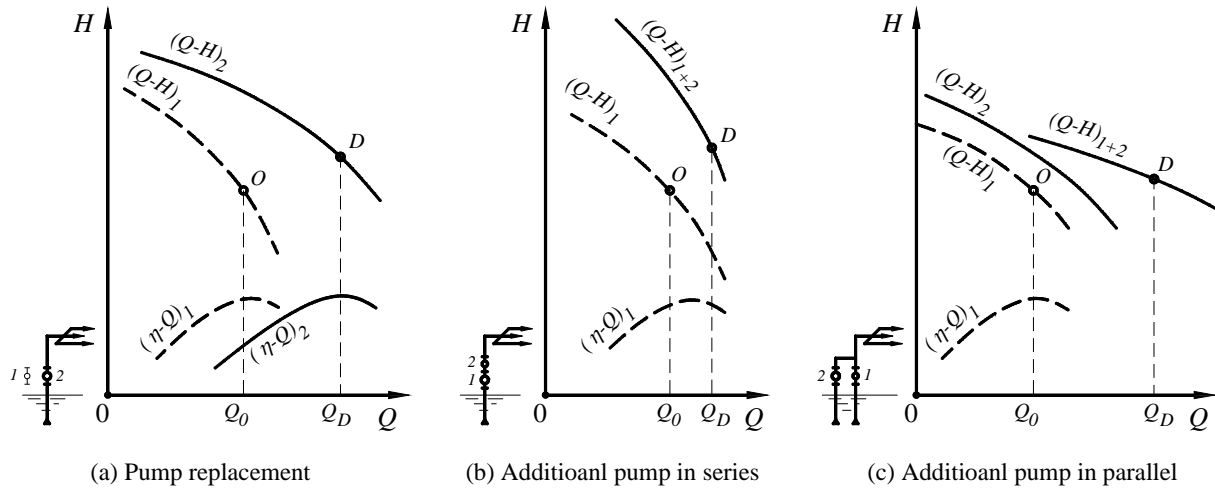


Fig. 1 Options to meet the increased demand in drip irrigation systems

It should be taken into account that the design points for the different stages (points **A**, **B** and **D** on **Fig. 2a** and **Fig. 2b**) are obtained for the worst combination of factors – the lowest water level in the water source, dirty filters and most unfavourable combination of simultaneously irrigating sectors. In case of clean filters the required head at p.o.i will drop down – for instance, the required duty point will move from **B** to **B'** on **Fig. 2a** and **Fig. 2b**. When classic pumps are used this will cause an excess head in the system, i.e. superfluous energy expenses. This is the main reason for usage of variable speed pumps for drip irrigation systems.

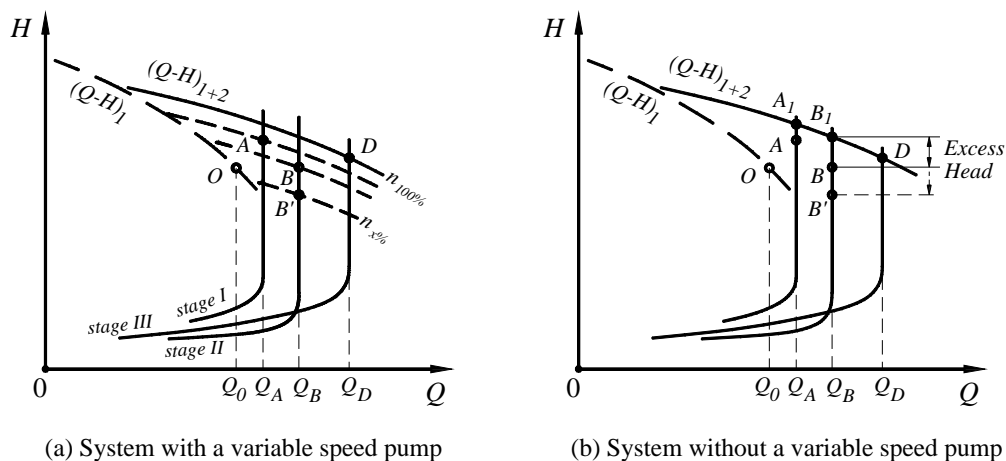


Fig. 2 Comparison between systems with and without a variable speed pump

The pump selection for extended network systems should be done keeping in mind that the pump have to provide not only the required discharge Q_D and head H_D for the last stage if extension. At the intermediate stages the pump should deliver the required discharges (Q_A and Q_B on **Fig. 2**) at minimum excess head. This is another reason for choosing a variable speed pump. When option **B** (**Fig. 1b**) or **C** (**Fig. 1c**) is chosen one of the pumps should have a variable speed control. For that reason it is recommended when option **A** is chosen to select a variable speed pump. In that case the actual duty points and the design points for the system will be identical (points **A**, **B** and **C** on **Fig. 2a**). If the classic pumps are used (**Fig. 2b**) the actual duty points (A_1 and B_1) will be higher than the design points (**A** and **B**) and the superfluous energy expenses will occur. It also should be kept in mind that in case of pumps without a variable speed control the design point usually does not coincide with the actual one.

The main specific of the extended network systems is the fact that the design discharge Q_D is the biggest one, obtained for the last stage of the extension, as the required total head at the p.o.i H_D , corresponding to Q_D may not be the highest obtained for the different stages. For instance, point **A** on **Fig. 2a**, representing the discharge and the required total head for the first stage of the extension, is above points **B** and **D**, representing the same parameters for the second and third stages. This deviation may be caused by the replacement of a few pipe sections at the second stage of the extension. The variation of the required total head depends on the way the network is used and how and at which stage the network is reconstructed.

The pump selection for extended network systems should be done considering not only the system parameters (Q_D and H_D) for the last stage of the extension, but also the parameters for the intermediate stages. The type and the moment for pipeline reconstruction works have to be specified in order to avoid malfunctions of the system. For instance, if the replacement of some pipeline sections is mistimed the design duty point for some intermediate stage may occur higher than $Q-H$ performance curve of the pump (point **B** on **Fig. 3**)

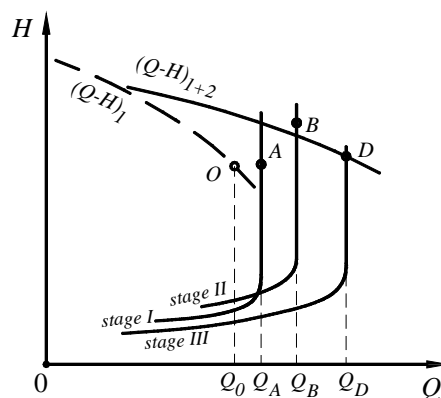


Fig. 3 Selected additional pump and mistimed pipe network reconstruction

In all cases of extended network systems a detailed hydraulic estimations for the network should be carried out in order the proper function of the system to be assured and the set values of the pressure reducing valves to be obtained.

2. RESEARCH DESCRIPTION

It is examined a drip irrigation system in the region of Dink village, Plovdiv District, Bulgaria (**Fig. 4**). The original system delivers water for raspberry-canets, covers rectangular area of 8 ha, divided in 8 equal sectors (*type I*). The shape and size of the sectors, network layout, sectors discharges and pipe diameters are shown on **Fig. 4**. The terrain is practically horizontal (slope under 5 ‰). The system is equipped with standard drippers

used at average operational free head of 10 m. The required free head at the entrance of the sub-main lines is 15,3 m. The original irrigation system is designed for 18 h/d operation, at 4 cycles, the design discharge is 7,4 l/s and the required head at the p.o.i is 46,0 m, including head losses at filter block, fittings and valves. The existing pump is submersible, fed by a diesel engine generator. The water source is a borehole well with a guaranteed capacity of 14,4 l/s (52 m³/h). The static water level is 3,0 m below the ground and the dynamic water level at the guaranteed capacity is 4,5 m below the ground.

The first stage of the extension consists of adding three sectors of *type 2* – marked as 9, 10 and 11 on **Fig.4**, for irrigation of 0,5 ha strawberries. Self compensating drippers are used at minimum free head of 5 m. Irrigation time for each sector is 1,5 h/d, the discharge of each sector is 1,8 l/s, or 5,4 l/s total. The required free head at the entrance of the sub-main lines is 8,0 m. Section between nodes 2 and 5 is built with a high density polyethylene pipe DN 75. The proper function of the system is ensured by regrouping of the simultaneously irrigating sectors or by prolonging of the operation time. The first stage of the extension was made without a consultation with an engineer and the existing pump is used.

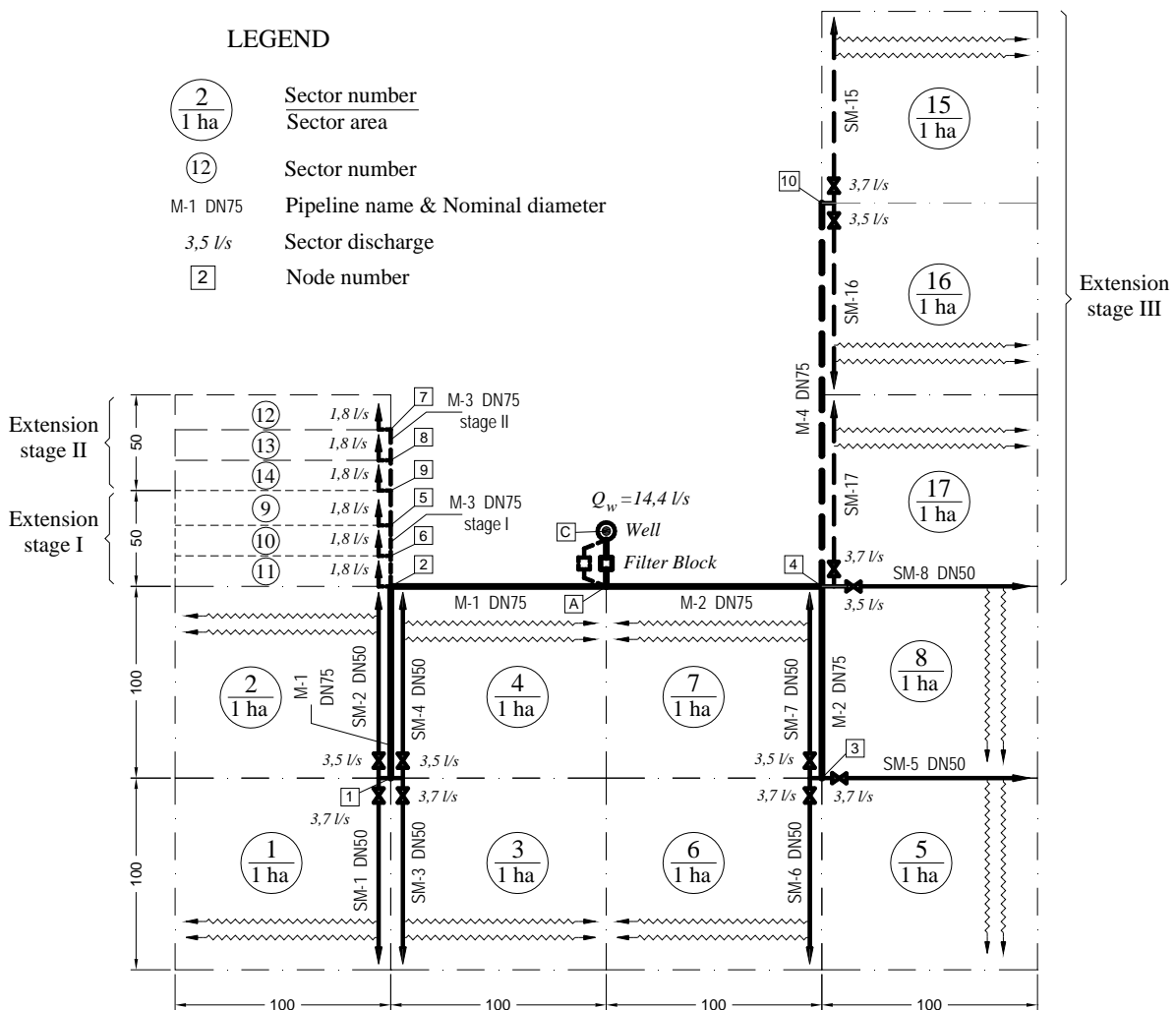


Fig. 4 Scheme of the drip irrigation system and extension stages

The second stage provides additional sectors 12, 13 and 14 of the same type and with the same specifics as sectors 9, 10 and 11. The last (third) stage consists of adding sectors 15, 16 and 17 for irrigation of raspberry-canes. The parameters of these sectors are not specified, except their size and area – the same as sectors 1 ÷ 8, so it is assumed that they will be of *type 1*.

The requirements of the owner are: (a) no or minimum reconstruction of the network; (b) an immediate selection of a new pump and (c) system operation time of maximum 18 h/d.

For obtaining the design points at each step of the extension a mathematical model of the network is prepared using *MS Excel*. Variants for the layout and the direction of the sub-main pipelines in sectors 15, 16 and 17 are examined. Also sub-variants for pipeline diameter of M-3 (stage II) and M-4 are investigated. For both stages and all the variants a parallel pipeline with DN 75 together with an additional filter block is provided between nodes A and C. After the extension the total irrigated area will become 12 ha, but the capacity of the well assures irrigation of maximum 16 ha at 18 h/d operation. The additional 4 ha can be planted in two ways – 3 ha of raspberry-canes and 1 ha of strawberries or vice versa. A possible future extension is also taken into account when the best variant is chosen. This variant is presented on **Fig. 4** – as a pipeline layout and pipe diameters.

The pump selection is made considering notes in paragraph 1.

3. RESULTS AND SIGNIFICANCES

The most significant constraint for the system operation is the guaranteed capacity of the well of 14,4 l/s. A slight surpass of 0,5÷1% can be accepted, but nevertheless the well should not be overdrawn. Second constraint regarding combination of simultaneously irrigating sectors is the diameters of the existing pipelines M-1, M-2 and M-3 (between nodes 2 and 5). These pipelines have DN 75, so M-1 and M-2 can supply only two sectors of *type 1*, while M-3 can supply maximum four or, if the velocity is 2,5 l/s, five sectors of *type 2*.

For each stage of the extension the most unfavourable combinations are taken into account, satisfying the constraints. Two kinds of combinations are examined at each stage. For the stage II they are named *normal operation* (a illustrative irrigation cycle) and *forced operation* (the whole capacity of the well is used). For the stage III these kinds are named *lightened operation* (the discharge is smaller than maximum) and *normal operation*. The required head is estimated for clean filters (H_{min}) and for dirty filters (H_{max}). The most significant results are presented in **Table 1** and **Table 2**. The accuracy of estimated head is 0,5 m.

Table 1. Pump discharge Q and head H required for the system extension, stage II

Irrigated Crops	Numbers of Sectors in Operation	Q	H_{max}	H_{min}
	-	l/s	m	m
Normal operation				
Raspberries & Strawberries	6, 7, 12, 13	10,8	39,0	36,0
Raspberries	1, 2, 5	10,9	39,0	36,0
Raspberries	3, 4, 8	10,7	39,0	36,0
Forced operation				
Raspberries & Strawberries	1, 5, 9, 10, 11	12,8	41,0	36,5
Raspberries & Strawberries	1, 6, 7, 12, 13	14,5	44,5	39,0

The accepted design point corresponds to normal operation for the stage III and the well discharge is not surpassed. Two more duty points are defined – point A ($Q = 10,8$ l/s; $H = 39,0$ m) presenting the normal operation of stage II; and point B ($Q = 12,6$ l/s; $H = 47,5$ m) corresponding to a part of irrigation cycle in stage III. When the filters are clean the alternative points A', B' and C' have required head 45,0 m, 43,0 m and 39,0 m respectively.

Table 2. Pump discharge Q and head H required for the system extension, stage III (final)

Irrigated Crops	Numbers of Sectors in Operation	Q	H_{max}	H_{min}
	-	l/s		m
Lightened operation				
Raspberries & Strawberries	12, 13, 14, 15, 16	12,6	47,5	43,0
Normal operation				
Raspberries	1, 2, 15, 16	14,4	50,5	45,0
Raspberries & Strawberries	1, 12, 13, 15, 16	14,5	50,5	45,0
	Design point	14,4	50,5	

On-line catalogues of two worldwide pump manufacturers – Grundfos [3] and Wilo [4] are used for proper pump selection. Variable speed, submersible, borehole pumps are selected and a few options are considered (Table 3). The criterion for pump selection includes not only the pump input power at the design duty point, but also the power input for points *A* and *B*. Considering that variable speed pumps are used the pump head and discharge are the same as for the duty points, so the pump power depends on pump efficiency only. The pump efficiency η for each duty point is obtained using the affinity laws [2]. In Table 3 the ratio between required and maximum pump speed n/n_{max} is presented, as well as the ratio between the required and the nominal discharge of the pump Q/Q_{NOM} .

Table 3. Selected pumps and pump parameters for the defined duty points

Pump	Q	H	n/n_{max}	η	$\eta_{average}$	Q_{NOM}	Q/Q_{NOM}
-	l/s	m	-	-		l/s	-
GRUNDFOS SP 46-8	14,4	50,5	0,964	0,702	0,715	12,5	1,15
		45,0	0,937	0,686			
	12,6	47,5	0,890	0,725			1,01
		43,0	0,866	0,715			
	10,8	39,0	0,789	0,733			0,86
		36,0	0,770	0,727			
GRUNDFOS SP 60-7	14,4	50,5	0,934	0,745	0,741	15,4	0,94
		45,0	0,898	0,744			
	12,6	47,5	0,878	0,740			0,82
		43,0	0,849	0,743			
	10,8	39,0	0,784	0,734			0,70
		36,0	0,761	0,738			
WILO TWI 6.50-07	14,4	50,5	0,997	0,728	0,739	12,0	1,20
		45,0	0,965	0,714			
	12,6	47,5	0,928	0,747			1,05
		43,0	0,901	0,739			
	10,8	39,0	0,826	0,755			0,90
		36,0	0,804	0,750			
WILO TWI 6.60-06	14,4	50,5	1,000	0,728	0,719	15,2	0,95
		45,0	0,962	0,731			
	12,6	47,5	0,942	0,715			0,83
		43,0	0,908	0,722			
	10,8	39,0	0,842	0,705			0,71
		36,0	0,817	0,712			

The best options for each of the manufacturers are as follows: Grundfos SP 60-7 and Wilo TWI 6.50-07-B. The performance $Q-H$ and $\eta-Q$ curves of the two pumps are presented on **Fig. 5**. The efficiency for both options is practically identical and any further selection should be based on other criterion – price, reliability, etc.

When only the design point is taken into account SP 60-7 is also the better option among Grundfos pumps, while the two Wilo pumps have identical efficiency. If the additional points are included in the criterion, the pump TWI 6.50-07 shows better performance.

Comparison between the better options from the two manufacturers shows that SP 60-7 achieves the design point with 93% of the maximum speed and the design discharge is smaller than the nominal (0,94). The discharge decrease (e.g. points B and A) leads to efficiency drop. As for the pump TWI 6.50-07 the design point is assured practically by no speed reduction ($n/n_{max} = 0,997$) and the ratio Q/Q_{NOM} is bigger than 1,00 – it is 1,20. The discharge decrease for points B and A leads to efficiency increase. It is seen from **Fig. 5** that TWI 6.50-07 runs near the end of its performance curve while achieving point D' . Any further decrease of the head in some operating cycles may lead to exit of the recommended $Q-H$ range. On the other side such pump characteristic prevents the well from overdraw. Contrary SP 60-7 has very good performance results both for the design and for the intermediate duty points. It has a reserve for small further extension of the network, but it should be operated carefully in order to prevent well overdraw. Smaller discharges at required heads smaller than the ones shown on **Fig. 5** are better delivered by TWI 6.50-07.

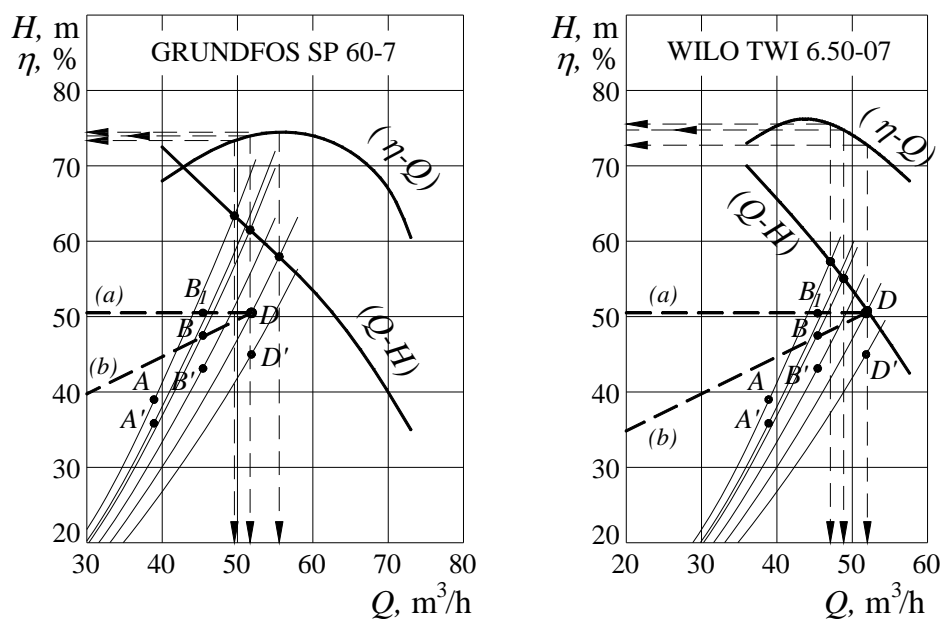


Fig. 5 Performance curves of the chosen pumps

It should be noted that results in **Table 3** are obtained assuming that every duty point is achieved and no mode for speed control is chosen. Depending on the applied control mode [5], [6] the results in **Table 3** will vary and the best option may differ. For example, if the water level in the well is constant and a constant differential pressure control mode is applied, then the actual duty points at different discharges are placed on the dashed line (a) on **Fig. 5**. In that case instead of duty point B point B_1 is achieved. If a proportional differential pressure control mode is assumed, then the actual duty points are placed on line (b). The discharge decrease causes leftwards moving of the duty points along these lines and in control mode (a) the points are higher than in control mode (b). Thus in control mode (a) the intersection between the parabola representing the affinity laws

and the Q - H curve is left from the intersection if control mode (b) is assumed. So in control mode (a) it is preferable to have $Q/Q_{NOM} > 1,00$ for the chosen pump, as in control mode (b) is better to have $Q/Q_{NOM} \leq 1,00$.

4. CONCLUSIONS

Pump selection for extended network systems should be done taking into account the following recommendations:

1. It is very important to have a clear concept about the system state at the last stage of the extension. It is decisive for determination of the design parameters (Q and H) of the pump and its selection, in order to make pump replacement at once.

2. Pump selection should be made after considering the pump parameters (Q and H) required at each stage of the extension. Thorough hydraulic estimations for the pipe network should be carried out, taking into account pipeline development and the way it is reconstructed at each stage. The parameters Q and H are co-related with the layout and the design of the pipe network and the way the network is used.

3. Placing an additional pump in parallel or in series with the existing one is a competitive variant in comparison with pump replacement. Such variant gives additional flexibility of system operation and it is much cheaper when it is possible. It is advisable to have one of the pumps with variable speed control.

4. When choosing a variable speed pump:

4.1. The pump control mode has to be chosen before the pump selection is started.

4.2. The design discharge Q_D should be as closer as possible to the nominal discharge Q_{NOM} . ($Q_D/Q_{NOM} = -10\% \div +10\%$);

4.3. If the design point is achieved by relatively big speed reduction ($n/n_{max} \leq 95\%$) then it is advisable to have $Q_D/Q_{NOM} < 1$ and vice versa – if the speed reduction is negligible, then Q_D/Q_{NOM} may be greater than 1,0;

4.4. If a proportional differential pressure control mode is assumed then it is preferable to have $Q_D/Q_{NOM} \leq 1,00$. If a constant pressure or a constant differential pressure control modes are assumed then it is better to have $Q_D/Q_{NOM} > 1$.

4.4. The most important factor is the absolute value of the pump efficiency.

Considering new drip irrigation systems for which a future extension is expected the following recommendations can be made regarding selection of pumps:

1. It is advisable that the design discharge Q_D is 80÷90% of the nominal discharge of the pump Q_{NOM} . This gives some reserve in capacity for future extension of the system.

2. A variable speed pump providing the design duty point at 85÷95% of the maximum speed is favourable decision. This also ensures reserve in capacity and causes high pump efficiency during operation regimes.

3. At general the optimised pipe network are not suitable for extensions and for that reason any optimisation of pipe diameters for systems subject to future extension should be considered carefully.

5. REFERENCES

- [1] Sakai, H *et al.* Pumping Station Engineering Handbook. Japan Association of Agricultural Engineering Enterprises, Tokyo, 1991, Vol. 1, ch. 1, p. 21-23.
- [2] Sakai, H *et al.* Pumping Station Engineering Handbook. Japan Association of Agricultural Engineering Enterprises, Tokyo, 1991, Vol. 1, ch. 9, p. 304-307.
- [3] * * *. Grundfos WebCAPS. Available at: net.grundfos.com/App/WebCAPS/
- [4] * * *. Wilo-Select Online. Available at: www.wilo-select.com
- [5] * * *. Grundfos E-pumps, Grundfos Data Booklet, 2005, p. 8-13.
- [6] * * *. Monoblock, Norm and Axial Split Case Pumps, Wilo Catalogue A3, 2007, p. 144-151.

Sewer System by SeWaCAD

Štefan Stanko

Abstract – Sewer networks in Slovakia consist mainly of combined sewer networks in the cities and separated in the villages. The new or extended sewer networks, according to EU approach process, are mainly built in villages and these are separated – dry weather sewer networks. The design of these networks needs very fast procedures and without the help of a software this process could be very difficult. The paper describes the SeWaCAD software developed by the paper's author in a few years, which is very successfully exploited in Slovak conditions. The software takes into account the Slovak standards and the outputs are hydro-technical calculations and drawings in CAD environment. The software is intuitive and it was verified by the experts. The main use of the software is focused on separated design, but the software allows very effective design of combined or storm water sewer system, because contains the rainfall database of 68 rainfall stations in Slovakia and computational procedures.

Keywords – appraisal, CAD, CSO, network design, sewage.

1. INTRODUCTION

The public sewerage system in Slovakia connects approx. 60% of the population. The remaining 40% are still a challenge for designing new effective and optimal sewerage networks equipped with waste water treatment plants and offer the design opportunity to many designers in Slovakia. The negative impact is the short time for the preparation and the old procedures, based on manual computation, don't offer the fast and accurate design with outputs in computer formats – CAD – DFX, DWG and their implementation in GIS systems in Slovakia.

The methodology of networking - sewer system design in Slovakia was developed more than 50 years ago. The methods for pipelines design, computation and drawings were customized for hand computation and hand drawing. This method was very slow, not very accurate and produced many mistakes caused by the designer. The relation between calculation and drawing was very heavily-handled. The designer had not enough time for making the mathematical “approximation” design and consequently for making drawings, used as plans for the structures building.

The 70s were the first years to experience computer based design. At first only the elementary tasks were solved by computer, and the graphical outputs were only a dream of the designers, but not reality. The computer hardware didn't allow them to produce the drawings. The end of the 70s promised better expectations for this dream. This period of the computer age was very surprising for the engineers, but everything was starting. The absence of the hardware, software had two reasons: 1. political –the war industry was preferred and 2. simply the level of hardware quality was low. [7] [8]

The expansion of software making took place in the 80s, when the computer industry developed the microprocessors, which brought the first personal computers, which allowed to produce not only computes, but

Manuscript received October 1st, 2011 and accepted November 10, 2011.

The paper was written with the support of the Scientific Grant Agency – projects VEGA No. 1/0559/10 dealt with the Department of Sanitary and Environmental Engineering of Slovak university of Technology

Author Assoc. Prof. Dipl. Eng. Štefan Stanko, PhD. is from the Slovak University of Technology, Faculty of Civil Engineering, Dept. of Sanitary and Environmental Engineering, Radlinského 11, 81368 Bratislava, Slovakia (corresponding author phone: +421-2-59274280; e-mail: stefan.stanko@stuba.sk)

graphical outputs on the screen too. It was a period, when some young engineers had the opportunity to make the software at the office in the absence of the big computer centres.

The 90s brought the enormous growth of the computer hardware and software. The new and not very expensive peripheral equipment – plotters, the new “quick” processors, the minimizing of computer dimensions with increasing operational memory, permanent memory and the quick graphical interface – graphical cards were the big call for software developers including the civil engineers.

Various software were developed in this period, which is not only a toy but a strong tool for design structures in the civil engineering branch. One of them is the system for pipeline design, developed in the Slovak Technical University – Faculty of Civil Engineering, which is in the newer version 2006. This is a complex system for inputs definition, hydraulic calculations, allowing changing the net topology with an easy approach and consequently to quickly produce the drawings as plans for building the line structures.

2. THE DESIGN PROCEDURE

The methodology, the know-how to design the pipelines comes from the history. The primary methodology was developed only for simple sewer network systems. The exploitation of computers provided only the calculations but no graphical outputs. The sewer network definition – the net – was very difficult and the check was not accurate every time. The 90s were the years of progress in the sewer system design. In Slovakia we developed the system Sewdes, which knew how to calculate the sewer system, but very long time only calculation without graphical outputs were possible. The SeWaCAD – the new software solved many problems concerning computer sewer design and offered to the public experts the possibility to exploit the software with a user-friendly interface and very fast computation ability with a short time for achieving the required results. The system was created in 2005. The system offers the possibility to use the continual data concept with a new software engine, with an intuitive approach of data definition, with the chance of additional data.

In the data definition process the user might cause various mistakes. The new system is susceptible of 2 basic approaches of data inputs: as input from some CAD system, the ACAD exploitation and very easy data definition in the software system environment, which doesn't need to hold the map, or with map – situation.

2.1 Exploitation of External Cad System

External CAD system exploits the system of data inputs, which is based on the method: “draw and XY capture”. This method shortly describes how to: draw the points of the nodes, and lines between nodes and after that, with the special software, to accurately record the XY data of the nodes for the next process. (Figure 1)

The module for processing the XY data called “digital”, produces the expert input of data for the design system environment. It contains the XY data, lengths between nodes, system of net topology contained in net matrix, the automatically named branches of the net. The level data is obtained after, by the self module, which grabs the data from the DXF file.

2.2 SeWaCAD Data

Inputs are based on data editing directly in the software environment. Manual input allows expanding the net upstream and downstream. It allows defining the length, if we need to keep the exact distances, or to omit the length – and define the exact place of the new node. After defining of a new node, editing of this node is allowed.

System allows the quick renaming of each branch by finding the branch and defining the new name – “combobox” routine.

Manual input is used on the graphical screen. The connection between the digital database and the graphical environment allows the visual check of the net for the designer, and very fast orientation in design process.

The difference between input from the CAD and the manual input is: The CAD input globally defines the new net with many nodes, allows defining not only one node at a time, but entire net. The main advantage is a very fast definition of the net, with distances and automatic names of the branches. On the other side, the manual input allows the user to exactly editing each node. The nodes are defined in the system and the new nodes are appended by automatic insertion with system attributes.

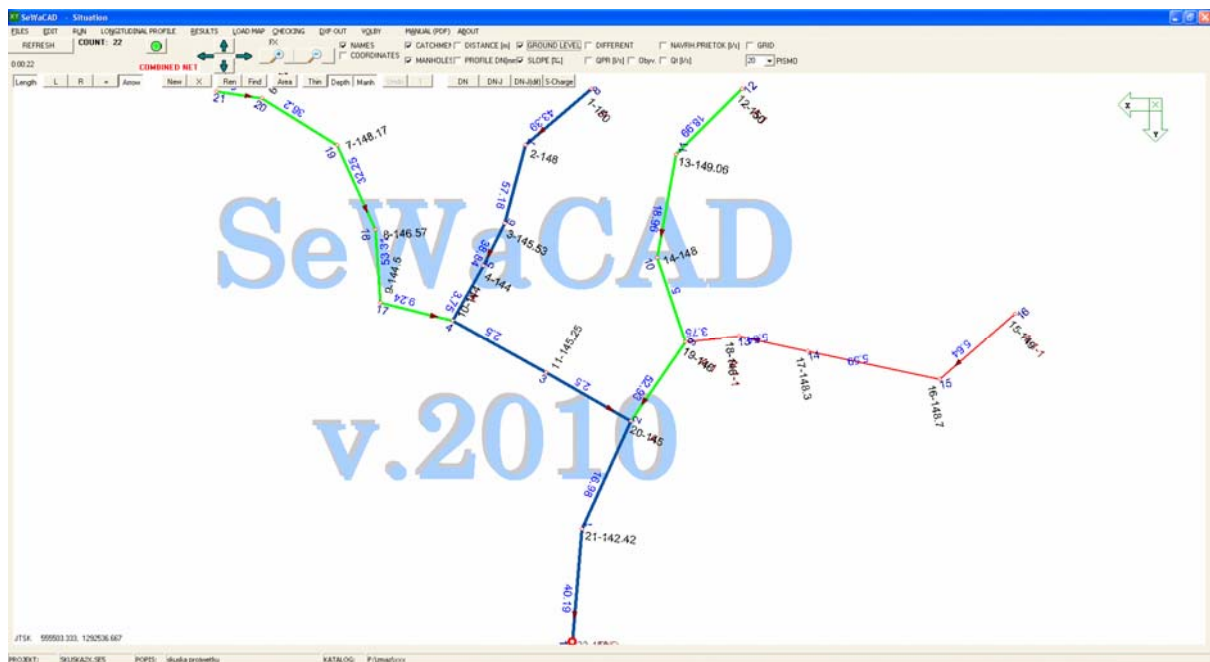


Fig. 1 The output from DXF file, transformed through the digital module (network example)

2.3 Data Checking

A very useful module is the module for data checking, which allows the logical system check and prevents against mistakes, which have a negative influence on hydrotechnical calculation. This is a very important module, because in large nets there is impossible for the user to manually check data. This checking concerns mainly net topology. The check is very easily enabled - by pressing the key, and in a moment the user can watch the results of the checking on the screen. The system shows the places – nodes, where problem were detected. The user can very easily repair the nodes which contain mistakes, and correct the fault values.

2.4 SLOPE GENERATOR

The design of longitudinal profiles is the challenge. User need to spend too much time for manual design of the longitudinal profiles. This challenge was the big initiator for creating the slope generator module, which allows in a short time to design the slopes on the entire net and in an iteration process of design, allows changing the specific parts of the sewer net. System of slope design allows the user to design the slopes by some approaches: the optimal computer design; the terrain replication; the defining of the own slope; function of slope generation on the idea bottom to bottom. The minimal slope is defined by empirical formula (1)

$$i_{\min} = \frac{1500}{D} \quad (1)$$

Where D is the sewer diameter in millimetres and the minimal slope defines the build-technical slope, which is possible to observe in building process. And this slope has no eligible value concerning sewage alleviation, where we need to define the sewer slope regarding the amount and quality of waste water.

Self-cleaning slope - The EN752 recommendation for the design of dewatering and sewer systems is explicit and wants to prevent the sewers against the permanent drift deposition, which increases the risk of flood involving the sewer system and following environmental pollution.

The sewers with the minimal bed slope are drifted and we need to clean them. The Čížek [1] in the 1953 advised to compute the sewer slope of the combined sewage by the use of the equation for critical tangential tension near the wall of the sewer pipe by the eq. (2)

$$\tau = \rho \cdot g \cdot R \cdot i_0 \quad (N \cdot m^{-2}) \quad (2)$$

Where

- τ - tangential tension - [Pa]
- g - gravitational acceleration - [$m \cdot s^{-2}$]
- R - hydraulic radius - [m],
- i_0 - slope

When we put $\tau_{\text{critical}}=4,0$ Pa for combined sewer system, after self-cleaning velocity is defined by eq. (3)

$$v_s = 0,02 \cdot R \cdot 0,167 \cdot n^{-1} \quad (m \cdot s^{-1}) \quad (3)$$

Where

- n - Manning's roughness coefficient.

In the case of dry-weather sewage we choose the τ critical=2,0 Pa [3]. The sewer bottom slope is equal is=0,00204/R, and the R is relative to the average dry-weather flow Q_{b24} .

Table 1. Recommended values of minimal slopes in dependency on sewage type [2]

Indicators	Recommended value				
	(1) DN	(2) Sanitary sewage	(3) x/D	(4) Combined sewage	(5) x/D
Minimal required slope	[mm]	[‰]	x	[‰]	x
	250	18	4500	12	3000
	300	14	4200	9	2700
	400	9	3600	6	2400
	500	7	3500	5	2500
	600	6	3600	4	2400
	800	5	4000	3	2400

2.5 SeWaCAD Exploitation in the Flat Areas

The use of design software for the flat areas (figure 3) is the effective tool for the alternative sewer system design. The hand calculation of sewer system takes too much time, and this operation might be inaccurate and very difficult. The used software offers the chance to investigate in a short time more alternatives of design, using more values for sewers diameters and solves the conception of sewer pumping station.

The Department of Sanitary and Environmental Engineering offers solution through the computational system SeWaCAD, which gives design alternative solutions with the possibility of alternatives compare. The use minimal diameter DN250 against DN300 in older period brought savings from the profile diameter, but not from excavation and number of pumping stations. The elaboration of alternatives could clear up the question of the most effective solution. And the answer to this question is quickly provided. For example the historical approach uses the minimal slope 3,33‰ with the profile DN300 against present minimal slope 6 ‰ together with the DN250 diameter use. It caused a loss of elevation of 60 cm – 33 cm = 27 cm for every 100 meters (figure 2), which represents a total elevation loss of 2,7 meters per 1 km of sewer length. So we can very easily assert that we need to build two times more pumping stations against older principles. If is it effective or not, we find this answer through the alternative design evaluation, from technical and economical viewpoint, by respecting the operational conditions and operational costs. We can say, that influence of terrain composition play an important role in sewer system design. Evaluation of many sewer system designs in various conditions allows us to declare, that saving profile diameters DN250 is not in every case the cleverest solution, but in many cases legitimate. And we can declare that only complex alternative solution could give answer to this question.

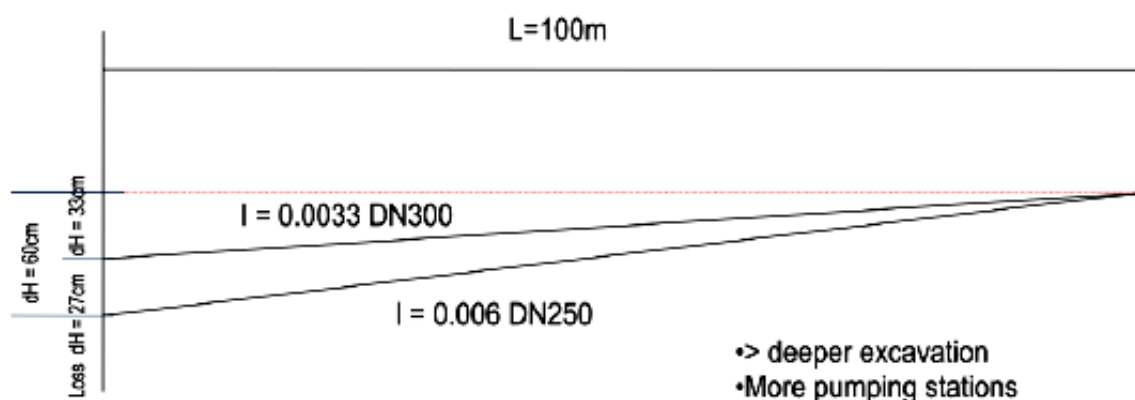


Fig. 2 Loss of deep in dependency on sewer slope

Hydrotechnical calculation is the process of input data transformation into the binary file, which contains the new data – hydro-technical results. These data are shown in graphical form on the screen.

The dimensions of profiles are shown in various colours, so it is very easily possible to see the dimensions of the profiles on the entire net. Hydrotechnical calculation module allows changing the type of the net and the number of population and the amount of water for the inhabitant per day. After data input the calculation is easily and immediately realized. User can view the maximum flow of the net, without using the module for result presentation.

The Slovak system of the nodes numbering is different from the numbering of catchments. System uses a very tide module, which allows nodes numbering by the system needed by practice. There are two ways – full automatic, or manual driving.

A very useful function is the possibility of computation appraisal.(Figures 3 and 4). The user can make CAD output with marked problematic segments. The decision of the high overload depends on system, but this is possible to change by the user. The figure is originally coloured. For example the red colour means much overloaded sewers. Description of the appraisal possibilities is more difficult and this is not to be described in this paper.

The possibilities of combined sewer design are based on rational formula. The system exploits the curves of rainfalls of the 68 rainfall stations in Slovakia [5]. The database contains the elaborated parameters from these stations with the periodicities 0.2, 0.5, 1.0 and 5.0. The rainfall curve is automatically computed by a chosen station or by iteration between three stations selected by the user.

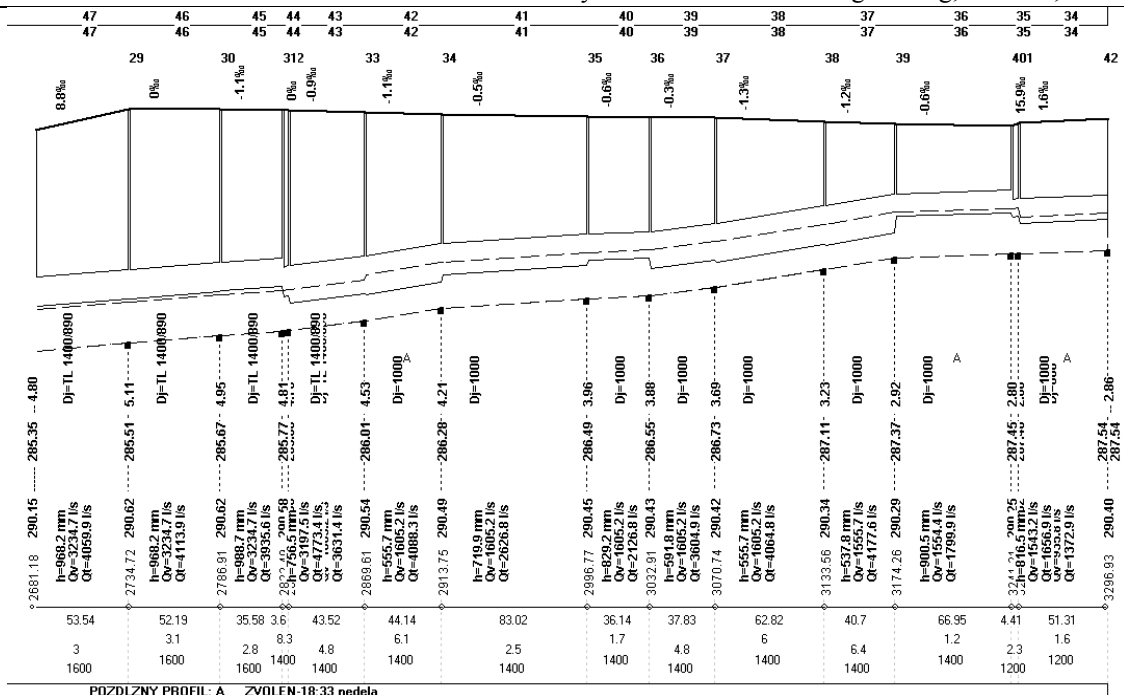


Fig. 3: Example of overload longitudinal profile with renew offer (draft sheet)

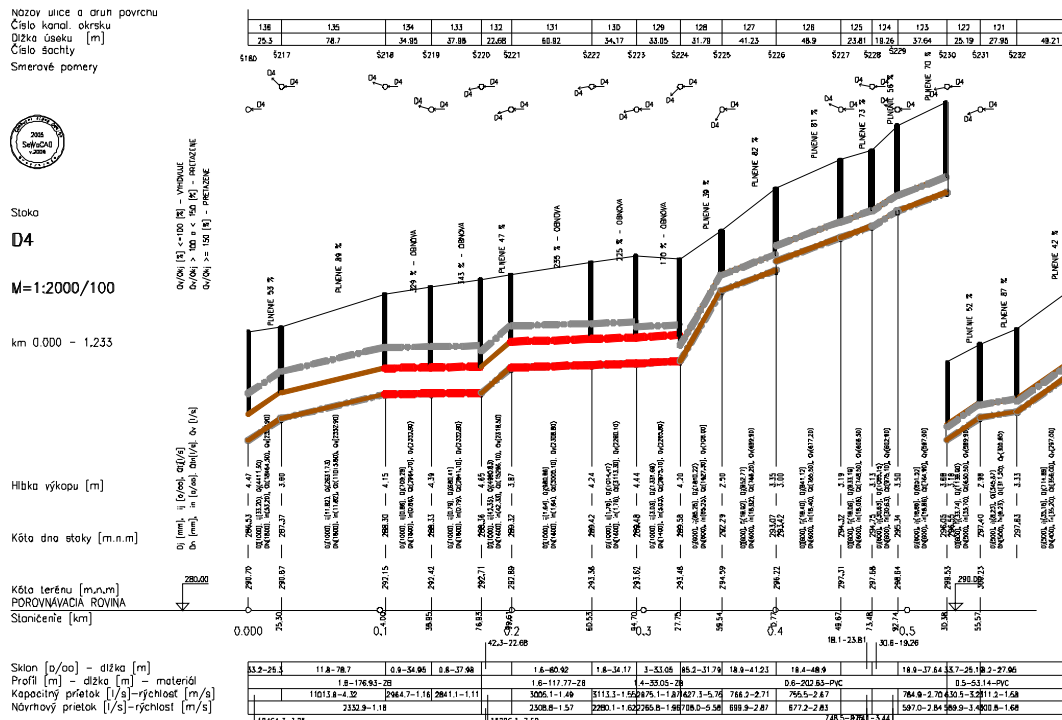


Fig. 4: Example of overload longitudinal profile with renew offer - final output

2.6 Longitudinal Profile – Drawing

This generation of longitudinal profiles allows the user to view these profiles on the screen. The system of viewing was designed on the idea to view the maximum of the design with a minimum pressing of the keyboard tastes and mouse. By this module, user can see all the longitudinal profiles only by using the mouse wheel. The drawing details are possible to zoom-in and zoom-out by clicking the left, or right button, or using the buttons on the screen. So the user can follow the changes operated in the system. (Figure 4)

If the user wants to make changes in these profiles, the system allows the use of the resident editor for deep defining, and switching to the situation allows the change of the details of the nodes. The view of longitudinal profiles shows only profiles which are not suitable as plan drawings, but only for creation of the optimal design. For the final drawings, the system contains composite module for profile generation in DXF form (Fig. 4).

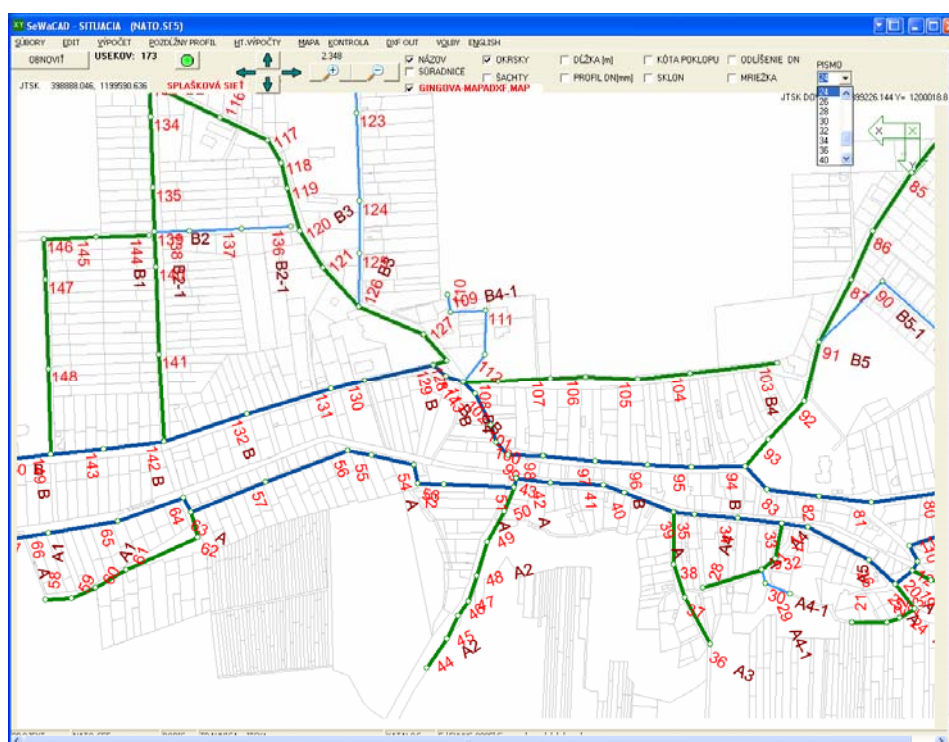


Fig. 5 Computational example of sewer system design in a flat area (SeWaCAD)

3. RESULTS AND SIGNIFICANCES

The purpose of the work was to develop a complex system for designing and evaluating the sewer systems. Combined, separated and storm sewer system are included. The combined sewer system includes the CSO (combined sewer overflow) structure with the possibility of dilution ratio and boundary rainfall. 68 rainfall station databases offer the combined sewer system design covering the whole Slovak region. System allows defining own rainfall IDF curves (intensity – duration – frequency). System contains two languages – Slovak and English mutation. The system was developed in the DELPHI program language. DELPHI is very sophisticated software and allows developing applications, which are user friendly, and with maximum exploitation capacity.

System is designed for the very fast effective design of pipelines with dimensions and allows fast output data transfer to the drawings – longitudinal profiles and various situations, which are used as plans for building the pipelines. The advantage is the interface for expert system MOUSE. As a consequence of this interface, the

system of pipeline design becomes a strong tool as an input editor for hydro-dynamical simulation. The main idea of the system is: in a short time create the plans of the pipelines for the villages and the cities in the Slovak republic.

The handling of this system needs some experience with the CAD systems work and know-how of system procedures. After user adoption the exploitation of this system becomes very effective.

Only clever and expert approach of main decision, supported by professionals could have an effective, optimal impact on dewatering the area from wastewaters. The system was developed by the author of this paper. The total program contains hundreds of pages of source code in the DELPHI environment and took a few years to be developed. The software verification was done by the testing on praxis. Many sewers were designed together with the Slovak highways. The next huge application was implemented on village sewages, mainly the dry-weather sewer. The cities such as Zvolen, Detva and others were appraised by the SeWaCAD.

4. CONCLUSIONS

At present time design and appraisal of sewer system and general water management requires the exploitation of computers through the software. The advantage is the fast and effective design. But the problem that still remains is that many users cannot exploit the software at hundred percent but with basic possibilities. This means that the optimisation process is not absolute. The software creation by the developer very often gives more possibilities, than the user can imagine. Only the training by the authorized teacher could improve the software exploitation. Besides, the user should be an expert in water management, because the software is clever, but the main decision depends on the user. So at final, only the user is responsible. Sometimes the user might wonder: why the software doesn't know this or this thing. My suggestion for the user is to think about the problem, to find solution together with the expert software exploitation and the engineer in water management. The expert system is an advantage and the SeWaCAD becomes a very strong tool which supports the experts.

5. ACKNOWLEDGMENTS

The article was written with the support of the Scientific Grant Agency – projects VEGA No. 1/0559/10 dealt with at the Department of Sanitary and Environmental Engineering of the Slovak University of Technology.

6. REFERENCES

- [1] ČÍŽEK, P.: Hydrologie stokových sítí, Stokování, 1.část, SNTL, 1961
- [2] STRÁNSKY, D., HAVLÍK, V, KABELKOVÁ , I., METELKA, T.SÝKORA, P, DOLEJŠ, M., HALOUN, R., MUCHA, A., PRYL, K.: Posouzení stokových systému urbanizovaných povodí, část III. – řešení balastních vod a výskytu sedimentů ve stokové síti, Vodní hospodářství, 08/2010.
- [3] STN 75 61 01 Stokové siete a kanalizačné prípojky
- [4] STN EN 752 Stokové siete a systémy kanalizačných potrubí mimo budov
- [5] Urcikán, P.: Analyse and using of rainfall data and hydrotechnical calculations of sewerage systems. Accademic dissertation, STU Bratislava, 1987
- [6] Act No.442/2002 Dig. on public water and sewerage systems
- [7] KRÍŽ, K. - BAREŠ, V. - POLLERT, J. - STRÁNSKÝ, D. - POLLERT, J. Risk analysis of sewer system operational failures caused by unstable subsoil In: Risk management of watersupply and sanitation systems. Dordrecht: Springer, 2009, p. 65-72. ISBN 978-90-481-2364-3, (2009)
- [8] HLAVÍNEK, P., Perspectives of decentra-lized wastewater treatment for rural areas, in Advanced Water Supply and Wastewater Treatment: A Road to Safer Society and Environment, ISBN 978-94-007-0279-0, Springer, Nederland, (2011).

Cracking Moment in Steel Fibre Reinforced Concrete Beams Based on Waste Sand

Jacek Domski

Abstract –The results of tests on cracking moment in steel fibre reinforced concrete beams based on waste sand are presented in this paper. The test defined cracking moment was compared with that calculated as proposed by Lok and Xiao, Tan, Paramasivam and Tan and by application of the methods contained in Eurocode 2 as well as in PN-84/B-03264. The best compatibility of the obtained test results with the calculated values was achieved for the Eurocode 2 method.

Keywords – beams, cracking moment, steel fibre, waste sand.

1. INTRODUCTION

The main objective for application of steel fibres in concrete elements is to limit cracking caused by external and internal loading. An important parameter describing the cracking phenomenon in steel fibre reinforced concrete “little beams” is the moment of appearance of the first crack [1]. This is determined, in most cases, on the basis of the load-strain relationship at the point in which the curve deviates from the straight line. Such interpretation is included in the majority of standards (ASTM C 1018, NBN B 15-238, JCI Standard SF-4) and recommendations (CUR, DBV, RILEM) [2], [3] regarding steel fibre reinforced concrete “little beam” testing irrespectively of their size. There is a big number of studies verifying the calculation methods included in the standards [4]–[8]. Unfortunately, those methods do not apply to calculations of full-size elements e.g. beams with longitudinal reinforcement and steel fibres because it is impossible to clearly define the cracking moment based on the load-deflection relationship [9], [10].

The fundamental parameter describing the cracking limit state is the cracking moment K . H. Tan, P. Paramasivam and K. C. Tan [11] have assumed that influence of fibres on the moment of inertia can be neglected and then the formula for the cracking moment would take the following form:

$$M_T = \frac{\varphi_{cr} I_g}{y_t} \quad (1)$$

where:

I_g – total moment of inertia,

y_t – distance from the centre of gravity to stretched cross-section edge,

Manuscript received October 1st, 2011 and accepted November 10, 2011.

Research work financed by the Polish State Committee for Scientific Research during the period of 2003 – 2006 as a research project (grant) No 5 T07E 021 24

J. Domski is with the Koszalin University of Technology, Department of Civil and Environmental Engineering, Śniadeckich Street no. 2, 75-453 Koszalin, Poland (corresponding author to provide phone: +48-94-3478581; fax: +48-94-3427652; e-mail: domski@wbiiis.tu.koszalin.pl).

φ_{cf} – strength for the first crack in steel fibre reinforced concrete little beams; it can be defined using an empirical formula proposed in 1974 by R. N. Swamy and P. S. Mangat [12] (recommended by ACI [13]), based on the so-called law of mixtures:

$$\varphi_{cf} = 0.843f_r(1 - V_f) + 2.93V_f \frac{l_f}{d_f} \quad (2)$$

where:

V_f – volume of steel fibre content in the entire mixture,

l_f & d_f – fibre length and diameter, respectively,

f_r – concrete little beams flexural strength [N/mm²]; it can be calculated as a product of constant 0.622 and square root of the compression strength defined for cylinders.

Another method for the calculation of the cracking moment for steel fibre reinforced concrete elements was proposed in 1995 by T. S. Lok and J. R. Xiao [14]. For the adopted relationship between load and strain (for the element before cracking) cracking moment per 1 m of element width was fixed:

$$M_{cr} = 0,236 \cdot H^2 \cdot f_t \quad (3)$$

where:

H – element height,

f_t – ultimate tensile strength.

2. EXPERIMENT DESCRIPTION

The aggregate used in the tests was the waste sand being a residue of the all-in aggregate hydraulic classification process [15], [16]. The fine aggregate and concrete matrix recipe was fixed for the required C12/15 class. The fixed composition of the fine aggregate and concrete matrix was modified by addition of a superplasticizer (FM 34) and hooked 50/0.8 mm or 30/0.55 mm steel fibres alternatively. The water content was controlled in such way so as to obtain a plastic consistency mixture compatible with ACI guideline [17]. In result, concrete of C25/30 and C30/37 was produced. The final composition of the steel fiber reinforced fine aggregate concrete mixtures has been indicated in Table 1.

Table 1. Steel fibre reinforced fine aggregate concrete mixture compositions for 1 m³

Concrete with steel fibres	Components					
	Waste sand [kg]	Cement [kg]	Water [litre]	FM 34 [litre]	Steel fibre [kg]	
					glued	loose
30/0.55 mm	1855	378	140	3.51	34	—
50/0.8 mm	1835	374	150	3.47	—	33

Additionally, for comparison purposes, plain (commercial) concrete has been made; its composition was devised by its manufacturer for fixed cube strength of 45 MPa.

The cracking moment tests were performed in 0.15×0.2×3.3 m beams. The test elements were made in 10 series that varied in type of concrete mixture (steel fibre reinforced fine aggregate and plain concrete), steel fibres applied (50/0.8 mm and 30/0.55 mm), beam element longitudinal reinforcement ratio (0.6 %; 0.9 %; 1.3 %; 1.8 %) and application (or not) of compressed reinforcement as well as stirrups vertical to the element axis spaced at every 130 mm (Table 2). Each test element series comprises 2 beams, 6 cylinders and 12 cubic samples intended for definition of strength features. They were demoulded after 24 hours as of concrete pouring. The thermal and humidity conditions during test element making and hardening were uniform.

The longitudinal beam reinforcement was made of ribbed steel (34GS grade) dia 8, 10, 12 and 14 mm, whereas the transversal reinforcement was made of smooth steel (St3SX-b grade) dia 4.5 mm. Only ribbed steel

was tested for its mechanical properties. The yield point within 424-454 MPa range, tensile strength from 678 MPa to 714 MPa and modulus of elasticity from 205 GPa to 223 GPa were obtained. It appears from the tests performed that ribbed steel used in this study featured a very distinct yield point.

Table. 2. The beam elements testing programme

Concrete	Fine aggregate with 50/0.8 fibres					Plain	Fine aggregate with 30/0.55 fibres				
Beam marking	A-1, A-2	B-1, B-1	C-1, C-2	D-1, D-2	G-1, G-2	F-1, F-1	H-1, H-2	I-1, I-2	J-1, J-2	K-1, K-2	
Reinforcement (top, bottom)	2#8, 3#8	2#8, 3#10	2#8, 3#12	–, 3#8	2#8, 3#14	2#8, 3#10	2#8, 3#14	2#8, 3#12	2#8, 3#10	2#8, 3#8	
Stirrups ϕ 4.5 mm	Spaced at every 13 cm			–	Spaced at every 13 cm						

The static diagram of the tested elements was a single-span freely supported beam loaded with two concentrated forces applied at 1/3 span between the support axes (Fig. 1). The forces were applied via a steel beam loaded with the hydraulic cylinder. At the bottom frame beam two supports, i.e. roller and pinned, designed in such way so that reaction measurement with tensometric force gauges could be performed. The amount of the load applied was controlled by beam support reaction reading with application of the SAD 256 computer data acquisition system.

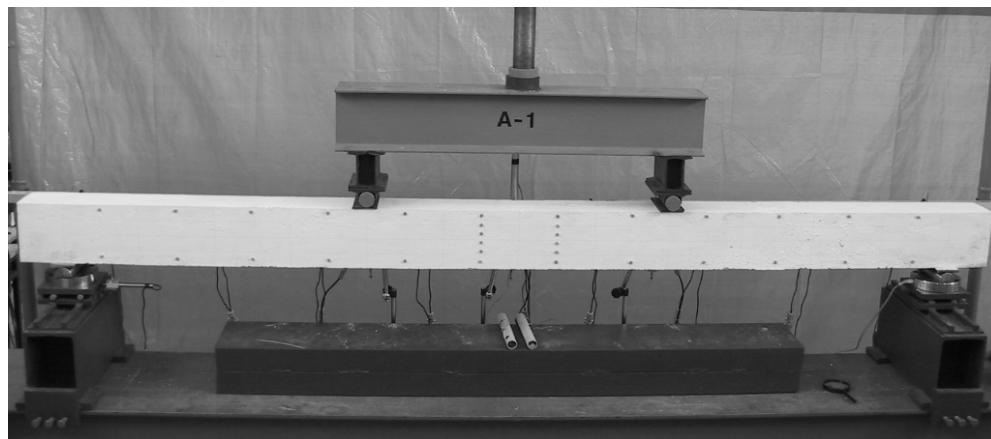


Fig. 1 General view of the test rig for A-1 beam testing (series A)

The system was used, in the presented study, also for measurement of beam tensioned reinforcement strain. It was measured with foil strain gauge glued (before concrete pouring) to two tensioned rods. TFS-5/120 foil strain gauges ($120.3 \Omega \pm 0.2\%$ resistance and gauge factor $k = 2.15 \pm 0.5 \%$) connected to SAD 256 system via the so-called Wheatstone's bridge have been applied.

The cross-section cracking moment was fixed during observation of the beam lateral surface with 5 x magnifying glass and from the graph of tensioned reinforcement strain in loading function.

3. RESULTS AND SIGNIFICANCES

The fundamental parameter of the reinforced concrete theory that describes transition of the bent element from the first phase of operation to the second one, is the cracking moment. Its determination in the steel fibre reinforced concrete elements is difficult because the composite may comprise the so-called "dead cracks" visible even without any loading applied, which do not grow with load increase. Therefore, the moment of occurrence of the first crack can be defined on the grounds of the displacement graph inclination change (e.g. deflection) depending on the load applied. This effect is visible, first and foremost, in the steel fibre reinforced concrete elements without any rod reinforcement because the transition between the operation phases is clear in such case [1]. In the steel rod reinforced concrete elements there are some objective problems with definition of the

cracking moment based on the change of the angle of inclination in the already mentioned graph because the reinforcement rods considerably moderate the between-the-phase transition [9], [10].

Values of the cracking moments have been determined, in the study presented herein, in a standard way through observation of the beam lateral surfaces and then compared with the values determined through analysis of the graphs of tensioned reinforcement strain in function of the bending moment, obtained from SAD-256 system. The reader can note a jump of strain values at a practically constant moment value in Figure 2 showing strain in reinforcement steel in the bending moment function. That value can be used as the cracking moment.

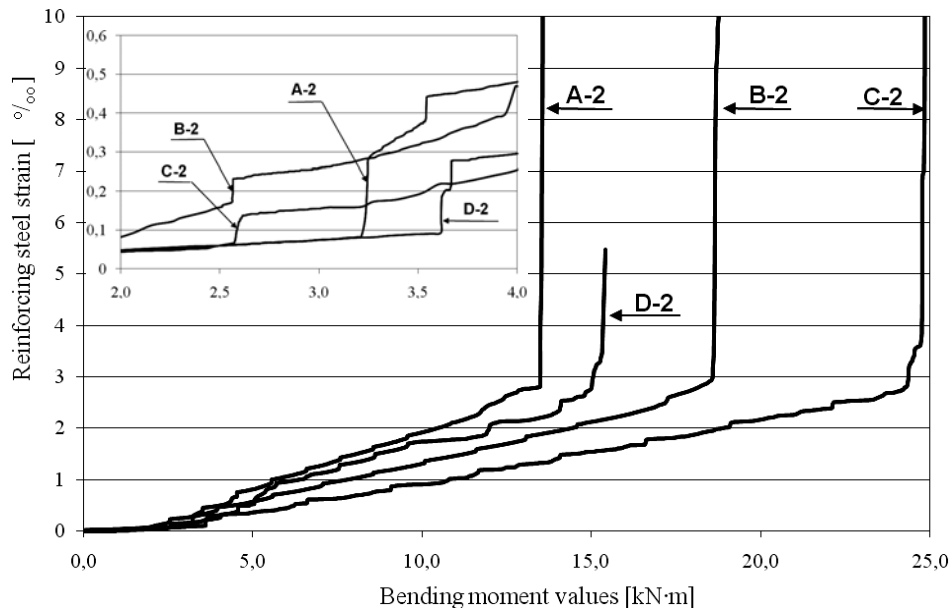


Fig. 2 Relationship between the cracking moment and strain in tensioned reinforcement for 50/0.8 mm fibre containing beams – second series.

Based on the analysis of the graphs of tensioned reinforcement strain in the bending moment function, in some cases the value of the cracking moment defined through observation of the lateral surfaces (A-2, C-2, D-2, G-2, I-2, J-1, K-1 and K-2) has been confirmed. The moment of a standard defined cracking could not have been confirmed for the other beams. This was probably caused by the fact that the first crack did not appear nearby the element mid-span, where the foil strain gauges were glued on. A jump at different values of the bending moment, or even lack thereof, has been observed for those beams in the strain graph. Also no change of the angle of inclination in the displacement graph in the loading function has been ascertained. Such situation confirms occurrence of problems in determination of the magnitude of the cracking moment in the steel fibre reinforced beams. Table 3 shows a comparison between the experimentally fixed cracking moments (M_{rys}) with those calculated in accordance with Eurocode 2 recommendations (M_{cr}) [18] and PN-84/B-03264 [19] (M_{fp}) as well as proposals of Tan, Paramasivam & Tan [11] (MT) and Lok & Xiao [14] (ML).

Small diversity in cracking moments has been ascertained for the steel fibre reinforced fine aggregate concrete beams (with single type fibres) due to practically imperceptible influences of the longitudinal reinforcement ratio (0.6 %, 0.9 %, 1.3 % and 1.8 %). The differences between the measured values of the cracking moments did not exceed 20 % (with exception of C-2 between containing 50/0.8 mm fibres). This proves that the magnitude of the cracking load is contingent, first and foremost, upon the tensile strength of the steel fibre reinforced fine aggregate concrete matrix. Comparing the average values obtained for plain concrete (F series beams) and steel fibre (50/0.8 mm) reinforced fine aggregate concrete (B series beams) tests one can see that they are practically identical. Lower values for steel fibre (30/0.55 mm) reinforced fine aggregate concrete are caused by respectively lower tensile strength. Also influence of the compressed reinforcement (comparison between A and D series beams) on the cracking moment value has not

been observed; this confirms the earlier observations that cracking moment's value is mostly contingent upon the matrix tensile strength. Very good compatibility of the experimentally fixed cracking moment values (determined through observation of beam lateral surfaces) with the values calculated for the plain concrete through application of EC 2 [18] has been achieved for all tested elements. The mean error did not exceed 6 % at the standard deviation of 8.6 %. The greatest divergence has been obtained for C-2 beam (25.9 %), for which very low value of the cracking moment (as for steel fibre (50/0.8 mm) reinforced fine aggregate concrete) was obtained; this was caused, most probably, by non-uniform distribution of the fibres or local cross-section weakening. Much bigger differences were obtained from comparison of the experimentally fixed moment values with those obtained by application of PN-84/B-03264 [19] and the methods proposed by Tan, Paramasivam and Tan [11] as well as Lok and Xiao [14], therefore, when the above methods are used, one should remember about the inflated values of the calculated cracking moments (for steel fibre reinforced fine aggregate concrete beams).

Table 3. Tested beam cracking moments' analysis

Beam marking	Experimentally fixed moment M_{rys}	Moment calculated from				$\frac{M_{rys} - M_{cr}}{M_{rys}}$	$\frac{M_{rys} - M_L}{M_{rys}}$	$\frac{M_{rys} - M_{fp}}{M_{rys}}$	$\frac{M_{rys} - M_T}{M_{rys}}$
		[18]	[14]	[19]	[11]				
		M_{cr}	M_L	M_{fp}	M_T	[%]	[%]	[%]	[%]
A-1	3.6	3.3	4.7	5.3	4.5	8.3	-30.6	-47.2	-25.0
A-2	3.2					-3.1	-46.9	-65.6	-40.6
B-1	3.8	3.6	5.1	6.3	4.7	5.3	-34.2	-65.8	-23.7
B-2	3.6					0.0	-41.7	-75.0	-30.6
C-1	3.6	3.4	4.9	6.2	4.6	5.6	-36.1	-72.2	-27.8
C-2	2.7					-25.9	-81.5	-129.6	-70.4
D-1	3.4	3.5	5.0	5.6	4.5	-2.9	-47.1	-64.7	-32.4
D-2	3.6					2.8	-38.9	-55.6	-25.0
F-1	3.5	3.8	—	6.8	—	-8.6	—	-94.3	—
F-2	3.7					-2.7		-83.8	
G-1	3.6	3.6	5.1	7.5	4.8	0.0	-41.7	-108.3	-33.3
G-2	3.5					-2.9	-45.7	-114.3	-37.1
H-1	2.6	2.7	3.9	5.9	4.0	-3.8	-50.0	-126.9	-53.8
H-2	2.4					-12.5	-62.5	-145.8	-66.7
I-1	2.5	2.7	3.8	5.4	4.1	-8.0	-52.0	-116.0	-64.0
I-2	2.5					-8.0	-52.0	-116.0	-64.0
J-1	2.6	2.9	4.1	5.5	4.1	-11.5	-57.7	-111.5	-57.7
J-2	2.4					-20.8	-70.8	-129.2	-70.8
K-1	2.6	2.9	4.2	4.9	4.1	-11.5	-61.6	-88.5	-57.7
K-2	2.6					-11.5	-61.6	-88.5	-57.7
Mean error [%]						-5.6	-50.7	-94.9	-46.6
Standard deviation [%]						8.6	13.3	28.4	17.4

4. CONCLUSIONS

The plain (commercial) concrete with declared C35/45 compressive strength class used in the test featured higher strength properties compared with two applied steel fibre reinforced fine aggregate concrete mixtures. Nonetheless, the cracking moments in beams made of steel fibre reinforced fine aggregate concrete containing 50/0.8 mm fibres and beams made of plain concrete were comparable; this indicates that the steel fibre reinforced fine aggregate concrete is less brittle compared with plain concrete.

Small diversity in the cracking moment values has been observed for the steel fibre reinforced fine aggregate concrete beams (with single type fibres) due to practically imperceptible influence of the longitudinal reinforcement ratio (0.6 %, 0.9 %, 1.3 % and 1.8 %). This proves that the magnitude of the cracking load is contingent, first and foremost, upon the tensile strength of the steel fibre reinforced fine aggregate concrete matrix.

The cracking moments calculated as per [14] and [11] (as for the steel fibre reinforced concrete elements) are considerably inflated compared with the test values. This is probably caused by the fact that the applied fine aggregate concrete matrix differs in properties from plain concrete.

The calculated cracking moments for steel fibre reinforced fine aggregate concrete beams can be determined based on Eurocode 2 [18] (as for the elements made of plain concrete), however, it should be remembered that the cracking moment values calculated that way are slightly higher than those obtained from tests.

The fine aggregate (waste sand) used in the study, being the aggregate hydroclassification waste, makes a perfect component of the fine aggregate concrete mixture with addition of steel fibres. Therefore, the proposed steel fibre reinforced fine aggregate concrete mixtures (based on waste sand) can make an alternative to the commonly used plain concrete.

5. REFERENCES

- [1] ASTM C 1018 "Standard test method for flexural toughness and first-crack strength of fibre-reinforced concrete (using beam with third-point loading)"
- [2] Rilem TC 162-TDF, "Test and design methods for steel fibre reinforced concrete: Bending test. Final Recommendation", Materials and Structures, November 2002, pp. 579-582
- [3] Rilem TC 162-TDF, "Test and design methods for steel fibre reinforced concrete: σ - ε Design method. Recommendations", Materials and Structures, March 2000, pp. 75-81
- [4] Balaguru P., Narahari R., Patel M.; "Flexural Toughness of Steel Fibre Reinforced Concrete", ACI Materials Journal November-December 1992, pp. 541-546
- [5] Chen L., Mindess S., Morgan D. R.; "Specimen geometry and toughness of steel-fibre-reinforced concrete", Journal of Materials in Civil Engineering, November 1994, pp. 529-541
- [6] Gopalaratnam V. S., Gettu R.; "On the characteristic of flexural toughness in fibre reinforced concretes", Cement and Concrete Composites, 1995, pp. 239-254
- [7] Johnson C.D., Skarendahl A.; "Comparative flexural performance evaluation of steel fibre-reinforced concretes according to ASTM C1018 shows importance of fibre parameters", Materials and Structures, 1992, pp. 191-200
- [8] Nataraja M. C., Dhang N., Gupta A. P.; "Toughness characterization of steel fibre-reinforced concrete by JSCE approach", Cement and Concrete Research, April 2000, pp. 593-597
- [9] Domski J.; „Load carrying capacity, deflection and cracking of fine aggregate concrete beams containing steel fibres under short time load”, PhD thesis, Koszalin 2005 (in Polish)
- [10] Piątek Z., Domski J., Staszak I.; „Cracking of beams with fine aggregate concrete with steel fibres”, L Conference N-T KILiW PAN i KN PZITB "Krynica 2004", 2004, vol 3, pp. 75-84 (in Polish)
- [11] Tan K.-H., Paramsivam P., Tan K.-C.; "Instantaneous and long-term deflections of steel fibre reinforced concrete beams", ACI Structural Journal, July-August 1994, pp. 384-393
- [12] Swamy R. N., Mangat P. S.; "A theory for the flexural strength of steel fibre reinforced concrete", Cement and Concrete Research, 1974, pp. 313-325
- [13] ACI 544.4R-88 (Reapproved 1994) „Design considerations for steel fibre reinforced concrete"
- [14] Lok T. S., Xiao J. R.; "Flexural strength assessment of steel fibre reinforced concrete", ASCE Journal of Materials in Civil Engineering, August 1999, pp. 188- 196
- [15] Katzer J.; "Employment of waste sand to compose fibre reinforced cement composites", Proceedings, Sustainable Construction Materials and Technologies, 11-13 June, 2007, Coventry, UK, pp. 91-99
- [16] Katzer, J., Kobaka J.; "Analysis of harnessing waste fine aggregate for sustainable production of concrete elements", Journal of Civil Engineering and Architecture, 2010 vol. 4, no. 7, pp. 42-58.
- [17] ACI 544.3R-93 (Reapproved 1998) „Guide for specifying, proportioning, mixing, placing and finishing steel fibre reinforced concrete"
- [18] Eurocode 2 (EN 1992-1-1:2004+AC: 2008): Design of concrete structures - Part 1: General rules and rules for buildings
- [19] PN-84/B-03264 „Polish Standard for plain, reinforced and prestressed concrete structures" Warsaw 1984, (in Polish)

Impact of the Grain-Size Distribution of the Fine Aggregate Cement Composites on the Rebound Hammer Test

Jacek Katzer

Abstract – The paper presents a research study of cement composites based on the fine aggregate. There were used 38 fine aggregates of glacial origin characterised by different grading curves. The natural fine aggregate was divided into 3 groups of fractions. Each of them contained particles of a diameter between specific limits. Such an approach enabled the author to use a mixture experimental design based on triangular surfaces. Cement composites made of these aggregates were then tested by a rebound hammer test. After establishing the rebound number, compressive strength of analysed composites was tested. On the basis of achieved results it was possible to draw contour plots depicting the relation between grading of fine aggregate and a rebound number. The main subject was to define the usability of the rebound hammer test in non-destructive quality control testing of fine aggregate cement composites.

Keywords –cement composite, concrete, fine aggregate, mortars, NDT, rebound hammer test.

1. INTRODUCTION

The strength of cement composite elements in existing buildings is often evaluated with the help of non-destructive testing (NDT). Using the NDT methods it is possible to quickly determine the mechanical properties of a building without damaging its structure, which is particularly important when the building is in a bad technical state or even at risk of collapse [8]. The most commonly used non-destructive method allowing the assessment of the strength of concrete (and other cement-based composites) was developed in 1948 by Ernest Schmidt [10]. This method employs the hammer, which measures the rebound of a spring-loaded mass, impacting against the surface of the specimen. The results are expressed with the help of arbitrary scale ranging from 10 to 100 (the so-called rebound height “L”). This method of testing is classed as indirect as it does not give a direct measurement of the strength of the material. It simply gives an indication based on surface properties and it is only suitable for making comparisons between concrete specimens and the real concrete structure. There are some calibration diagrams provided by hammer manufacturers. Different national codes and instructions [7] suggest other diagrams. Because the stiffness of cement composite is influenced by the type of aggregate used, harnessing “global” diagrams relating the hardness number and strength is inadvisable [10]. The most accurate procedure is to establish the relation between the rebound number measured on specimens and their actual strength experimentally.

The non-destructive methods have a number of imperfections that affect the accuracy and reliability of the achieved results. In case of using the rebound hammer, the biggest problems with assessing the strength is related to local variability of the analysed cement composite surface, the execution of the test and the impact of environment that could weaken or harden the analysed material surface [1]. If it is impossible to calibrate the

Manuscript received October 1st, 2011 and accepted November 10, 2011.

Jacek Katzer Author is with Koszalin University of Technology, Department of Civil Environmental Engineering, ul. Sniadeckich 2, 75-453 Koszalin, Poland (e-mail: jacek.katzer@tu.koszalin.pl).

hammer on cast specimens in situ, the granular composition of aggregate used to prepare the cement composite may become an important factor causing significant divergence of achieved results.

2. EXPERIMENT DESCRIPTION

The main aim of the research program was to determine the influence of the fine aggregate composition on the rebound hammer test results of cement composites. There were considered only cement composites based on natural fine aggregate available in Pomerania region in Poland. These aggregates and cement composites based on them were thoroughly described in numerous previous publications [4]- [6].

In order to generate a mathematical experimental design that would reflect grading of all fine aggregates possible to employ, the whole aggregate was divided into three fraction groups (x_1 from 0 to 0.5mm; x_2 from 0.5 to 2mm and $x_3 > 2$ mm, with the note that the biggest grains were < 8 mm), whose sum always equals 100%. Due to this simple procedure it was possible to apply an integral simplex design also called 'a mixture design' [2]. This design was described in detail in Table 1 and spacing of measuring points was shown in Figure 1. The object of the experiment was considered as a complex material whose structure is unknown and unavailable for an observer. Still the 'input' and 'output' parameters are known, [11]. The examination results were statistically processed and values bearing the gross error were assessed on the basis of Smirnow-Grabbs criterion. The objectivity of the carried out experiments was assured by choosing the sequence of the realization of specific experiments from table of random numbers.

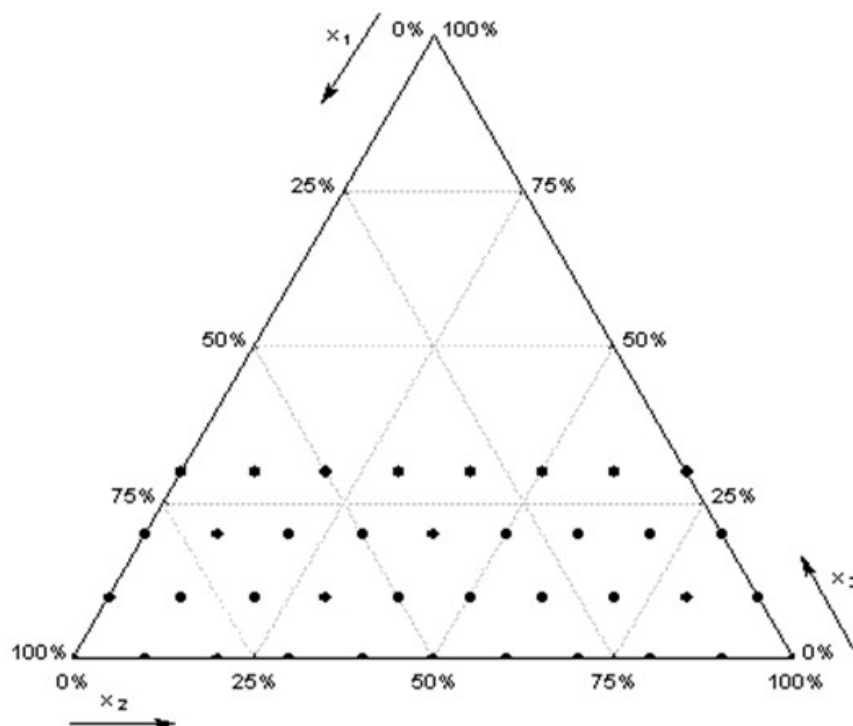


Fig. 1 Scheme of testing points spacing

All calculations connected with specifying and graphic interpretation of the received mathematic model were carried out with the help of Statistica 8.0 computer programme [3]. Contour plots were achieved by using polynomial fit.

Table 1. Mix proportions

N°	Aggregate Mixture	Aggregate Fractions (kg/m ³)			Cement (kg/m ³)	Water (kg/m ³)
		0-0.5	0.5-2.0	2.0-4.0		
1	0/100/0	0	1570	0	358	189
2	10/90/0	157	1417	0	397	209
3	20/80/0	309	1235	0	394	207
4	30/70/0	480	1121	0	384	202
5	40/60/0	614	921	0	422	222
6	50/50/0	755	755	0	429	226
7	60/40/0	878	585	0	452	238
8	70/30/0	1007	432	0	488	257
9	80/20/0	1107	277	0	487	256
10	90/10/0	1225	136	0	478	251
11	100/0/0	1362	0	0	492	259
12	0/90/10	0	1480	164	380	200
13	10/80/10	163	1303	163	360	190
14	20/70/10	319	1118	160	398	210
15	30/60/10	479	958	160	405	213
16	40/50/10	617	771	154	419	221
17	50/40/10	751	601	150	403	212
18	60/30/10	850	425	142	474	249
19	70/20/10	1025	293	146	418	220
20	80/10/10	1141	143	143	472	248
21	90/0/10	1279	0	142	457	241
22	0/80/20	0	1285	321	370	194
23	10/70/20	167	1167	333	350	184
24	20/60/20	331	996	331	375	198
25	30/50/20	512	853	341	376	198
26	40/40/20	628	628	314	429	226
27	50/30/20	810	491	327	410	216
28	60/20/20	904	302	302	439	231
29	70/10/20	1065	152	304	425	224
30	80/0/20	1226	0	306	420	221
31	0/70/30	0	1209	518	354	186
32	10/60/30	168	1008	504	346	182
33	20/50/30	344	860	516	341	180
34	30/40/30	522	696	522	343	181
35	40/30/30	670	502	502	379	200
36	50/20/30	817	327	490	378	199
37	60/10/30	948	158	474	403	212
38	70/0/30	1084	0	465	431	227

Fitted functions are characterized by correlation coefficient equal to at least 0.90. The experimental design described above covers completely the grading field of all the fine aggregates. There were planned 38 different aggregates to be used during the tests. The aggregates were prepared individually according to the planned percentages of different groups of fractions.

For each aggregate composition 4 specimens were cast. In total 152 cube specimens 15x15x15 cm were analysed. Cement composites were prepared on the basis of CEM I 32.5 and water/cement ration was equal to

0.53 for all mixes. To ensure consistency of results, no additives or admixtures were added. The consistency of the fresh cement composites mixes determined with the help of the Vebe test was equal to $8s \pm 1s$. Proportions of all cast mixes are presented in Table 1.

A rotary drum mixer was used to prepare composite mixtures. Compaction of fresh concrete mix was performed externally using a vibrating table. Each specimen was vibrated in two layers, with each layer filling half of the thickness. Each layer was vibrated for 20 s (until a thin film of bleed water appeared on the surface). The first step of curing was to keep the specimens in their moulds covered with polyethylene sheets for 24h. The specimens were then removed from their moulds and cured by storing them in temperature of $+20^{\circ}\text{C}$ and relative humidity of 60% for 27 days.

The rebound hammer test was performed on specimens subjected to compressive stress of 2 MPa. Original Schmidt hammer type N, characterized by impact energy equal to 2.207 Nm was harnessed. On each specimen 12 measurements were conducted - 6 measurements on two opposite faces of the specimen (orthogonal to the casting direction). The rebound hammer test was followed by testing ultimate compressive strength of a specimen.

3. ANALYSIS OF THE RESEARCH RESULTS

Average rebound height "L" in a form of a contour graph is presented in Figure 2. The relation between fine aggregate composition and average rebound height "L" shown in Figure 2 is described by the following equation.

$$L = 15.05x_1 + 16.56x_2 + 2.02x_3 + 12.48x_1x_2 + 36.14x_1x_3 + 57.83x_2x_3 \quad (1)$$

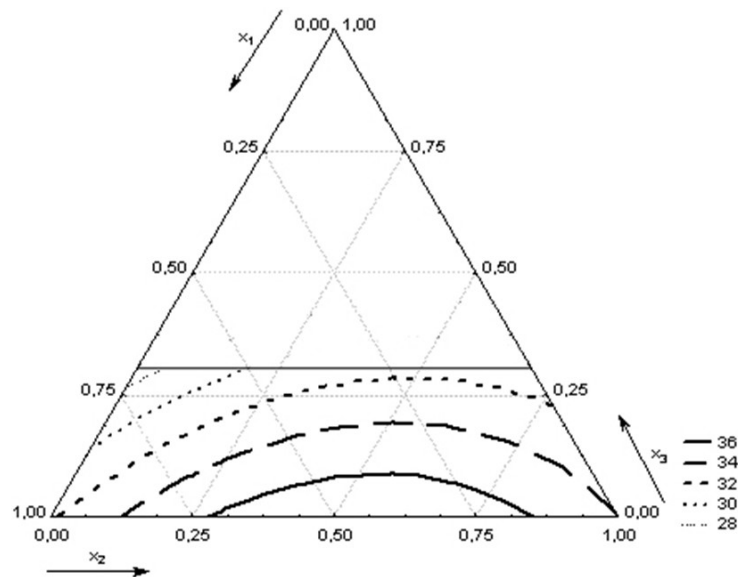


Fig. 2 Average rebound height "L"

The relation shown in Figure 2 allows determining the scope of the optimal aggregate composition, characterized by the highest values of the rebound height. In this field should also appear composites characterized by the highest values of compressive strength. Limits of the optimal field can be defined as: for the group of fractions x_1 , from 40% to 50%, for the group of fractions x_2 , from 40% to 60%, and for the group of fractions x_3 , from 0% to 10%.

The standard deviation of the average height of the rebound hammer test is presented in Figure 3. The relation between fine aggregate composition and standard deviation of rebound height "L" shown in Figure 3 is described by the following equation:

$$S_L = 1.89x_1 + 1.01x_2 - 2.21x_3 - 2.91x_1x_2 + 3.37x_1x_3 + 6.55x_2x_3 \quad (2)$$

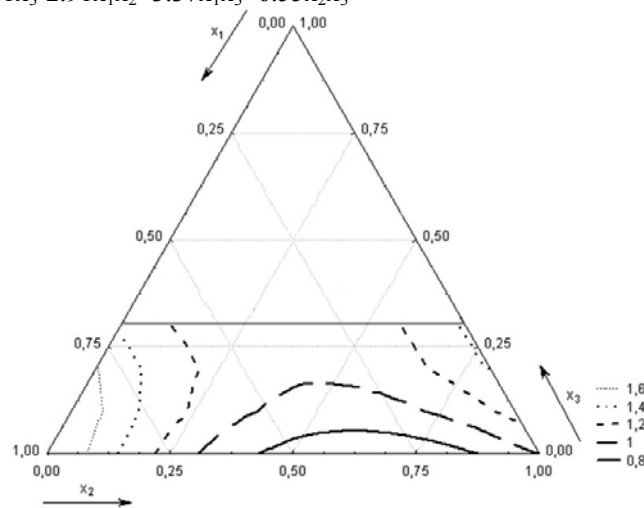


Fig. 3 Standard deviation of the rebound height “L”

The area corresponding to the lowest values of standard deviation covers the area of aggregate mixtures determined as the most optimal for the rebound height “L”. The highest values of the standard deviation (exceeding 1.2) are located in the right and left part of the diagram. The right part of the diagram represents aggregate mixtures where percentage of the group of fractions x_1 varies from 0% to 20%, the group of fractions x_2 varies from 60% to 70% and the group of fractions x_3 varies 15% to 30%. The left part of the diagram represents the aggregate mixtures where percentage of the group of fractions x_1 varies from 60% to 100%, the group of fractions x_2 varies from 0% to 20% and the group of fractions x_3 varies from 0% to 30%.

The ultimate compressive strength of analysed cement composites is presented in the Figure 3. The relation between fine aggregate composition and ultimate compressive strength shown in Figure 4 is described by the following equation:

$$f_{c,cube} = 15.05x_1 + 16.56x_2 + 2.02x_3 + 12.48x_1x_2 + 36.15x_1x_3 + 57.83x_2x_3 \quad (3)$$

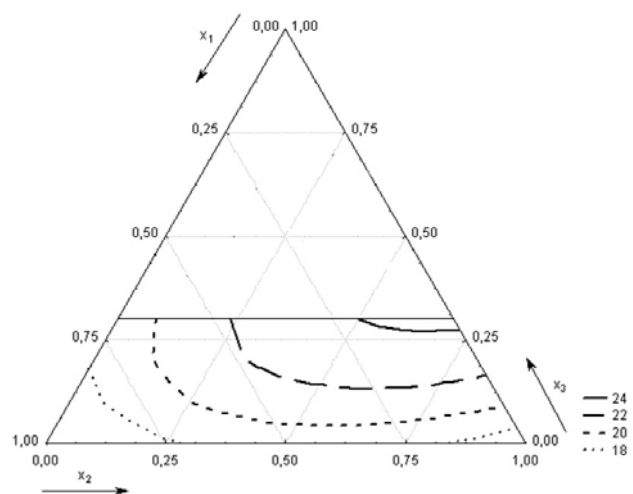


Fig. 4 Ultimate compressive strength $f_{c,cube}$ [MPa]

The compressive strength $f_{c,cube}$ ranged from 18 to 24 MPa depending on the composition of the aggregate used. Composites characterized by the highest compressive strength are those based on to the aggregate where the percentage of fractions x_1 varies from 0% to 20%, the percentage of fractions x_2 varies from 60% to 70% and the percentage of fractions x_3 varies from 15 % to 30%.

4. CONCLUSIONS

Rebound hammer test is sensitive to local variations in the cement composite internal structure, e.g. the presence of a large piece of aggregate immediately underneath the plunger would result in an abnormally high rebound number; conversely, the presence of a void in a similar position would lead to a low result. It must be also remembered that the rebound hammer test measures the properties of only the surface zone of concrete, the depth of this zone is about 30mm. In case of tested cement composites these limitations of rebound hammer method are not very important because of the specific character of the fine aggregate cement matrix. There are no large aggregate grains that could influence the hammer reading when located under the plunger or a void of relatively large diameter.

It has also been shown that the majority of area of optimal grain-size distribution determined during the compressive test is also characterized by the lowest standard deviation of the rebound height "L".

6. REFERENCES

- [1] Amasaki S., "Estimation of strength of concrete in structures by rebound hammer", CAJ Proceedings of Cement and Concrete, N° 45, 1991
- [2] Bayramov, F. et al., "Optimalisation of steel fibre reinforced concretes by means of statistical response surface method". Cement & Concrete Composites, 26/04: 665-675
- [3] Borovikov, I.P. & Borovikov, V.P., "STATISTICA: Data Preparation and Analysis". Filini, Moscow 1998, Russia
- [4] Katzer J., Kobaka J., "The assessment of fine aggregate pit deposits for concrete production", Kuwait Journal of Science & Engineering, Vol. 33, Issue 2, 2006
- [5] Katzer J., Kobaka, J., "Influence of Fine Aggregate Grading on Properties of Cement Composite", Silicates Industriels, Vol. 74, No.1-2/2009, 9-14
- [6] Katzer, J., "Properties of Precast SFRCC Beams Under Harmonic Load", Science and Engineering of Composite Materials, Vol.15, No.2, 2008, 107-120
- [7] Komlos, K., et al., 1996. "Ultrasonic Pulse velocity Test of Concrete Properties as Specified in Various Standards", Cement and Concrete Composites, 18 (1996), 357-364
- [8] Kujawiński K., Pietraszak P., "Complex use of ultrasonic and sclerometric methods for evaluation of concrete strength in construction in the aspect of technical investigations", Nondestructive Testing in Civil Engineering, Warszawa-Jadwisin, Poland, p. 173, 1981
- [9] J. Jones. (1991, May 10). Networks (2nd ed.) [Online]. Available: Mann, H.B., "Analysis and design of experiments", Dover Publications, New York 1950, NY, USA
- [10] Neville A.M., "Properties of concrete", England, Longman, 1997
- [11] Schenk, H., "Theories of Engineering Experimentation", Hemisphere Publishing Co. 1979, USA.

The Response of Maritime Structures with Vertical Walls at Braking Wave Forces in Terms of Duration of the Impact

Mirela Popa, Gabriela Drăghici, Cosmin Filip

Abstract –Usually for design and verification of maritime structures, the effects of forces generated by waves are obtained by static calculation, even for these actions is clearly evident the time variation. This because of the large difference between waves period and natural period of maritime structure and it is expressed by a dynamic amplification factor less than or close to 1. Recent researches have shown that, under certain conditions, the impact waves on maritime structures generate high intensity pressures that vary quickly in time. In such cases it requires a dynamic analysis. The dynamic analysis, unlike static analysis in which the wave action is described only by its maximum value, requires the loading history's definition. The loading history can be approximated like a triangular time-history described by three quantities: the maximum amount of impact force, rise time and total duration. The structural response to the dynamic action depends not only from the external forces but also its dynamic characteristics, like its natural periods. For this reason care have been given to how you can obtain a discrete model as simple and which takes into account the special boundary conditions, using type SPRING finite element. In this way the natural periods can be obtained quickly, using FREQUENCY modules implemented in finite element programs. From the modal time history analysis revealed a significant increase in the response obtained from the dynamic analysis to those obtained by static analysis, which is expressed by high levels of the dynamic amplification factor. This paper presents the results from a study of the structural response (the form of top displacement) in order to determine the dynamic amplification factor and it depend of the rise time (t_r) and the total duration (t_d) of shock. Also, through response spectra, we studied how the maximum displacement response values vary depending on the natural period and on the time characteristics of shock, for the constant value of the maximum force.

Keywords – dynamic amplification factor, equivalent static force, response spectra, response time history, rise time, total duration, triangular shock.

1. INTRODUCTION

For maritime structure the main load to which they are exposed is the horizontal force given by the waves. Especially for the structures or the structural elements with vertical walls, the breaking is a dangerous phenomenon. Usually, for design and verification of maritime structures, the static analysis is made because between the waves period and natural period of structure is a big difference. Typically, for these analyses, the wave's forces are evaluated using by Sainflou or Goda relationships.

If conditions are all right for breaking waves, especially for structures with vertical walls, the wave forces reach very high values in a very short time.

Manuscript received October 1st, 2011 and accepted November 10, 2011.

M. Popa is with Ovidius University of Constanta, Bd. Mamaia nr. 124, 900356-Constanta, Romania (corresponding author to provide e-mail: mpopa@univ-ovidius.ro).

C. Draghici is with Ovidius University of Constanta, Bd. Mamaia nr. 124, 900356-Constanta, Romania

C. Filip is with Ovidius University of Constanta, Bd. Mamaia nr. 124, 900356-Constanta, Romania

Many studies concentrate on the developing methods to estimate the wave pressures caused by breaking in front of the vertical walls; a lot of them are often accompanied by experimental studies. A review of these is made in [3].

When waves break close to forming a vertical front just before contact with the wall and are contained only a negligible amount of air will result a high pressure intensity and short duration. Time history of load shows a single peak, followed by very small oscillations, as is revealed by the results of large-scale models [5]. This load history of forces can be approximated with a triangular time-history. Based on the load history it could easily define a time curve for finite element analysis.

On the other side, as it is known from the theory, the structural response to the dynamic actions depends not only by external forces but also its dynamic characteristics, like its natural periods. Dynamic analyses with finite element are very laborious and therefore it is fine to start analysis by comparing the total duration shock with the significant natural periods. Therefore, the first part of paper shows how we have obtained these dynamic characteristics.

Further on, the paper shows how time characteristics of the shock influence the structural response. Results that will be presented in the paper show that the simple static analysis would lead to the underestimated displacement values than those obtained from dynamic analysis, which justifies the assessment of dynamic amplification factor. The paper shows how the dynamic amplification factor for a constant value of maximum force depends by the total duration of shock and its shape.

To assess the maximum displacements, according to its dynamic characteristics of structures, the authors propose the use of response spectra. Therefore the authors have constructed families of spectra of response, depending on the characteristics of shock.

2. THE REPLACING OF THE RIGID CONNECTION WITH THE ELASTIC CONNECTION

Breaking is a dangerous phenomenon for vertical front structures as they are caisson type breakwaters and walls of concrete caps in extreme cases when the run up reaches the superstructures of rubble-mound structures.

The considering of a rigid connection between the concrete structure and rubble-mound would introduce significant errors of to the real situation and lead to lower values of their natural periods.

Therefore numerical modelling of such structures requires to meshing the rubble-mound or introducing boundary conditions that reproduce the elastic connection between the vertical element and the rockfill or rubble-mound.

From this observation has resulted an objective of the study, namely the identification of an efficiency method for numerical modelling the contact between the vertical element and rubble - mound.

Introducing the SPRING type finite element at the contact between the vertical wall and rubble-mound solved this problem.

SPRING is a 2-node uniaxial element for structural models. Two degrees of freedom (one translation and one rotation) are considered for each node in the element local coordinate system. The element has the capability to perform as a longitudinal and/or torsional spring in one-, two-, or three-dimensional applications. The study has consisted of two-dimensional analyses that consider only the longitudinal spring.

For the analysis performed it was chosen to make the modelling of a structure that is known both of geometric and material characteristics, and values of loads waves. In paper [6] are presented records of horizontal forces and movements for a small-scale model developed at the University of Hanover for the study of the relationship between wave-induced loads and dynamic response of caissons. Tests were conducted in a channel with a length of 110m, width of 2.2 m and a depth of 2 m. Structural model used for the analysis was based on this model.

For caisson's modelling were used four sets of materials, proper concrete and granular material in submerged state and emerged state (see Fig. 3).

For the elastic connection, axial spring stiffness was associated with the longitudinal elasticity modulus of the rubble-mound materials. We considered two granular materials, characterized by the longitudinal elasticity modulus 90000 kPa and 50000 kPa. Comparative results (as the horizontal top displacement from 44 node and

first natural period) are presented for these two cases and the case rigid connection. The mesh for cross section with elastic connection it is shown in Fig. 4.

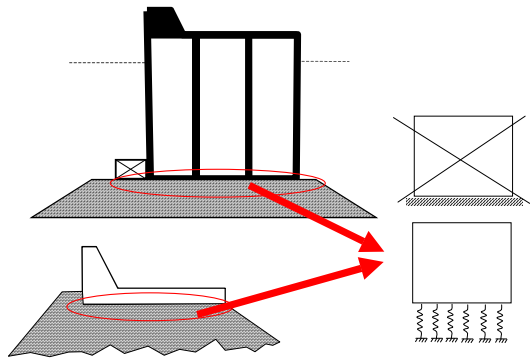


Fig. 1 Modelling contact with rubble-mound

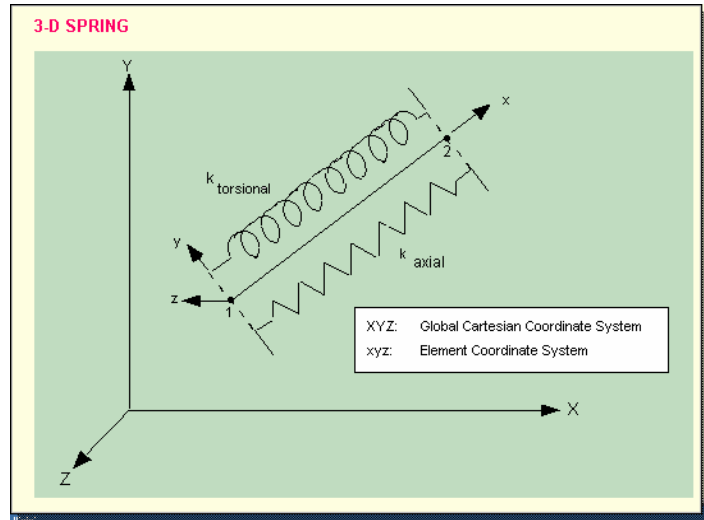


Fig.2 The SPRING type finite element used in COMSOS/M software

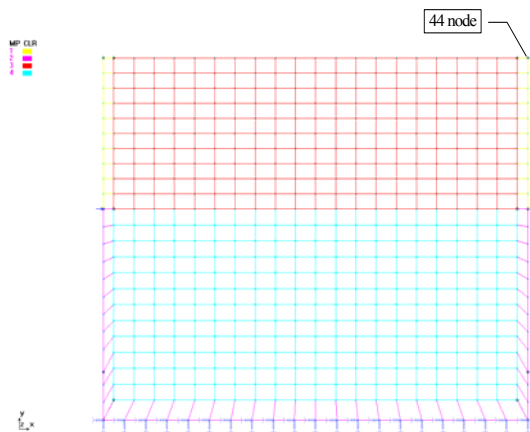


Fig. 3 PLANE2D mesh with four sets of different material characteristics and rigid connection with rubble-mound

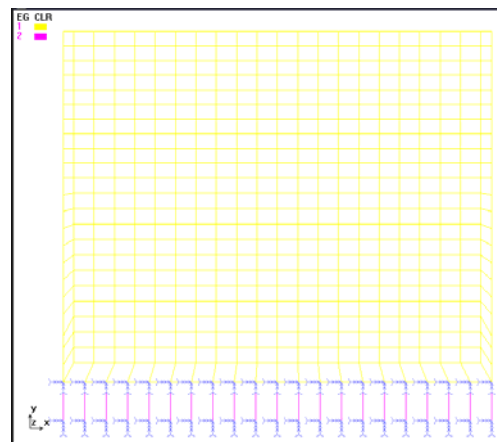


Fig. 4 Mesh with two type finite element: PLANE2D and SPRING with axial stiffness

Table 1. Comparison of results, depending on the modelling of contact with rubble-mound

Structural model	T_1 (ms)	Horizontal top displacement u_{st} (mm)
Rigid connection	27.0	0.107
Elastic connection SPRING – axial stiffness $k_{axial}=90000$ kN/m	29.6	0.130
Elastic connection SPRING – axial stiffness $k_{axial}=50000$ kN/m	31.0	0.145

For subsequent dynamic analysis, the contact between the wall and rubble-mound was modelled using SPRING finite elements with $k_{axial} = 90000$ kN/m.

3. BREAKING WAVE FORCE'S APPROXIMATE BY TRIANGULAR SHOCKS

In paper [8], based on investigation carried out of several large-scale models of structures with vertical walls, for the magnitude of impact horizontal forces is proposed the following relationship:

$$F_{h,max} = 15 \rho g d^2 \left(\frac{H_s}{d} \right)^{3.134} \quad (1)$$

Starting from the theory of solitary waves was deduced relationships between the maximum relative forces of impact, rise time t_r and total duration t_d .

$$F'_{h,max} = \frac{F_{h,max}}{\rho g H_b^2} \quad t_r = k \cdot 8.94 \sqrt{\frac{d_{eff}}{g}} \quad t_d = t_r \left(2 + 8e^{-18 \frac{t_r}{T_p}} \right) \quad (2)$$

where H_s – the significant wave height; d – the water depth d_{eff} – can be assumed to be identically to the breaking depth, T_p - the peak wave's period.

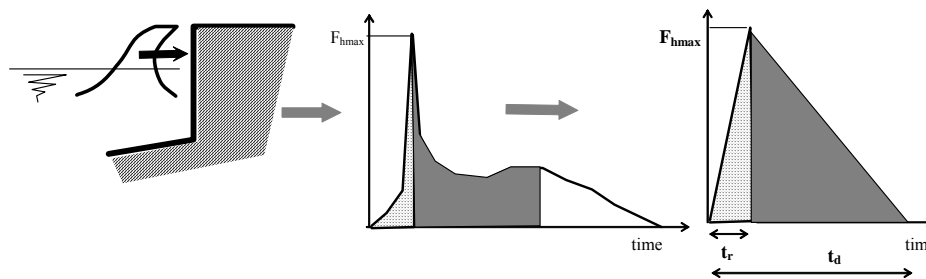


Fig. 5 The replacement of impact load history by a triangular load

As is known, the response structure at this type of actions it is depend on the ratio of pulse duration and natural period. Moreover, for structures approximated as systems with one dynamic degree of freedom, if total duration (t_d) is greater than half of natural period ($T/2$) also loading speed is important, meaning the time when the force reaches its maximum values (t_r).

Based on this observation, this paper has been going to highlight how ratio t_r/T_1 and t_d/T_1 affects the response time history, the dynamic amplification factor and the response spectra. For this purpose dynamic analyses were performed that were considered different values of rise time (t_r) and total duration (t_d).

4. THE VARIATION OF DYNAMIC AMPLIFICATION FACTOR DEPENDING ON THE RISE TIME AND TOTAL DURATION

For simplified structural model was obtained 29.6 ms for the first natural period of vibration and 0.13mm for the static horizontal top displacement in the 44 node. In static analysis wave loads are replaced with maximum value of force.

The dynamic analysis was done by modal time history, using COSMOS /M and a curve loads was required to introduce the time variation of the applied load.

The hydrodynamic force was schematized as a triangular shock described by $F_{h,max}$, t_r and t_d . We have

considered several values of the time t_r , $F_{hmax} = 8kN$ and $t_d=10 \cdot t_r$ (as a result of [1]).

The following graphs (Fig. 6 to Fig. 8) shows the response-time histories for top horizontal displacements for three forces that are different by t_r value and therefore by t_d value.

The results obtained by dynamic analysis shows that the maximum horizontal displacement is much higher than those provided by static analysis performed for the same amount of force F_{hmax} .

It shows that applying a static calculation, based on the replacement of wave loads with maximum values of impact force, leads to underestimated values of the displacement response for the breaking waves.

The static calculation might be replaced by the pseudostatic calculation, considering an equivalent static force that can be able to produce the same displacement of the structure as that obtained from a dynamic analysis. The value of this force can be obtained by multiplying the maximum force with a dynamic amplification factor.

$$\mu = \frac{\max(u_x)_{dynamic}}{u_x_{static}} = \frac{F_{ech}}{F_{hmax}} \Rightarrow F_{ech} = F_{hmax} \cdot \mu \tag{3}$$

In this paper were calculated the dynamic amplification factors for the five cases presented in the table below, as obtained from the ratio of the maximum displacement obtained for modal analysis and the displacement from a static analysis.

In Fig. 9 was graphically represented the dynamic amplification factor depending of the ratio between rise time t_r and fundamental period (T_1). This dependence has been studied, also, for another value of the fundamental period of vibration. For this purpose it was considered the same structural model that had the material properties changed (for this model to obtain the fundamental period 33.4 ms and a static horizontal top displacement of 0.17 mm)

In the next phase of the study was performed a dynamic analysis to show how the dynamic amplification factor varies depending on the total duration if rise time is constant ($t_r = 3ms$). We have considered two structural models again, distinguished by material characteristics. The results are summarized in Table III and represented in Fig. 10.

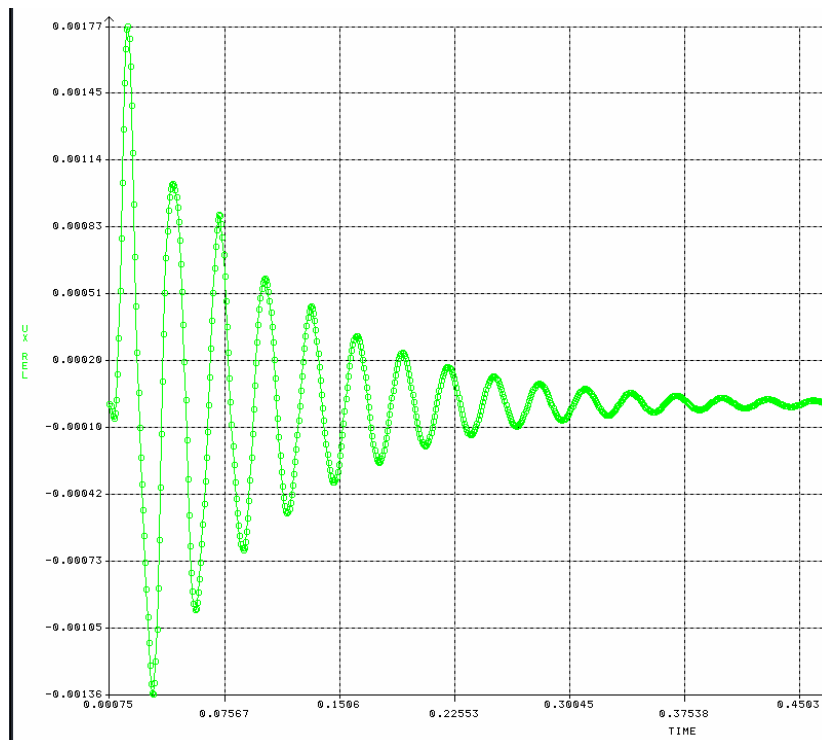


Fig. 6 Response time history for $t_r=1.5$ ms, $t_d=15ms$, $T_1=29.6ms$

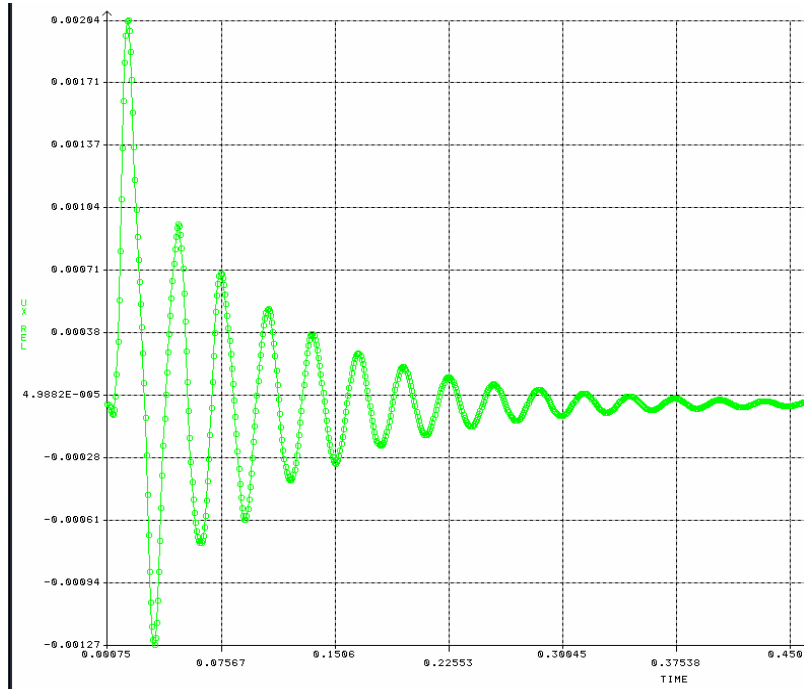


Fig. 7 Response time history for $t_r=3$ ms, $t_d=30$ ms, $T_1=29.6$ ms

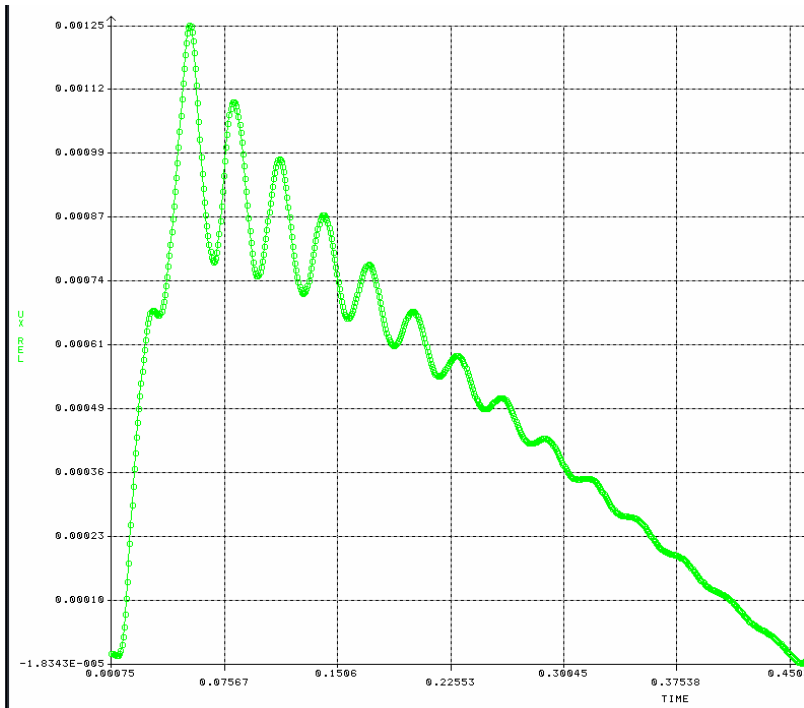


Fig. 8 Response time history for $t_r=15$ ms, $t_d=150$ ms, $T_1=29.6$ ms

Table 2. Dynamic amplification factors for two structural models in term of ratio t_r/T_1 for $t_d=10t_r$

$t_d=10t_r$						
$T_1=29.6ms, u_{st}=0.13mm$			$T_1=33.4ms, u_{st}=0.17mm$			
t_r (ms)	t_r/T_1	$u_{x_{max}}$ (mm)	μ	t_r/T_1	$u_{x_{max}}$ (mm)	μ
1.5	0.05	1.77	13.62	0.05	2.14	12.59
3	0.1	2.04	15.69	0.1	2.53	14.88
15	0.5	1.25	9.62	0.5	2.30	13.53
30	1	1.1	8.46	1	1.49	8.76
45	1.5	1.25	9.62	1.5	1.60	9.41

Table 3. Dynamic amplification factors for two structural models in term of ratio t_d/T_1 for $t_r=3ms$

$t_r=3ms$						
$T_1=33.4ms, u_{st}=0.17mm$			$T_1=29.26ms, u_{st}=0.12mm$			
t_d (ms)	t_d/T_1	$u_{x_{max}}$ (mm)	μ	t_d/T_1	$u_{x_{max}}$ (mm)	μ
7	0.21	1.45	8.53	0.24	1.23	10.25
15	0.45	2.19	12.88	0.51	1.77	14.75
35	1.05	2.57	15.12	1.20	2.03	16.92
70	2.10	2.74	16.12	2.39	2.13	17.75
300	8.98	2.85	16.76	10.25	2.20	18.33

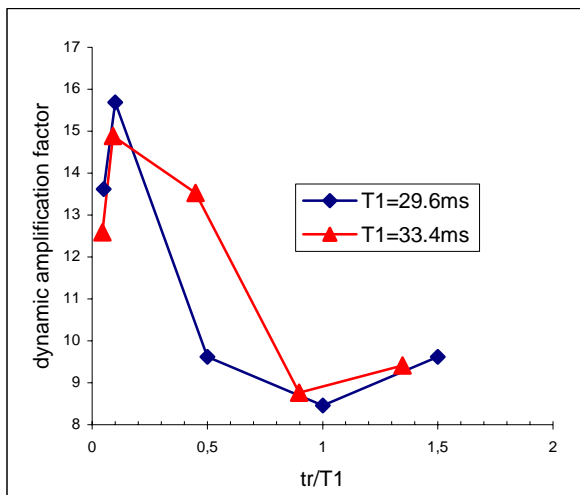


Fig. 9 The variation of dynamic amplification factor depending on the ratio t_r/T_1

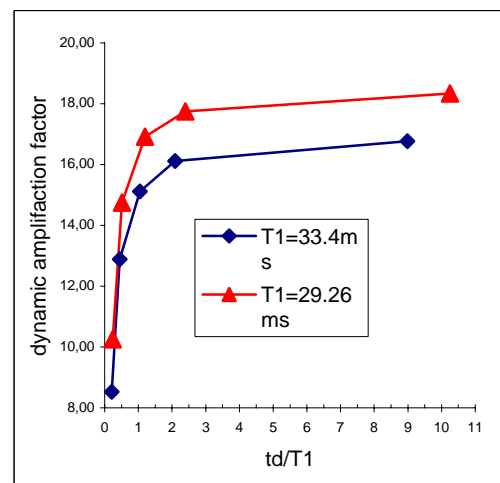


Fig. 10 The variation of dynamic amplification factor depending on the ratio t_d/T_1 for $t_r=3ms, F_{h_{max}}=8kN$

5. SPECTRA RESPONSE OF SHOCK TYPE ACTIONS

To determine the maximum amount of top displacement without doing modal analysis, the response spectra can be used, provided that the natural dynamic characteristics of the structure to be known.

Therefore, in this section will be presented spectra response of triangular shock actions used earlier.

To watch how they are or not affected by the two quantities that define the duration of shock, t_r and t_d , the individual spectra provided by the program COSMOS/ M have been processed and represented as families of spectra. All the spectra were calculated for a modal damping of 5%.

Spectra represented in Fig. 11 is obtained for a maximum value of force 8kN, and a total duration $t_d = 10t_r$. It is noted that for a $t_r < T/10$, respectively t_d near the natural period, its own maximum response displacement is about 6-7 times higher than the response of a structure for which T_1 has the same order with t_r .

We studied how the independent change of quantities t_r and t_d goes or not at changes in response spectra (Fig. 12 and Fig. 13). For studied range of circular frequency, corresponding to natural periods from 20ms to 1.3s, it resulted that simply modifying of the pulse shape by varying the quantity of t_r did not significantly alter the maximum response value, as seen in the family of spectra given in Fig. 12.

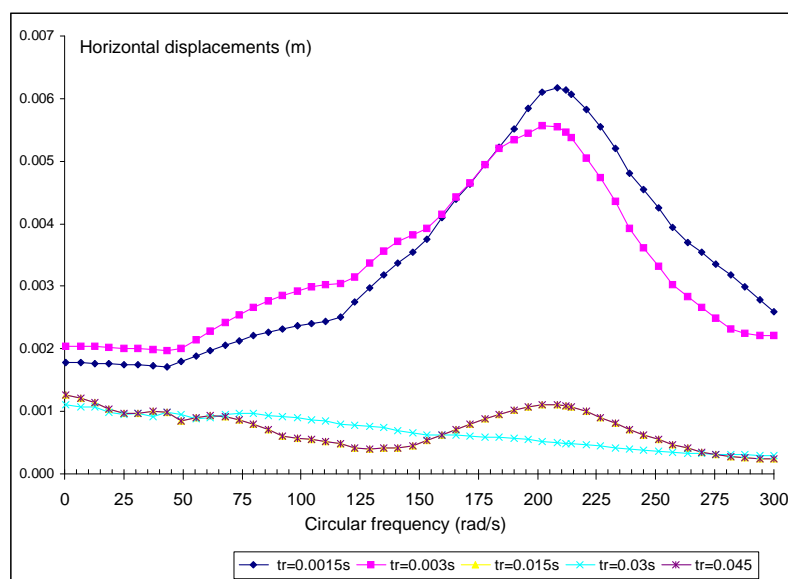


Fig. 11 Response spectra of horizontal displacement for hydrodynamic forces approximated by triangular shock with $F_{max}=8$ kN, $t_d=10t_r$

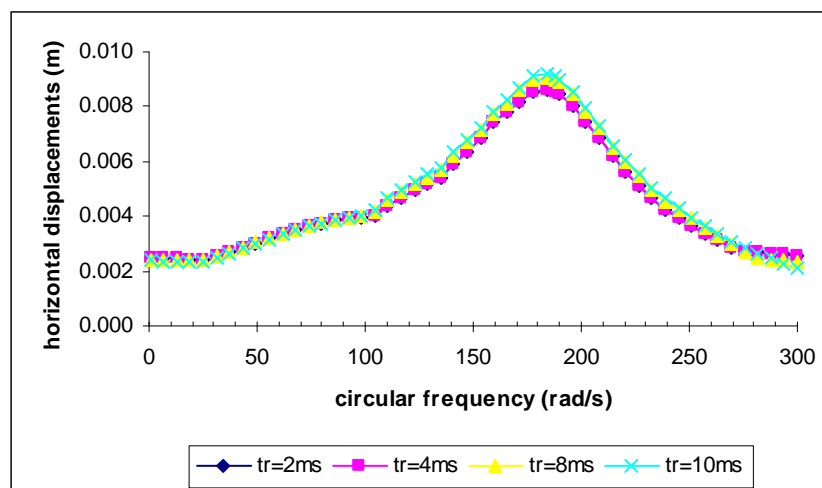


Fig. 12 Response spectra for same total duration shock, and various rise time, $F_{max}=8$ kN

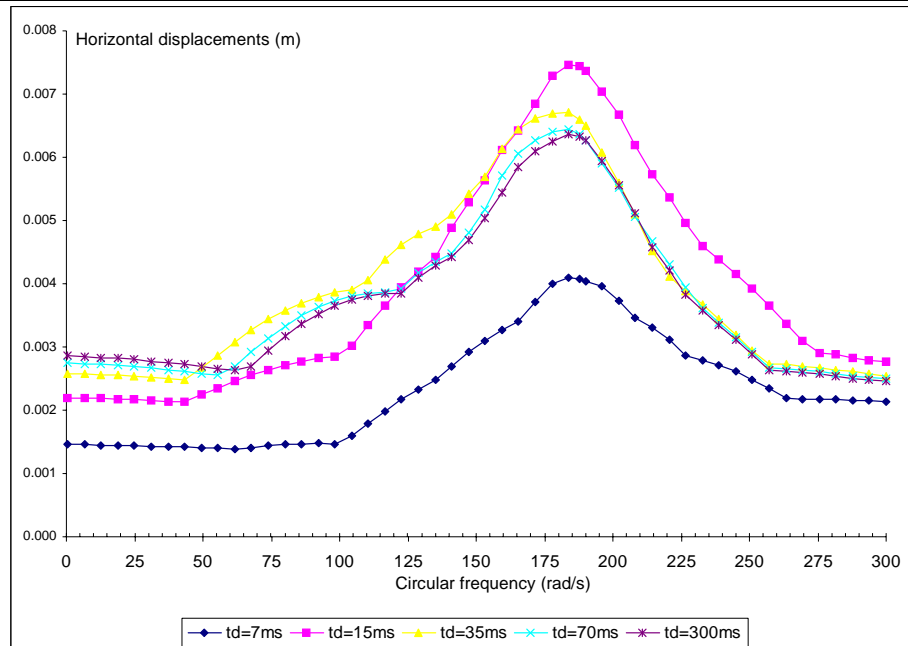


Fig. 13 Response spectra for same rise time, and various total duration, $F_{max}=8kN$

6. CONCLUSION

The study conducted on the impact action shows that treat these requests as dynamic actions lead to results significantly different from those obtained by static analysis. In applying these observations to more efficient and practical design in some simplifications are proposed:

- the using of some simple discrete models to determine of the significant natural periods;
- the using of the equivalent static forces, evaluating a dynamic amplification factor;
- the using of the response spectra to determine the maximum response, depending of the natural periods.

These observations lead to the belief that it would be useful to find a relationship of the dynamic amplification factor and values t_d , t_r , T_1 . Graphic definition of such relationships would allow the current practice of design to easily find an equivalent static force generated by a broken wave.

These kinds of graphics exist in the technical literature, but only for particular cases. Because of this, in the future, is intended the development of a graphics set, that are able to applied at the vertical structures from the Romanian ports.

Another direction of future research plans to build response spectra such as those in this work, for impact forces evaluated according to the sea state and the structural characteristics.

7. REFERENCES

- [1] Popa M., Filip C. – “*Ways to estimate broken waves forces on vertical structures*” in International Conference Water Across Time In Engineering Research, Ovidius University Annals of Constanta, Series Constructions, vol.12, Constantza, 2010, pp. 65-72 ISSN 1584 – 5990,

-
- [2] Popa M. – “*Broken wave forces on structures with vertical wall*” in Scientific Buletin of the POLITEHNICA, University of Timisoara, Romania, Transactions on Hydrotehnics, Tom 53(67), Fascicola 2, 2008, pp 79-86 ISSN 1224-6042
- [3] Giovanni Cuomo, William Allsop, Tom Bruce, Jonathan Person – “*Breaking wave loads at vertical seawalls and breakwaters*” in Coastal Engineering 57 (2010) p424-439, ELSEVIER
- [4] Giovanni Cuomo, Rudolfo Piscopia, William Allsop – “*Evaluation of wave impact loads on caisson breakwaters based on joint probability of impact maxima and rise times*” in Coastal Engineering (2010) –Vol. 58, 1 ian2011, pp 9-27 ELSEVIER
- [5] Obhrai C., Bullock G., Woltres G., Muller G., Peregrine H., Bredmose H., Grune J. – “*Violent wave impact on vertical and inclined walls: large scale model test*”, in Proc. 29th International Conference on Coastal Engineering ASCE Lisbon, 2004
- [6] Oumeraci H., Kortenhauss A, Klammer P – “*Displacement of caisson breakwaters induced by breaking wave impacts*” in Advanced coastal structures and breakwaters, Thomas Telford, London, 1996
- [7] Burchartch H.F., Hughes, S.A, “*Coastal Engineering Manual, Fundamentals of desingn*”, EM 1110-2-1100, pp II-4-1...II-4-6 VI-5-3...VI-5-18, VI-5-154...VI-5-160, VI-5-206...VI-5-209
- [8] Kortenhau A., Oumerac H.,; Allsop N.W.H., Mcconnell K.J., Van Gelder P.H.A.J.M, Hewson P.J., Walkden M., Müller G., Calabrese M., Vicinanza D., “*Chapter 5.1: Wave impact loads - pressures and forces*” available <http://www.tudelft.nl/live/binaries/ec906edd-af0e-4ba1-bcd8-18e7e7cd73ab/doc>

Seismic Assessment of the Faculty of Land Reclamation and Environmental Engineering, Bucharest according to norm P 100-3/2008

Camelia Slave

Abstract – The actual design methods of structures under the influence of permanent, effective and climatic (wind, snow) loads, need an elastic behaviour of the structure and a static action of loads. The dynamic aspect of seismic action and inelastic behaviour of the structures affected by major earthquakes require specific design methods, governed by seismic design regulations. In Romania the field is covered by Seismic Design Code- part III –provision for seismic evaluation of Existing buildings, indicative P 100-3/2008. The article presents a calculation model of body A, building of Faculty of Land Reclamation and Environmental Engineering, Bucharest and also correlation and regression analysis of mathematical results to seismic evaluation of buildings, using MATHCAD PROFESSIONAL Software.

Keywords – correlation function, regression function, seismic risk, seismic force.

1. INTRODUCTION

The case study presented below aims to establish seismic risk class of an existing building of reinforced concrete. The building selected for evaluation is body A of the Faculty of Land Reclamation and Environmental Engineering, University of Agronomical Sciences and Veterinary Medicine of Bucharest. The building is carried out between 1968 and 1970, has a resistance structure on reinforced concrete frames. Designed according to the design concepts of that period the building does not meet many of the requirements of current seismic design codes (**Fig. 1**).



Fig.1 The building chosen for seismic assessment

Manuscript received October 1st, 2011 and accepted November 10, 2011.

C. Slave Author is with USAMV, Bd.Marasti nr. 59, 011464-Bucuresti, Romania (corresponding author to provide phone 0723.31.30.54; e-mail: camellia_slave@yahoo.com).

2. EXPERIMENT DESCRIPTION

Specifying conditions on seismic site. The building selected for evaluation is located in Bucharest. According P100-1/2006, the area is characterized by a peak ground acceleration $a_g = 0.24g$ for design and control period (corner) of the response spectrum $T_c = 1.6$ sec.

Normalized elastic response spectrum shape for horizontal acceleration of ground movement associated components for Bucharest is presented in **Fig. 2**.

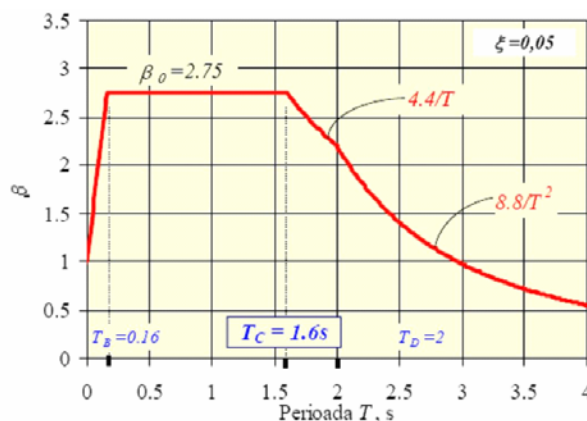


Fig. 2 Normalized acceleration spectrum for. $T_c = 1.60$ s, according P100-1/2006

Building characteristic data. The Faculty of Land Reclamation and Environmental Engineering is located in the north of the town. In the same area are the Village Museum, Free Press House and Romexpo Pavilion. The building consists of three independent sections separated by expansion joints of about 50 mm. For example the evaluation of seismic body has been selected (**Fig. 1**). The assessed building consists of a ground floor and 4 levels with a total height of about 19 m. The non-structural walls are made for compartmentalization of masonry, bricks being arranged in "American" system: two separate longitudinal lines with bricks put on their lateral side and, from time to time, bricks put across. The result is a wall with lower weight lower than the classic solution, having acceptable properties of thermal insulation, but mechanical and deformation properties much lower. The foundation is isolated type (reinforced bushings and plain concrete blocks) under the columns, associated with rectangular network of balancing beams under the masonry walls of the basement. The foundation layer is a brown-yellow dusty clay, plastic consistent, with a conventional pressure of 250 kPa at 2.00 m depth.

Regarding the reinforcement of concrete frame elements it should be noted that they were designed under "Normative conditioning design construction in seismic regions": P13-1963. Given the limited knowledge of seismic engineering at the time, sectional effort design of beams and columns are associated with a shear force base of 4.5% weight of the building. In addition, compliance and reinforcement of concrete elements are strongly influenced by the requirements and design concepts of "gravity" system of STAS 1546-56. Thus, both plates and beams are reinforced in the "gravity" of straight and inclined bars.

In terms of reinforcement the columns have identified 27 different sections. It is noted that the ends of the stirrups up columns is higher than the values specified in current seismic design standards. Structural elements are of B 200 concrete and smooth brand OL38. Concrete quality, confirmed by a limited number of non-destructive testing by sclerometry corresponds to a concrete class of C12/15.

The level of knowledge. Based on the information presented above should determine the appropriate level of knowledge. P100-3/2008 defines three levels of knowledge

- KL1: limited knowledge;
- KL2: normal knowledge;

- KL3: complete knowledge. Thus, the knowledge selected and allowed calculation method determines the value of confidence factor (CF).

As for the construction analysed: (a) overall dimensions of the structure and the structural elements are available based on the original plans and the validity of such data was confirmed by random checks on the field, (b) the composition of structural elements, reinforcement details are known from an incomplete set of the original plans of execution and the validity was verified by limited field checking of the elements considered most important and (c) mechanical characteristics of materials are obtained from the specifications of the original project and are confirmed by limited field tests; it was agreed that appropriate knowledge level is KL2: normal.

According to table 4.1 of P100-3 is allowed "Any method of calculation, according to. P100-1: 2006 "and the trust factor that will be used to establish material characteristics of the existing structure is" $CF = 1.20$ ". Thus, for the calculation of structural capacity (checked against the requirements), the average values of resistance obtained by in-situ tests and the original design specifications falls in values of trust factors.

Qualitative assessment of the structure. Determination of the indicator R1 by determining "the degree of fulfillment of conditions of seismic structure -R1" aims to establish the extent of compliance with general rules of structures, structural and non-structural elements that are stipulated by the current seismic design code P100-1: 2006.

Table 1. R1 values associated seismic risk classes

Seismic risk class			
I	II	III	IV
R1 values			
<30	30-60	61-90	91-100

Body A of the F.I.F.I.M. building falls in seismic risk class RsIII - buildings which, under the effect of design earthquake, could have non-significant structural degradation but important non-structural degradation.

The degradation assessment. Determination of indicator R2. Assessment of degradation of the structural elements is quantified by calculating the value of "degree of structural damage -R2". Its determination is based on scores given in Table B.3 in Appendix B of the code P100-3, for different types of degradation identified. Other types of degradation can be considered further by a reduction factor R2.

Following the evaluation results a "high degree of structural damage" $R2 = 89$ points. Seismic risk class associated factor score of R2 is determined according to table 2, which is a reproduction of table 8.2 P100-3/2008 code:

Table 2. R2 values associated seismic risk classes

Seismic risk class			
I	II	III	IV
R2 values			
<40	40-70	71-90	91-100

Thus, depending on the state of degradation of the resistance structure, Body A of the FIFIM building falls in seismic risk class RsIII, very close to the border with RsIV class of seismic risk.

Analytical evaluation by calculation. Determination of R3. Assessment by calculation is a quantitative method which checks if the existing structures, damaged or not meet the requirements limit states considered in computing seismic action associated with them. The choice of seismic risk classes is based on the value obtained for the indicator "R3 - the degree of seismic structural insurance."

The new code provides three P100-3/2008 seismic evaluation methodologies for assessing construction, defined by the conceptual level of refinement of calculation methods and level of detail of checking operations:

1. Methodology Level 1 is a simplified methodology;
2. Methodology Level 2 is commonly used methodology for the current type for ordinary construction;

3. Methodology Level 3 uses the methodology of calculation methods for to nonlinear and complex construction or of particular importance when they are available the necessary data. Level 3 is the recommended methodology for the current type construction, due to higher degree of confidence provided by the method of investigation, when a classification based on risk group R3 coefficient is not obvious. The following is part of the assessment methodology that has been used for Level 1.

According to a level P100-3/2008, methodology Level 1 can be applied for regular constructions of reinforced concrete, with or without filling masonry walls, up to three floors, located in seismic zones with values $a_g \leq 0.12 g$. However, for example, a level 1 methodology will be used as an exercise that allows a comparison with results of other two approaches. These efforts fall to acceptable and consistent efforts to obtain such insurance different values of the degree of structural seismic: RN3 values associated with axial forces and RV3 values with shear forces associated. To establish the value of normalized design acceleration is necessary to determine the fundamental period of vibration of the structure. This is estimated using one simplified equations:

$$T = k_T H^{3/4} = 0,007 \times 19^{3/4} \approx 0,65 \text{ s} \quad \text{or} \quad T = 0,1 x_n = 0,1 \times 5 \text{ levels} \approx 0,50 \text{ s} \quad (1)$$

Since the height level of 3,80 m is significantly higher than the usual one for residential buildings or offices, and considering the relatively small cross section of columns, it was considered that the first equation provides a value closer to the real. The fundamental period corresponds to an acceleration normalized $\beta = 2.75$ design. According to Table 6.1 of P100-3/2008 - methodology Level 1, for reinforced concrete structures the value of behaviour factor is $q = 2.5$. Since the analysed building has a capacity of over 200 people on total exposed area, it should be of class II, characterized by an importance factor of 1.20. Since the surface of the current floor is of 690 squares meters, and the equivalent load is 1.10 t / m for this type of construction, results a total mass of approximately 3,800 t and an equivalent static seismic force of:

$$F_b = \gamma_1 S_d(T_1) m \lambda = \gamma_1 \frac{a_g \beta(T_1)}{g q} \lambda (mg) = 1,20, \frac{24g}{g} 2, \frac{75}{2}, 50,85G \quad (2)$$

$$F_b = 0,27G = 0,27 \times 3800 \times 9,81 \Rightarrow F_b \approx 10000kN \quad (3)$$

Simplified vertical distribution of seismic force is associated with a deformed linear equivalent. Follows:

Table 3. Distribution of seismic force level

Level	Level table $m_i(t)$	High level $Z_i(m)$	Seismic force level $F_i(kN)$	Share forces level "P" (kN)
E4	759	18.93	3341	3341
E3	759	15.13	2671	6012
E2	759	11.33	2000	8012
E1	759	7.53	1329	9341
P	759	3.73	659	10000

The Level 1 methodology consists in determination of the **structural seismic insurance degree** associated with shear forces in vertical elements using equation (8.1a) of P100-3/2008:

$$R_a^V = \frac{V_{adm}}{qV_{med}} \quad R_a^V = \frac{V_{adm}}{qV_{med}} \quad (4)$$

where: V_{med} represents average tangential effort, calculated as the ratio of shear force level and total area of cross sections of columns at that level, v_{adm} represents the reference admissible value for tangential unit effort in the vertical elements. According to Annex B of P100-3 $v_{adm} = 1.4 f_{ctd}$, f_{ctd} is design tensile resistance of

concrete. Thus $f_{ctd} = 0.67 \text{ N/mm}^2$ for concrete class C12/15 and considered a reliable factor of $CF = 1.2$ and $v_{adm} = 0.93 \text{ N/mm}^2$. For each level of the structure results following values of the structural seismic insurance degree associated with shear forces.

Table 4 Distribution by level of the structural seismic insurance degree R_3^V

Level	Share forces level "i" (kN)	Total area of columns $A_c(m^2)$	Tangential effort average $V_{med}(N/mm^2)$	R_3^V
E4	3341	6.67	0.50	0.74
E3	6012	6.67	0.90	0.41
E2	8012	7.71	1.04	0.36
E1	9341	8.58	1.09	0.34
P	10000	9.84	1.02	0.37

It is noted that due to changes in cross sections of columns the minimum structural seismic insurance degree is recorded on the ground floor, where " $R_3^V = 0.34$ ".

3. RESULTS AND SIGNIFICANCES

Simple correlation refers to two variables X and Y. If Y acts on two or more c is called multiple correlation. Simple correlation can be positive (direct) or negative (reverse). In the first case, as X increases, increases also the average distribution of Y. Simple correlation is negative when the independent variable X values increase and decrease the average distribution of variable Y. Correlations can be highlighted by graphics or tables of correlation. Independent variable is chosen as a variable that can be measured easily and accurately. Characteristics are chosen as the dependent variables to be determined by the independent variables. The purpose of correlation analysis is to find an easier way to determine characteristics without direct measurements, but expressed by statistical relationships. In statistical terminology, the concept of correlation is sometimes, of very large interest, between quantitative and qualitative variables. Sometimes, the concept of correlation means only the relationships between quantitative variables.

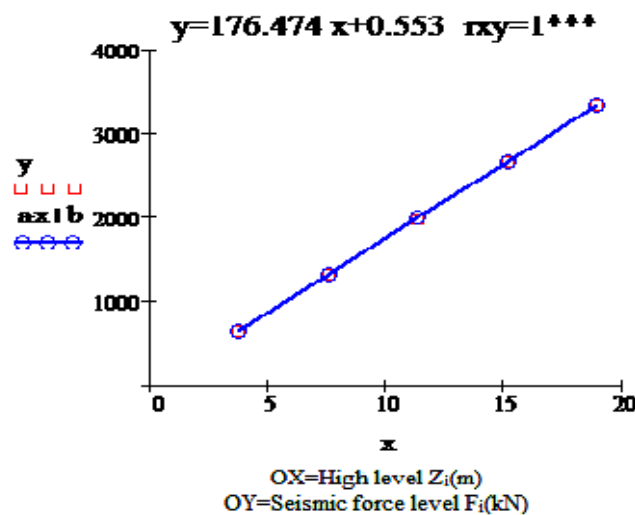


Fig 3 The regression function graph of seismic force and height level

Graphs obtained in this chapter are performed using MATHCAD PROFESSIONAL Software. These graphs are obtained by successive attempts looking at table 3 (distribution of seismic forces) and was established

following the simple correlation between seismic force level considered variable Y and height level. In this case the function is a straight line regression and correlation ratio is $r_{xy} = 1$ which means that there is a very significant connection between the two variables.

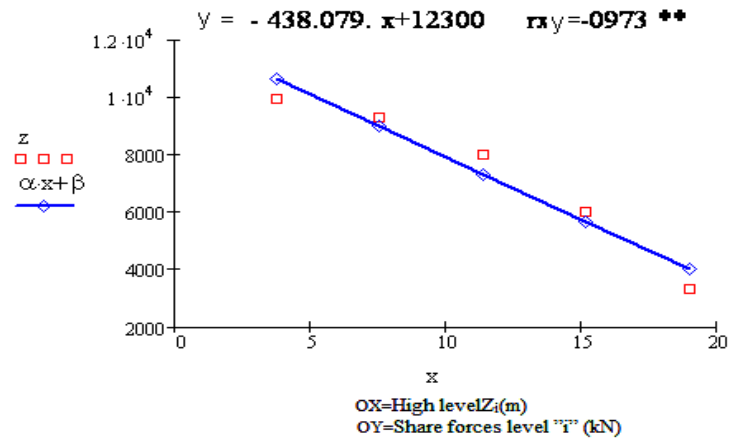


Fig 4 The regression function graph of share force level and height level

4. CONCLUSIONS

For the final evaluation of structural safety of existing building needs to be done the consolidation of the results achieved in each stage of the evaluation process:

1. In terms of qualitative assessment results a "degree of fulfilment of the terms of seismic structure" - $R1 = 69.5$ points corresponding to seismic risk class R_{sIII} .
2. In terms of assessing the state of degradation results a "high degree of structural damage" - $R2 = 89$ points corresponding to seismic risk class R_{sIII} .
3. In terms of analytical evaluation by calculation results the following values of the "structural seismic insurance degree"
 - The methodology level 1: $R3 = 34\%$ - CSR seismic risk class
 - The methodology level 2: $R3 = 39\%$ - R_{sII} seismic risk class
 - The methodology level 3: a. linear static calculation: $R3 = 46\%$ - R_{sII} seismic risk class; b. nonlinear dynamic calculation: $R3 = 44\%$ - R_{sII} seismic risk class; conclusion: Resistance of body A, FIFIM building falls in seismic risk class R_{sII} including construction that under the effect of design earthquake may suffer major structural degradation, but the loss of stability is unlikely.

Therefore, it is mandatory to design a major intervention on the resistance structure in order to enhance the safety of the building.

5. REFERENCES

- [1] Armeanu I, Petrehuş V. Probabilities and statistics, Editura Matrix Bucureşti 2006
- [2] Alexe R, Călin A, Călin C, Nicolae M, Pop O, Slave C, - Earthquake risk reduction of university buildings. Proceedings of European Conference on Earthquake Engineering and Seismology, Geneva, Switzerland, 5-8 September 2006, paper#522
- [3] Alexe R, Călin A, Călin C, Nicolae M, Pop O, Slave C, - Post – seismic Interventions to Buildings and Balancing with the Environment. Proceedings of the European Conference on Environmental research and Assessment, Bucharest, Romania, 5-8 october 2006, pp 146-188.
- [4] Slave C. Seismic risk assessment of existing structures, PhD Thesis, UTCB, September 2010

The Quantification of Potential and Actual Evapotranspiration in the Process of Soil Draught Creation

Milan Gomboš, Branislav Kandra

Abstract – Soil draught is defined as the lack of water in soil, which plants can use for their growth. If plants have no access to the water, they wither. Accessibility of soil water for plants is determined by soil moisture potential (h_w). Soil moisture potential increases with the decrease of water content. In order to determine water accessibility characteristic values were defined on the retention curve, or $pF = \log h_w$. These are wilting point (WP), threshold point (TP) and field water capacity (FWC).

This paper presents the quantification of the course of actual and potential evapotranspiration with regard to the soil water storage. Soil water storage is evaluated according to the FWC, TP and WP. The impact of evaporation deficit on the soil water deficit in the course of and after the state of soil draught was also monitored. The results presented herein come from the investigation realized in the area of Eastern-Slovakian Lowland, Slovakia.

Keywords – actual evapotranspiration, potential evapotranspiration, soil draught, soil water storage.

1. INTRODUCTION

The occurrence of the periods of soil draught has been on the rise in the recent years due to the ongoing climatic changes. Generally speaking, draught is the state of water deficit in the natural environment. Manifestations of draught are considered from the point of view of various social interests and needs. Therefore the criteria for the quantification of soil draught are manifold, including, among many more, meteorological, hydrologic, physiologic, socio-economic and soil criteria [6], [11].

Soil draught is defined as the lack of water in soil, which plants can use for their growth. If plants have no access to the water, they wither. Accessibility of soil water for plants is determined by soil moisture potential (h_w). Soil moisture potential increases with the decrease of water content. In order to determine water accessibility limit values were defined on the retention curve. To assess the available water storage for the plant cover, we conventionally use the following characteristic points of the moisture retention curve (soil-water content), wilting point (WP) representing the value ($\log h_w = pF$) of $pF = 4,18$ (it is a soil moisture state where the plant cover is permanently insufficiently supplied with water and wilts), threshold point (TP) representing the value of $pF = 3,3$ (it is a soil moisture state where the physiological processes in the plant cover are limited by the lack of water), field water capacity (FWC) representing the value of $pF = 2,0$ to $2,7$ (Field capacity is the quantity of water that a well-drained soil would hold against the gravitational forces) [8], [9].

The start of soil draught is defined at the potential of TP. Evaporation is one of the fundamental processes which influence the water content in soil. The aim of the paper is the quantification of the actual (ET_a) and potential (ET_0) evapotranspiration in the process of creation, duration and end of soil draught [1], [5].

Manuscript received October 1st, 2011 and accepted November 10, 2011.

M. Gomboš is with Institute of Hydrology Slovak Academy of Sciences, Hollého 42, 071 01 Michalovce, Slovakia (corresponding author to provide phone: 00421-056-6425147; fax: 00421-056-6425147; e-mail: gombos@uh.savba.sk)

B. Kandra is with Institute of Hydrology Slovak Academy of Sciences, Hollého 42, 071 01 Michalovce, Slovakia (e-mail: pavelkova@uh.savba.sk)

2. EXPERIMENT DESCRIPTION

The process of evaporation was examined in the central part of Eastern-Slovakian Lowland in the area of Milhostov ($\phi = 48^{\circ}40'11,08''$; $\lambda = 21^{\circ}44'18,02''$; 100 m). The locality is characteristic of medium-heavy clayish soil with clay particles of 18 – 39 % **Fig. 1**.

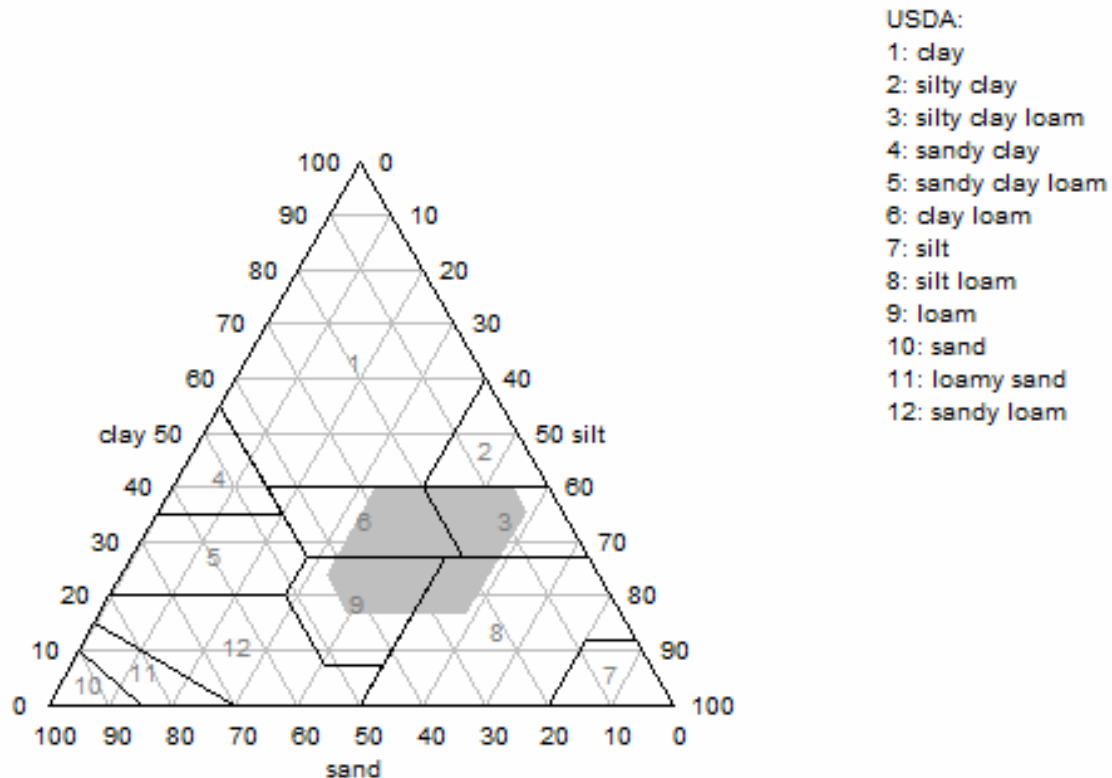


Fig. 1 Texture of the examined soil profile according to the triangular classification diagram USDA (sand 0,05-2,0mm, clay <0,002mm, dust 0,002-0,05mm)

The issues in question were analysed by way of field measurements, laboratory measurements and numerical simulation on the mathematical model GLOBAL [4].

The measurements were focused on the monitoring of volumetric moisture in the vertical direction of the soil profile to the depth of 0,8 m, by the layers of 0,1 m. The monitoring has been carried out once a week since the year 2000. A part of field works was sampling, necessary for the determination of retention curve, texture and other basic hydro-physical characteristics of soil profile [2], [3]. In the area, there is located an agro-ecological climatic and research station. This station provided all the data concerning hydro-meteorological elements and plant cover characteristics required for numerical simulation on the mathematical model GLOBAL [7], [10].

The model GLOBAL is a simulation mathematical model of soil water transfer which enables the calculation of moisture potential distribution or soil moisture in real time. The model was tried and verified for the monitored soil water storage to the depth of 0,8 m. After successful completion of the verification process, it was possible to launch numerical simulation of the course of ET_0 , ET_a and water regime components in the chosen vegetation periods (VP). The simulation of the course of water regime components was executed to the depth of 3,0 m under the surface. In this depth, majority of field plants roots is located. Time-course of soil water

storage was analysed to the depth of 1,0 m. Numerical simulation was carried out with 1-day step. The inputs of meteorological and plant cover parameters and the inputs necessary for the formulation of boundary conditions were adjusted accordingly.

The background data bases used for the choice of vegetation periods analysed in this paper was the period between 1970 and 2008. Four VP were chosen according to the evaluation coefficients. Two of them were normal from the meteorological point of view and slightly dry from the soil analysis point of view (1995, 2004). The other two VP were extremely dry (1986, 2007). The following evaluation coefficients were used: Refer to (1) – (4).

$$D_{ET(VP)} = \sum ET_a - \sum ET_0 \quad (1)$$

$$P_n = \frac{\sum ET_a}{\sum ET_0} * 100 \quad (2)$$

$$B_{i_0} = \frac{\sum P}{\sum ET_0} \text{ and } B_{i_a} = \frac{\sum P}{\sum ET_a} \quad (3)$$

$$A_{(VP)} = \frac{1}{n} \sum_{i=1}^n [\theta_a - \theta_{WP}] / [\theta_{FWC} - \theta_{WP}] \quad (4)$$

where

- $D_{ET(VP)}$ - evapotranspiration deficit during VP [mm]
- P_n - proportional number [mm]
- $B_{i_0(a)}$ - balance index between precipitation and evapotranspiration [mm]
- $A_{(VP)}$ - agronomical classification
- $\sum ET_0$ - potential evapotranspiration sum during VP [mm]
- $\sum ET_a$ - actual evapotranspiration sum during VP [mm]
- $\sum P$ - precipitation sum [mm]
- θ_a - actual water content [%]
- θ_{TP} - water content at the threshold point [%]
- θ_{WP} - water content at the wilting point [%]

The increase in evaporation deficit was analysed using 7-day moving average ($D_{ET,7}$). For illustration there are also shown the 7-day moving averages of precipitation (P_7) and actual evapotranspiration ($ET_{a,7}$). The beginning of the creation and the course of evaporation deficit indicate the lack of water in the soil profile. Duration and intensity of evaporation deficit with regard to the changes of soil water storage and TP and WP were analysed. The results are shown in tables and graphs.

3. RESULTS AND SIGNIFICANCES

Table 1 shows the evaluation of the vegetation periods in the analysed years according to various parameters.

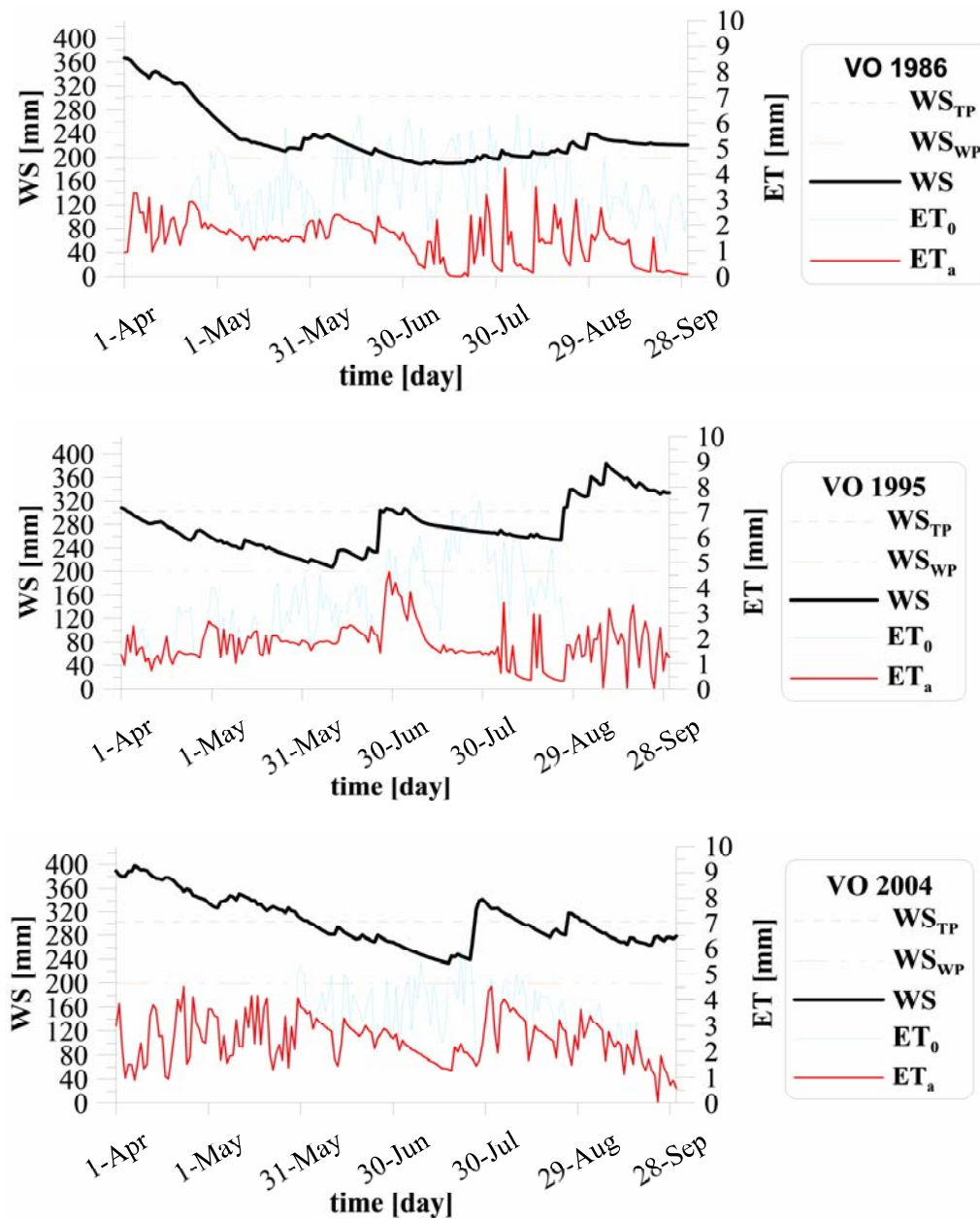
The parameters characterize the years in question in terms of water storage, evaporation and precipitation. Pursuant to the table, it is obvious that the VP of 1986 and 2007 were dry with regard to the soil water storage. The average soil water storage to the depth of 1 m under the surface was below the long-term average values of the years 1970 – 2008 (275,59 mm). The periodicity of the occurrence of such dry periods is 0,14 and 0,11; the reference years for the calculation being 1970 – 2008. These years were characteristic of high evaporation deficits. The actual evapotranspiration ratio out of the potential evapotranspiration was 42 % (1986) and 33 % (2007). According to $PDSI$ evaluation, the year 1986 is considered moderately dry, while the year 2007 extremely dry. The years 1995 and 2004 are close to the normal state. The periodicity of the occurrence of the identified average water storage in VP is 0,42 and 0,53. The average soil water storage were slightly below the normal values of the years 1970 – 2008. The actual evapotranspiration ratio out of the potential was 57 % (1995) and 81 % (2004).

Table 1. Evaluation coefficients in selected VP with Palmer drought severity index ($PDSI$), exceedance probability (p) of average soil water deficits in investigated VP and soil water storage deviation (ΔWS_n) from the water storage average in normal period (1970 – 2008)

Indicator	1986	1995	2004	2007
\overline{WSWS} [mm]	233,07	276,64	304,57	220,90
ΣET_a [mm]	255,99	322,86	450,11	221,43
ΣET_0 [mm]	607,35	568,21	558,66	664,12
Precipit. ΣP [mm]	274,6	499,3	458,3	328,6
$D_{ET(VP)}$ [mm]	351,36	245,35	108,55	442,69
P_n [%]	42,15	56,82	80,57	33,34
$PDSI$	-1,19	0,24	-0,05	-3,74
B_{i0}	0,45	0,88	0,82	0,49
B_{ia}	1,07	1,55	1,02	1,48
p [%]	14	42	53	11
ΔWS_n [mm]	-42,52	1,05	28,98	-54,69
$A_{(VP)}$	0,13	0,27	0,36	0,09

Figure 2 shows the daily course of WS , ET_0 , ET_a , WS_{TP} (WS at the TP level = 303 mm) and WS_{WP} (WS at the WP level = 200 mm). At the beginning of the VP , the soil profile is in the state of draught (2007) or close to it (1986). In 2007 the soil profile shows constant water deficit $ET_a < ET_0$. Water storage was slowly and gradually decreasing until reaching the wilting point. Only September rains did increase the water storage level again. One of its manifestations was the fact that the actual evapotranspiration drew closer to the potential one. Until the very end of the VP the soil profile persisted in the state of soil draught. The 1986 soil profile, which was also a dry year, reached the state of soil draught in mid-April and this state continued to the end of the VP . Further calculations revealed that the occurrence of draught was not fully compensated for during the winter season, and thus was partly transferred to the new VP . In the soil profiles of average years the formation, duration and end of soil draughts was also observed. In 1995, for example, the lack of water was observed at the beginning of the VP . Evaporation deficit gradually increased and the water storage decreased until reaching the wilting point. Precipitation at the end of May and beginning of June increased the water storage to the level of TP , while ET_a was close to ET_0 . During the following no-precipitation period, however, evaporation and water storage deficit, causing new soil draught. The precipitations at the end of July and beginning of August refilled soil water storage deficit and water storage gradually exceeded TP level – $ET_a = ET_0$. In terms of water regime, the year 2004 was the most positive, also due to the soil water storage accumulated during the winter season. At the beginning of May, soil water storage in the soil profile reached TP , ET_a level and dropped with regard to ET_0 . End-of-July precipitations increased soil water storage until reaching TP level, at which point it oscillated till the end of the VP .

Figure 3 shows the impact of soil water storage in a soil profile on the evaporation deficit. During the no-precipitation periods soil water storage decreases. When the soil water storage reaches 300 mm, ET_a drops below ET_0 . Under the conditions of the area under consideration this is critical moisture and it equals the moisture level of app. TP .



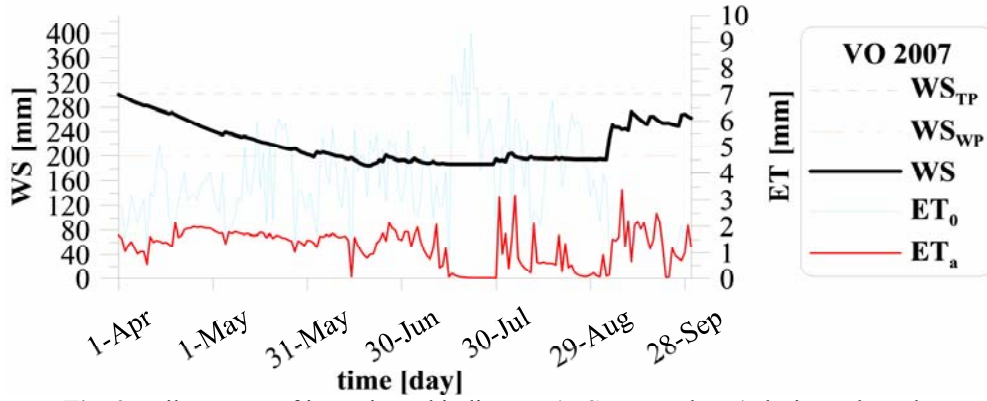


Fig. 2 Daily course of investigated indicators (WS , ET_0 and ET_a) during selected VP

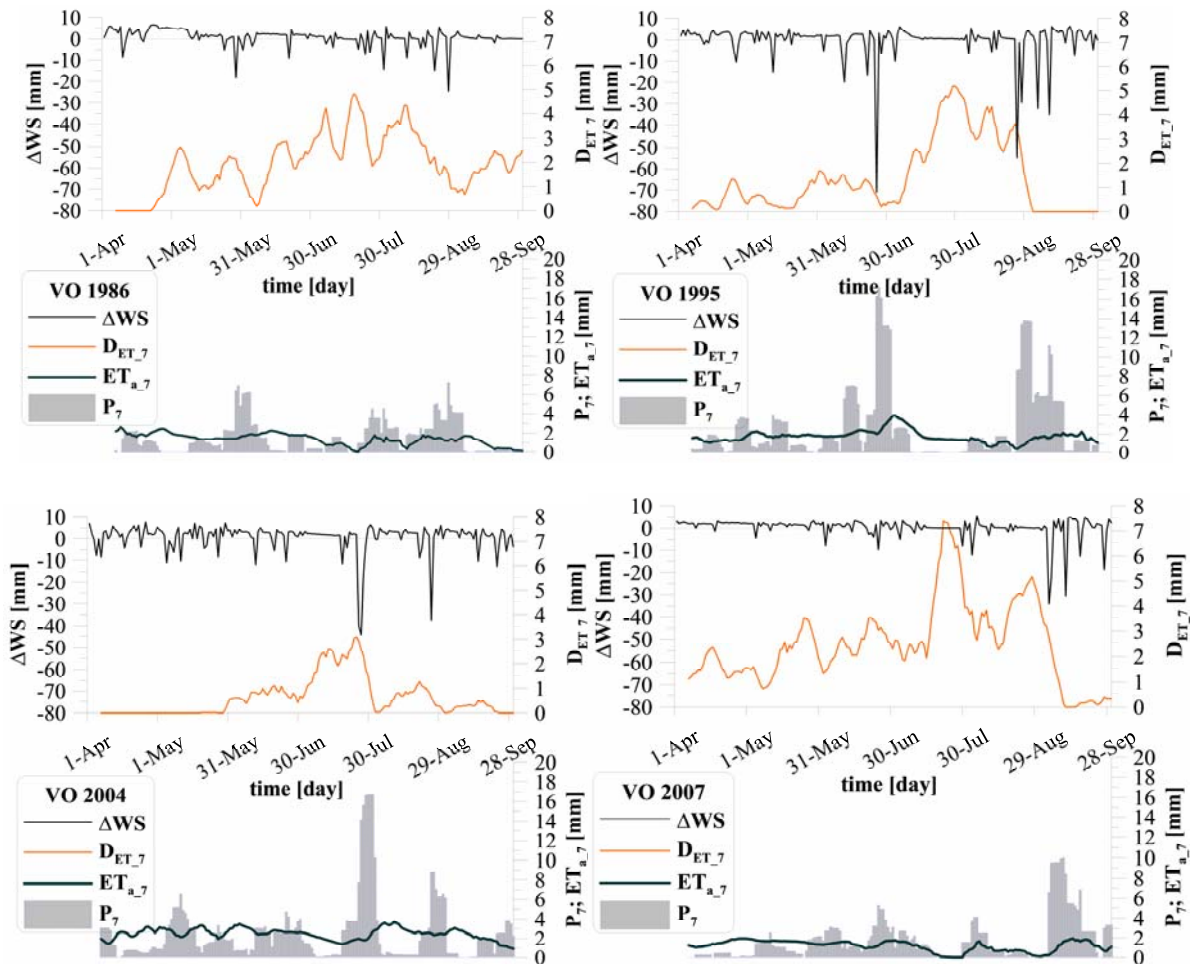


Fig. 3 The course of the analysed parameters (daily deviations ΔWS , course of 7-day moving averages $D_{ET,7}$, P_7 and $ET_{a,7}$) during the vegetation periods of the years

4. CONCLUSIONS

The paper quantifies the actual and potential evapotranspiration in the course of formation, duration or end of the soil draught. Soil draught is defined as the water storage in the root zone of a soil profile at TP level. It has been found out that if there is enough water in the soil profile, $ET_a = ET_0$. When water storage up to the depth of 1 m drops to 300 mm, evaporation deficit is created and $ET_a < ET_0$. In the analysed area this corresponds to the water storage at the TP level. At this point, the soil profile shows the lack of water and it gets to the state of soil draught. Under very adverse hydro-meteorological conditions it can reach WP and plant cover withers. Vegetation period can end in the state of water deficit. If the following non-vegetation season is also dry, the conditions are created for the soil draught in the next vegetation period. It was found out that the maximum daily evaporation deficit could reach 9,3 mm. Summary evaporation deficit during the whole VP in the extremely dry year 2007 was 443 mm.

5. ACKNOWLEDGMENTS

This contribution is the result of the project implementation: Centre of excellence for the integrated river basin management in the changing environmental conditions, ITMS code 26220120062 supported by the Research & Development Operational Programme funded by the ERDF.



Agentúra
Ministerstva školstva, vedy, výskumu a športu SR
pre štrukturálne fondy EÚ



We support the research activities in Slovakia/ The project is co financed by the EU sources.

The authors would like to thank for the kind support of the project APVV-0139-10, APVV-0271-07 and project VEGA 2/0130/09.

6. REFERENCES

- [1] I FAO., 1990. Annex V: FAO Penman-Monteith formula. Report from the Expert Consultation on revision of FAO methodologies for crop water requirements, 28-31 March 1990, Rome, Italy.
- [2] Van Genuchten, M. T. 1980. A closed equation for predicting the hydraulic conductivity of unsaturated soil. In Soil Science Society of America Journal. 1980, no. 44, p. 892-898.
- [3] Kotorová, D., Mati, R. 2008. The trend analyse of water storage and physical properties in profile of heavy soils. In: Agriculture (Poľnohospodárstvo), roč. 54, 2008, č. 4, s. 155-164. ISSN 0551-3677
- [4] Majerčák, J., Novák, V. 1994. GLOBAL, one-dimensional variable saturated flow model, including root water uptake, evapotranspiration structure, corn yield, interception of precipitations and winter regime calculation : Research Report. Bratislava : Institute of Hydrology S.A.S. 1994, 75 s.
- [5] Novák, V. 1995. Vyparovanie vody v prírode a metódy jeho určovania. (Evaporation of water in nature and methods of determining.) Bratislava : Veda, 260 s.
- [6] Palmer, W. C. 1965. Meteorological drought. In: Research Paper č. 45, s. 201 – 232. U.S. Department of Commerce Bureau, Washington, D. C.
- [7] Štekauerová, V., Šútor, J. 2000. Úloha monitoringu pri numerickej simulácii vodného režimu zóny aerácie pôdy. Acta Hydrologica Slovaca, ISSN 1335-6291, vol. 1, 2, 203-212.
- [8] Štekauerová, V., Skalová, j., Šútor, J. 2002. Using of pedotransfer functions for assessment of hydrolimits. Rostlinná výroba (Plant production), 48, 9, 407-412.

- [9] Štekauerová, V., Skalová, J., Nováková, K. 2010. Assignment of hydrolimits for estimation of soil ability to supply plants by water. *Növénytermelés*, Vol. 59, ISSN 0546-8191, Supplement, p. 195-198.
- [10] Šútor, J., Štekauerová, V., Nagy, V. 2010. Comparison of the monitored and modeled soil water storage of the upper soil layer: the influence of soil properties and groundwater table level. *J. Hydrol. Hydromech.*, ISSN 0042-790X, 4, s. 279-283.
- [11] Tall, A. 2008. Application of the palmer drought severity index in east Slovakian lowland. *Cereal Research Communications*, ISSN 0133-3720, vol. 36, 1.190-IF2008, 1, pp. 1195-1198.

The Impact of Groundwater Level Position on the Actual Evapotranspiration in Heavy Soils in Eastern-Slovakian Lowland

Milan Gomboš, Dana Pavelková

Abstract – Water evaporation is one of the most important elements of hydrologic cycle. The paper analyses the impact of groundwater on intensity and course of actual evapotranspiration. Analysis is based on numerical experiment using the mathematical model GLOBAL. Prior to the experiment, the model was verified by comparing calculated and measured soil water storage in the examined localities at the depth of 0,8 m. The experiment quantifies the groundwater level (GWL) impact on actual evapotranspiration. Three phases of groundwater influence were identified. Threshold values of GWL were identified in the examined profiles. They are borders between non-linear and residual phase of the impact. At the residual phase, GWL impact on potential evapotranspiration intensity is negligible.

Keywords – actual evapotranspiration, groundwater level, potential evapotranspiration.

1. INTRODUCTION

Water evapotranspiration is a thermodynamic process during which mass converts from solid or fluid phase to gaseous phase. It is the most decisive regulator of energy flow in the hydrologic cycle. Process of evaporation from plants and water or soil surface is called evapotranspiration. Maximal possible evaporation from land covered by vegetation under particular meteorological conditions is called potential evapotranspiration (ET_0). Real evaporation from land covered by vegetation is called actual evapotranspiration (ET_a). Evapotranspiration is one of the key elements in water balance in nature [7]. It crucially effects biomass creation and water storage in unsaturated zone of soil profile. Unsaturated zone (UZ) is water source for the biosphere. If there is enough water in a soil profile then $ET_0 = ET_a$. If $ET_0 > ET_a$, it indicates the water deficit in the root zone of a soil profile and the beginning of soil profile drying [3]. Unsaturated zone is determined by surface runoff and, on the lower boundary, by a position of groundwater level (GWL). Apart from evaporation and rainfall, the amount of water in UZ in lowland conditions, and also root zone of a soil profile, is influenced by groundwater level (GWL). For some time during rainless periods, groundwater can supply water storage in the root zone of a soil profile by capillary rise [5]. Thereby water availability for plants improves and actual evapotranspiration intensity rises [8]. In consequence of the water transfer, GWL lowers and therefore unsaturated zone is enlarged. When the groundwater level drops under certain critical level, the water transfer from GWL to the root zone is negligible. During long-lasting rainless period the intensity of the actual evapotranspiration slowly decreases due to the lack of water in the root zone [4]. Surface soil horizon and consequently the whole root zone is getting into the state of soil drought. It is a state in which the creation of biomass decreases and physiological activity of the plants is focused merely on survival due to the water deficit [9]. It is defined as a threshold point (TP) for potential $pF=3,3$ on the retention curve.

Manuscript received October 1st, 2011 and accepted November 10, 2011.

M. Gomboš is with Institute of Hydrology Slovak Academy of Sciences, Hollého 42, 071 01 Michalovce, Slovakia (corresponding author; phone: 00421-056-6425147; fax: 00421-056-6425147; e-mail: gombos@uh.savba.sk)

D. Pavelková is with Institute of Hydrology Slovak Academy of Sciences, Hollého 42, 071 01 Michalovce, Slovakia (e-mail: pavelkova@uh.savba.sk)

The aim of the article is to quantify the impact of GWL on the course and intensity of actual evapotranspiration in vegetation period (VP - April to September). Apart from this, the aim is to determine the threshold values of GWL in the examined areas. The threshold values are the values indicating that the impact of groundwater on actual evapotranspiration is negligible. The impact of GWL was examined in lowland areas with plant cover, where main part of their root zone is located less than 1m under the surface. Research works are based on field measurements and numerical simulation on mathematical model global.

2. EXPERIMENT DESCRIPTION

Research works were carried out on East-Slovakian Lowland, in the Kamenec area ($\phi = 48^{\circ}21'02.9''$; $\lambda = 21^{\circ}48'52.6''$; 95 m) and Horeš area ($\phi = 48^{\circ}22'32.4''$; $\lambda = 21^{\circ}53'54.4''$; 94 m). In both areas winter wheat was grown during the examined year. The major part of the root zone of winter wheat is less than 1m under the ground. In terms of soil types the first one is clayey, in second one is predominantly silty-clayey loam (**Fig. 1**).

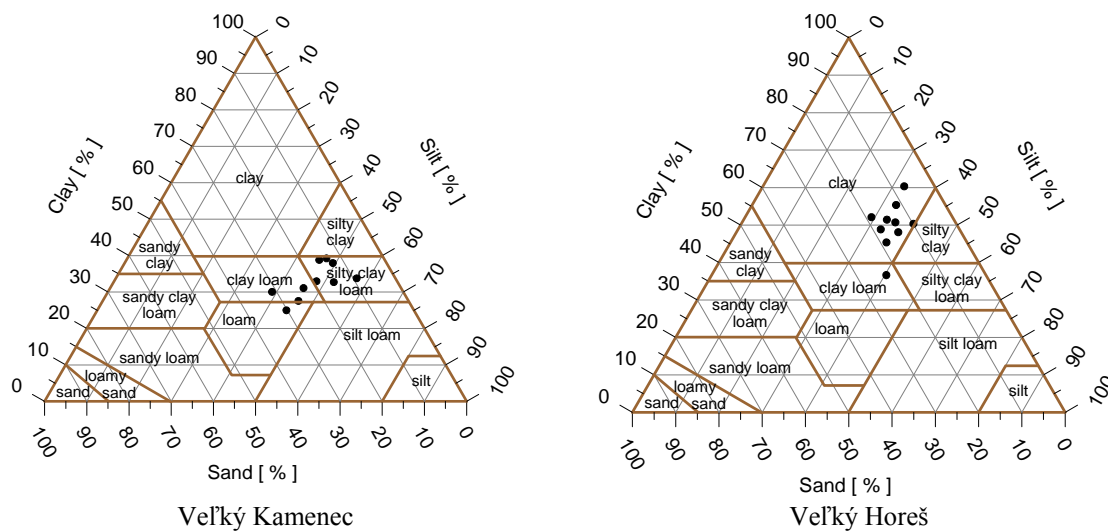


Fig. 1 Specification of soil types by means of triangular classification diagram by vertical line of the soil profiles Kamenec and Horeš into the depth of 1m by 0,1m layers.

To examine the issues in question the vegetation period of the year 2007 was chosen. In terms of soil water storage, this period was one of the driest periods in the last 30 years. The investigation was carried out by way of numerical experiment on the mathematical model GLOBAL.

The model GLOBAL is a simulation mathematical model of soil water transfer which enables the calculation of moisture potential distribution or soil moisture in real time [6]. The principle of the model is numerical calculation of the following non-linear partial differential equation of water movement in the aeration zone:

$$\frac{\partial h_w}{\partial t} = \frac{1}{c(h_w)} \frac{\partial}{\partial z} \left[k(h) \left(\frac{\partial h_w}{\partial z} + 1 \right) \right] - \frac{S(z, t)}{c(h_w)} \quad (1)$$

h_w soil moisture potential;

z vertical coordinate;

$k(h_w)$ unsaturated hydraulic conductivity of the soil;

$S(z, t)$ intensity of the water take-off by the plants roots from unit soil volume per time unit ($\text{cm}^3/\text{cm}^3 \cdot \text{d}^{-1}$);

θ bulk soil moisture (cm^3/cm^3).

The model GLOBAL enables the simulation to be executed with one day time-step. Daily values are used as the basic inputs for setting up the boundary conditions. Similarly are used the inputs for the meteorological and vegetation parameters. Hydro-physical characteristics of the soil (retention curves, saturated and unsaturated hydraulic conductivity of the soil, hydrolimits and some physical properties of the soil as porosity, density and bulk density, moisture of saturated soil) also enter the model GLOBAL. Moisture retention curve is described by the formula of van Genuchten [2].

Potential evapotranspiration ET_0 is calculated according to FAO, by Penman's method of Monteith [1]. For determining the actual transpiration or evaporation intensities the method developed on IH SAS was used. According to this method the evapotranspiration structure depends on the value of leaf area index (LAI). Intensity of potential evaporation E_{eo} is calculated from the value of potential evapotranspiration ET_0 using the formula:

$$E_{eo} = ET_0 \cdot \exp(-m_1 \cdot LAI) \quad (2)$$

The value of empirical coefficient ($m_1 = 0,463$) was gained by field measurements in the wheat plant cover. Calculation of the actual evapotranspiration intensities and its structure is based on the knowledge of potential evapotranspiration ET_0 and the relationship between E_{eo}/ET_0 and moisture of the soil profile, i.e.:

$$ET_r = E_{eo}/ET_0 = f(\theta) \quad (3)$$

Used calculation method is based on the assumption that mean value of soil moisture in the root zone in case of calculation transpiration or value of moisture of the upper layer of soil profile in case of evaporation calculation, in which evaporation starts to decrease (critical value θ_k), depends on the intensity of evaporation. The higher the evaporation intensity is, the higher is the value of θ_k , in which evaporation starts to decrease. This method was verified using the model GLOBAL and there was shown conformity of the calculated values with the values gained by field measurements in real conditions. Modelling shows soil moisture distribution and soil moisture potential, daily interception and evapotranspiration rates and their elements, infiltration, existing water deficiency in the soil and more information. Results of monitoring of water storage into the depth of 0,8 m are available for both localities. Model GLOBAL was verified in 2007 on these results in two localities.

Experimental research of the impact of GWL on actual evapotranspiration rate is based on actual evapotranspiration rate quantification for different simulated positions of average GWL during vegetation period of the year 2007. Variability of GWL, as well as hydrometeorologic and other input data remains the same. Calculation process during numerical experiment was the same in both cases, following these steps:

1. Average GWL in vegetation period of the year 2007 was calculated.

2. Course of GWL in vegetation period 2007 (lower boundary condition) was shifted by vertical so that average values of GWL_i^k in vegetation period had in every k^{th} shift different characteristic position of GWL_{VP}^k where :

GWL_{VP}^k is the position of GWL in i^{th} day of vegetation period for k^{th} shift that is k^{th} average GWL.

$\overline{GWL_{VP}^k}$ is average GWL during vegetation period in k^{th} shift.

Value $ET_{a,i}^k$ and $ET_{a,VP}^k$ was calculated for every GWL_i^k and $\overline{GWL_{VP}^k}$

where $ET_{a,i}^k$ is the value of actual evapotranspiration ET_a in i^{th} day of vegetation period in k^{th} average GWL.

$$ET_{a,VP}^k = \sum_{i=1.4.2007}^{30.9.2007} ET_{a,i}^k \quad (4)$$

3. There were considered three basic levels as characteristics position of \overline{GWL}_{VP}^k : lower edge of the root zone of a soil profile, 1m deep under the \overline{GWL}_{VP}^1 , average \overline{GWL}_{VP}^2 in vegetation period of the year 2007 and average value \overline{GWL}_{VP}^3 at which is the influence of GWL on ET_a negligible (threshold level of GWL position). In addition, two other positions of GWL were chosen in the interval $\langle \overline{GWL}_{VP}^1; \overline{GWL}_{VP}^2 \rangle$ for representation of the course of the dependency. Threshold level of groundwater level \overline{GWL}_{VP}^3 was identified by progressive selection of subsequent groundwater levels GWL so that $\overline{GWL}_{VP}^k < \overline{GWL}_{VP}^2$. Threshold value of groundwater level \overline{GWL}_{VP}^3 is identified after fulfilling the condition:

$$\left(ET_{a,VP}^k - ET_{a,VP}^{k-1} \leq 0,01 \times ET_0 \right) \wedge \left(\overline{GWL}_{VP}^k - \overline{GWL}_{VP}^{k-1} \leq 0,5 \right) \Rightarrow \overline{GWL}_{VP}^k = \overline{GWL}_{VP}^3 \quad (5)$$

4. The following dependencies were gained in the examined areas $ET_{a,VP} = f(\overline{GWL}_{VP})$ (6)

3. RESULTS AND SIGNIFICANCES

Table 1. Basic hydrophysical characteristics of soils.

Locality	Veľký Kamenec		Veľký Horeš		
Type of soils	Heavy soils		Very heavy soils		
Layers	0 – 40	40 – 100	0 – 50	50 – 60	60 - 100
Alpha	0,0103	0,0093	0,0154	0,0158	0,0131
n	1,4143	1,4655	1,3130	1,3149	1,3888
Theta s	0,396	0,413	0,442	0,483	0,4895
Theta r	0,0788	0,0806	0,0919	0,0988	0,0966
Ks	3,37	5,09	7,48	10,7	15,3
Available WC	224		200		

From **Table 1** and **Fig. 1** results that heavy soils occur in Kamenec locality. Two calculation material layers were considered for improvement of the calculation precision during the simulation. There are very heavy soils in the locality of Horeš (**Table 1** and **Fig.1**). Three calculation profiles were considered here.

Table 2 shows the basic characteristics of GWL position in the examined areas during the vegetation period in 2007, as well as the total volume of precipitation (P) during the vegetation period in question.

Table 2. Average position of GWL and total volume of precipitation in the examined areas during the vegetation period in 2007.

	$\overline{GWL}_{VP}^{2007}$	$\overline{GWL}_{VP}^{2007}$	Standard deviation	$GWL_{max}-GWL_{min}$	ΣP_{VP}^{2007}
Locality	m n.m.	m under surface	m	m	mm
Veľký Kamenec	94,87	2,34	0,62	0,65	308,80
Veľký Horeš	95,49	2,15	0,48	0,86	308,80

During the period under consideration, water regime and its components were simulated to the depth of 4m. They were analysed in detail to the lower boundary of the root zone, to the depth of 1m under the surface. Calculation time-step was 1 day. Hydro-meteorological inputs and lower boundary condition (GWL) were entered the calculations accordingly.

Figure 2 shows the results of the verification of the model GLOBAL. In both areas, the verification was executed by means of field measurements of volumetric soil moisture, to the depth of 0,8 m under the surface.

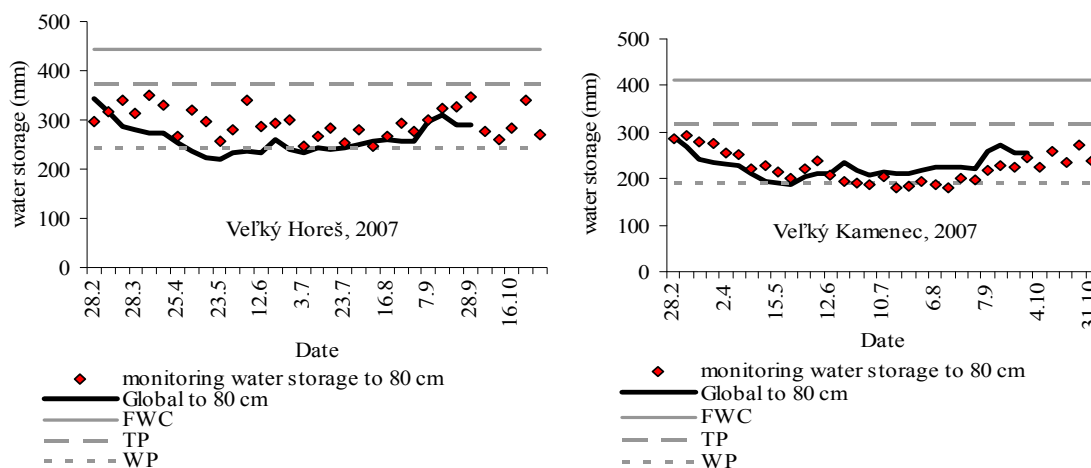


Fig. 2 Monitored and calculated (by model GLOBAL) soil water storage into the depth of 0,8 m in the localities of Kamenec and Horeš and hydrolimits FWC (pF=2,52), TP (pF=3,3), WP (pF=4,18)

From the course of measured and calculated values is obvious that in terms of soil water storage it is a dry year. Soil water storage into the depth of 0,8 m was during whole vegetation period in between the wilting point and threshold point. This confirms evapotranspiration deficiency:

$$ED = ET_0 - ET_a \quad (7)$$

During the vegetation period 2007, ED was 289 mm in Kamenec area and 293 mm in Horeš area. The deficit represents 62% and 63% of total potential evapotranspiration during the whole vegetation period. **Figure 3** and **Figure 4** show the course of totals daily values of ET_a , ET_0 and precipitations in VP of 2007.

Figure 5 is a graphic representation of the results of the calculation of dependency characterized by the formula (6). It shows that the GWL position affects the evapotranspiration rates in both areas where winter crop is grown. Three phases can be identified in the curve of dependency characterized by the formula (6) – linear phase, non-linear phase and residual phase.

Linear phase starts at the GWL position at \overline{GWL}_{VP}^1 . When GWL drops under certain point, the dependency becomes non-linear. At this phase, the impact that groundwater has on the actual evapotranspiration rates decreases. Hydraulic connection between the root zone and groundwater is negligible. The dependency (6) then becomes residual. At the residual stage the impact line asymptotically approaches the line parallel to the vertical axis of GWL depths. Considering the condition described in (5), the residual phase starts at the interval between two lowest points. In this case, the lowest points of the interval are located in the depth of 3,73 m.

Under the conditions of the profiles in question, these are the threshold levels of \overline{GWL}_{VP}^3 . Water transfer from GWL to the root zone of a soil profile at the depth of 3,73 m is negligible. The impact on the actual evapotranspiration and biomass production is minimal as well. The course of the dependency and the limits of

the individual phases are influenced mainly by hydrological characteristics of the environment and variations of GWL position.

Figure 6 and 7 illustrate the courses of daily values of actual and potential evapotranspiration during the vegetation period in question in the positions \overline{GWL}_{VP}^1 , \overline{GWL}_{VP}^2 and \overline{GWL}_{VP}^3 . It is obvious that the GWL position has a great influence on water evaporation from soil. At the threshold position \overline{GWL}_{VP}^3 the actual evapotranspiration in both areas was 135 mm and 117 mm. Actual $ET_{a,VP}$ at \overline{GWL}_{VP}^2 was 178 mm and 74 mm.

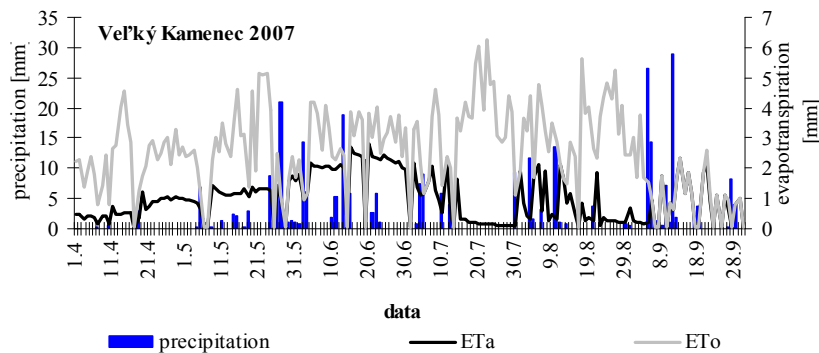


Fig. 3 The course of total daily values of ET_0 , ET_a , Z in the vegetation period of 2007 in Kamenec area

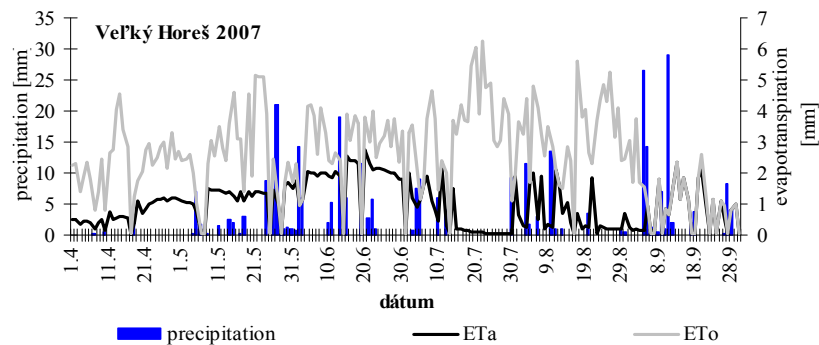


Fig. 4 The course of total daily values of ET_0 , ET_a , Z in the vegetation period of 2007 in Horeš area

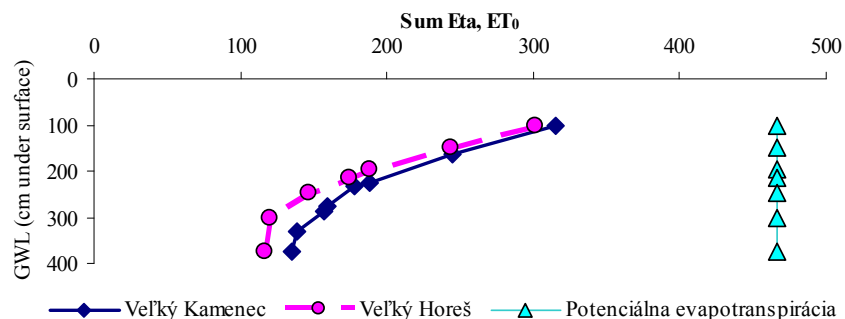


Fig. 5 The course of the dependency (6) and ET_0 in Kamenec and Horeš areas

The real impact of groundwater on $ET_{a,VP}$ in the examined areas was 24% and 33% from the total amount of evaporation during the vegetation period (**Fig. 8**).

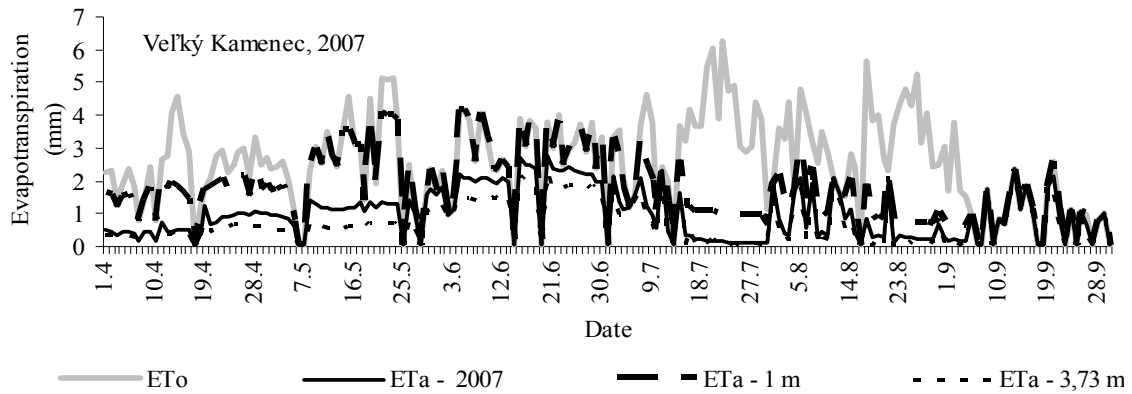


Fig. 6 The course of daily values of ET_0 and total daily volumes of ET_a at the positions of $\overline{GWL_{VP}}^1$, $\overline{GWL_{VP}}^2$ and $\overline{GWL_{VP}}^3$

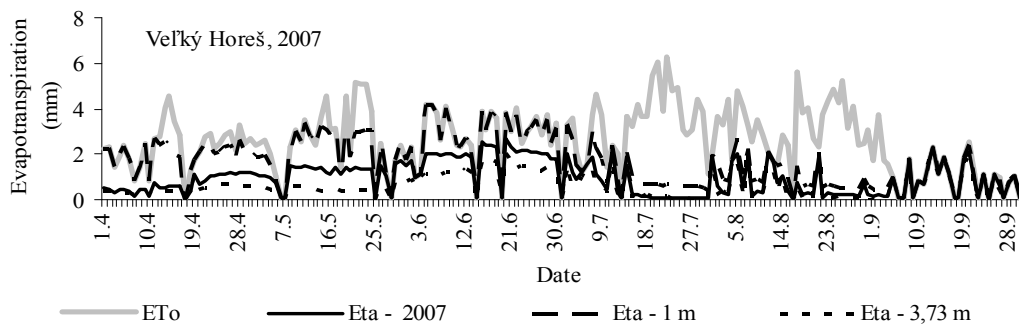


Fig. 7 The course of daily values of ET_0 and total daily values of ET_a at the positions of $\overline{GWL_{VP}}^1$, $\overline{GWL_{VP}}^2$ and $\overline{GWL_{VP}}^3$

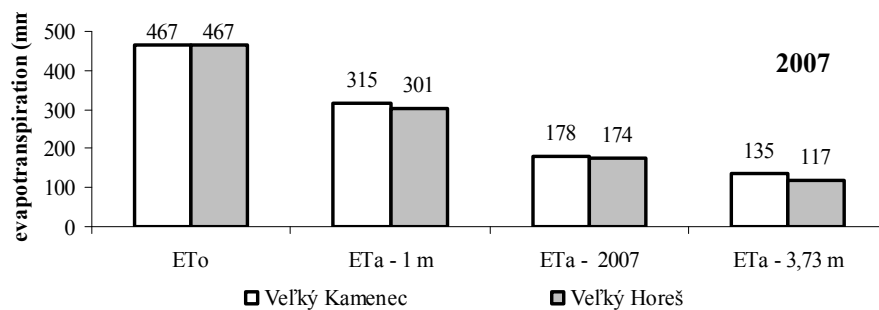


Fig. 8 The sum of potential evapotranspiration rates during the whole vegetation period and the sums of actual evapotranspiration rates at the positions $\overline{GWL_{VP}}^1$, $\overline{GWL_{VP}}^2$ and $\overline{GWL_{VP}}^3$

4. CONCLUSIONS

The experiment confirmed the significant role of groundwater in the hydrologic cycle. The impacts of GWL position on the course of evapotranspiration rate, as well as the values of the actual evapotranspiration were quantified. The impact of groundwater on water evaporation from soil was divided into three phases – linear, non-linear and residual phase. The boundary between linear and non-linear phase was determined as GWL threshold position. It is a position, where water transfer from GWL to the root zone is negligible and its impact on evaporation is minimal. In the particular conditions of the experiment, GWL threshold position was located 3,7 m under the ground. For the purposes of the experiment, extremely dry vegetation period of 2007 was chosen. The evaporation deficit during this period was 62 % and 63 % of the potential evaporation. It was shown that 24 % - 33 % of the water evaporated from the surface of the ground came from groundwater supply.

The results show that the impact of groundwater on the evaporation rates is directly proportionate to the hydro-physical characteristics of soil and GWL variations. GWL regulation could be an effective measure of soil water regulation during the periods of soil draught.

5. ACKNOWLEDGEMENTS

The authors would like to thank for the kind support of the project VEGA 2/0130/09 and project APVV-0139-10.

6. REFERENCES

- [1] FAO, 1990. Annex V: FAO Penman-Monteith formula. Report from the Expert Consultation on revision of FAO methodologies for crop water requirements, 28-31 March 1990, Rome, Italy.
- [2] Van Genuchten, M. T. 1980. A closed equation for predicting the hydraulic conductivity of unsaturated soil. In Soil Science Society of America Journal. 1980, no. 44, p. 892-898.
- [3] Kandra, B., Tall, A. 2011. Determining the intensity and duration of soil drought by the method of effective precipitation. *Növénytermelés*, ISSN 0546-8191, vol. 60, p. 373-376.
- [4] Kandra, B. 2010. The creation of physiological stress of plants in the meteorological conditions of soil drought. *Növénytermelés*, Vol. 59, ISSN 0546-8191, Supplement, p. 307-310.
- [5] Kotorová, D., Mati, R. 2008. The trend analyse of water storage and physical properties in profile of heavy soils. In: *Agriculture (Poľnohospodárstvo)*, roč. 54, 2008, č. 4, s. 155-164. ISSN 0551-3677
- [6] Majerčák, J., Novák, V. 1994. GLOBAL, one-dimensional variable saturated flow model, including root water uptake, evapotranspiration structure, corn yield, interception of precipitations and winter regime calculation : Research Report. Bratislava : Institute of Hydrology S.A.S. 1994, 75 s.
- [7] Novák, V. 1995. Vyparovanie vody v prírode a metódy jeho určovania. (Evaporation of water in nature and methods of determining.) Bratislava : Veda, 260 s.
- [8] Štekauerová, V., Skalová, J., Nováková, K. 2010. Assignment of hydrolimits for estimation of soil ability to supply plants by water. *Növénytermelés*, Vol. 59, ISSN 0546-8191, Supplement, p. 195-198.
- [9] Šútor, J., Štekauerová, V., Nagy, V. 2010. Comparison of the monitored and modeled soil water storage of the upper soil layer: the influence of soil properties and groundwater table level. *J. Hydrol. Hydromech.*, ISSN 0042-790X, 4, s. 279-283.

Trends of Extreme Precipitation Events in Dobrudja

Judicaël Deguenon, Alina Bărbulescu

Abstract – This work presents some results on the trend of climate extreme indices, computed by RCLimDex 1.9.0, for a part of the region of Dobrudja (Romania). The database contains the daily precipitation series, collected at two meteorological stations (Sulina and Tulcea), in the period 1953 - 2008, respectively 1961 - 2005. Kendall's tau based slope estimator has been used to compute the indices' trends. Statistical tests come to infirm the hypothesis of a linear trend existence for Tulcea series, but confirm its existence for 6 precipitation indices associated to Sulina series. We notice a light trend of increasing of number of days with precipitation over 10, 20 25 mm for the last series.

Keywords – climate change, extreme indices, precipitation.

1. INTRODUCTION

The study of extremes is of major importance in the nature sciences, when the extreme events could have disastrous effects for the human activity and life [1].

Based on surface temperature data from 100 European stations, ECSN reports an increment in air temperature during the 20th century. The climate change scenarios for Europe indicate a warming rate between 0.10C and 0.40C per decade [2]. This warming is greatest over Southern and Northeast Europe.

Land degradation/ desertification and drought affect many parts of Central and Eastern Europe. The climate in much of the region, notably in Armenia, Azerbaijan, Bulgaria, Georgia, the Republic of Moldova, Romania, the Russian Federation and Ukraine, is classified as dry sub-humid; some areas, such as that along the northwest coasts of the Black Sea and the Caspian Sea, are even drier and are classified as semi-arid [3]. Therefore, the study of extreme events is of high importance in the design of irrigation systems and of water supply, in a region where the drought period is between 5 and 6 months per year, as Dobrudja. [4]

The analysis of the changes in extremes can be performed using climate extreme indices [5] – [8].

In this study we present only the results obtained after analysing the climate extremes indices for the Sulina and Tulcea meteorological stations, situated in Dobrudja, Romania.

It comes to complete our previous researches concerning the climate evolution in this region of Romania [9] – [12].

2. METHODS

The database is formed by the daily precipitation series collected in the period 1953 - 2008, respectively 1961 – 2005. In this study, RCLimDex software [13] has been run to calculate 11-rainfall extreme indices [14] for Sulina and Tulcea series.

Manuscript received October 1st, 2011 and accepted November 10, 2011.

Judicaël Deguenon is with Université d'Abomey – Calavi, École Polytechnique d'Abomey - Calavi, 01 BP 2009 Cotonou, BENIN (e-mail: tjudy73@yahoo.fr).

Alina Bărbulescu is with Abu Dhabi University, College of Art and Sciences, Department of Applied Sciences and Mathematics, P.O. Box 59911, Abu Dhabi, UAE (e-mail: alina.barbulescu@adu.ac.ae).

In addition to classical indices such as the annual total precipitation (RTOT) and the annual total of wet days, the simple day intensity index (SDII) as the average rainfall from wet days has been also calculated. Two indices consider annual maximum rainfall recorded during 1 and 5 days (Rx1day, Rx5day) and two are based on the 95th and 99th percentiles.

The percentile values are calculated from the daily rainfall data over the chosen periods.

The 95th percentile, defined as a very wet day, corresponds to the 547th highest value recorded over the 30-year reference period. The 99th percentile corresponds to the 110th highest value of the periods and is qualified as an extreme rainfall event.

Very wet day and extreme rainfall frequency are based on the annual count of days with rainfall greater or equal to 95th and the 99th percentiles of the period (R95p and R99p). Very wet day and extreme rainfall intensity corresponds to the annual total precipitation recorded from days with rainfall greater or equal to 95th and 99th percentiles of the period (R95pSUM and R99pSUM) and gives an indication on the rain received from very wet or extreme rainfall. We don't report these results, since they are not significant.

The calculated indices, their measure units and short definitions are as follows [13]:

- Rx1day [mm] - *Maximum 1 - day rainfall* - Annual maximum 1 - day rainfall;
- Rx5day [mm] - *Maximum 5 - days rainfall* - annual maximum 5 - days rainfall;
- SDII [mm/day] - *Simple day intensity index* - average rainfall from wet days;
- R10mm [day] - Annual count of days when the precipitation quantity was ≥ 10 mm;
- R20mm [day] - Annual count of days when the precipitation quantity was ≥ 20 mm (day);
- R25mm [day] - Annual count of days when the precipitation quantity was ≥ 25 mm (day);
- CDD [day] - Maximum length of dry spell - maximum number of consecutive days with the daily precipitation amount less than 1mm;
- CWD [day] - Maximum length of wet spell - maximum number of consecutive days with the daily precipitation amount greater or equal to 1mm;
- R95p [day] - Very wet day frequency - annual count of days with rainfall greater or equal to 95th percentile of 1961 - 1990;
- R99p [day] - Extreme rainfall frequency - annual count of days with rainfall greater or equal to 99th percentile of 1961 - 1990;
- PRCPTOT [mm] - precipitation total - the annual total precipitation.

Before the index calculation, the data has been checked for quality and homogeneity. The quality control involved the data evaluation and outliers detection. Data homogeneity is assessed using the RHtestV2 program [15], based on two-phase regression model with a linear trend for the entire base series [16].

3. RESULTS

In Figure 1 we present the position of the hydro meteorological stations and, in Table 1, their identification data. Tulcea is situated at the mouth of the Danube and Sulina, 13 km off shore.

Table 1. Identification data for meteorological stations

Station	LAT	LON	height (m)	Period
Sulina	+45:10	+29:44	3	1953-2008
Tulcea	+45:11	+28:49	4	1961-2005

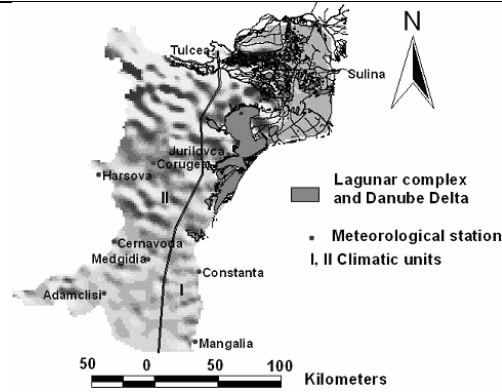


Fig.1 The map of Dobruja and the meteorological stations

In Figs. 2-13 we present the evolution of the indices defined in the previous section, corresponding to Tulcea station.

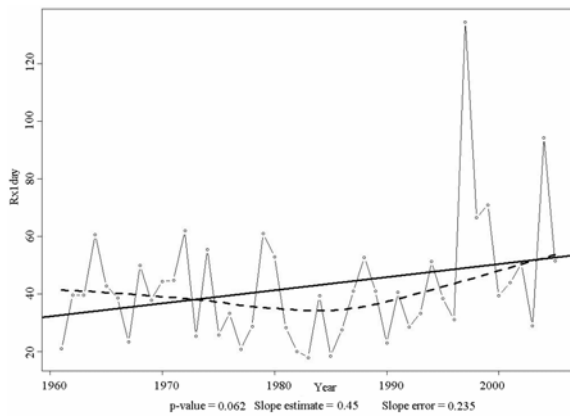


Fig.2 Rx1day evolution for Tulcea series

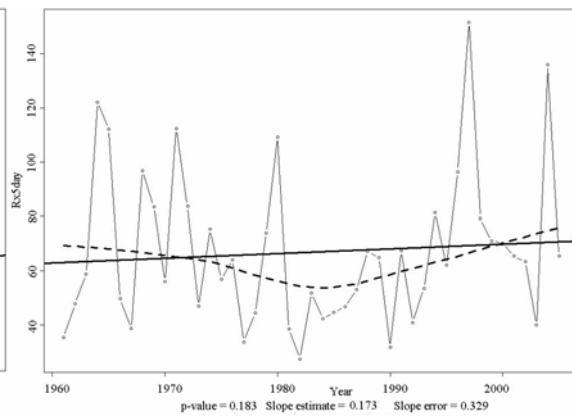


Fig. 3 Rx5day evolution for Tulcea series

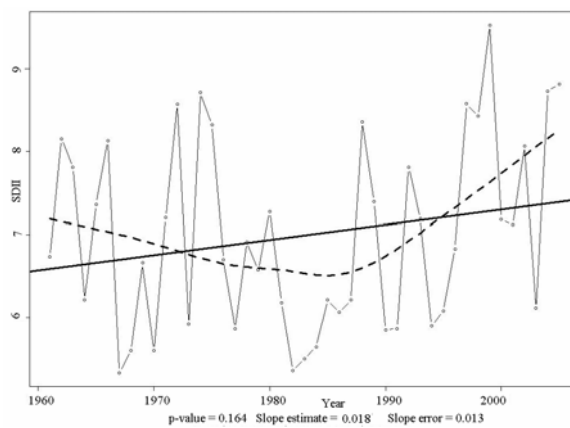


Fig. 4 SDII evolution for Tulcea series

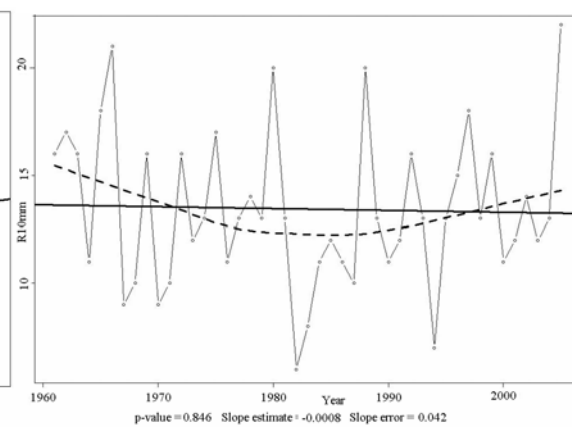


Fig. 5 R10mm evolution for Tulcea series

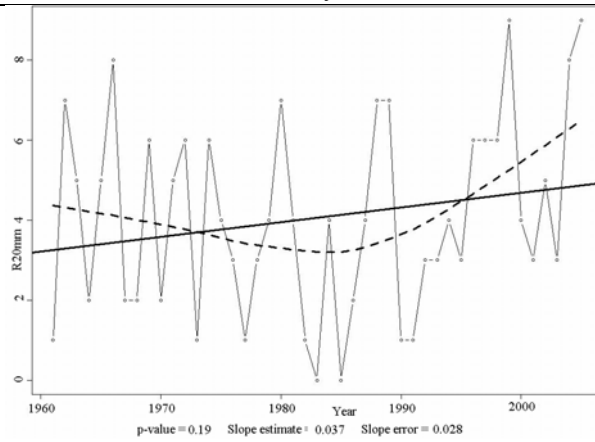


Fig. 6 R20mm evolution for Tulcea series

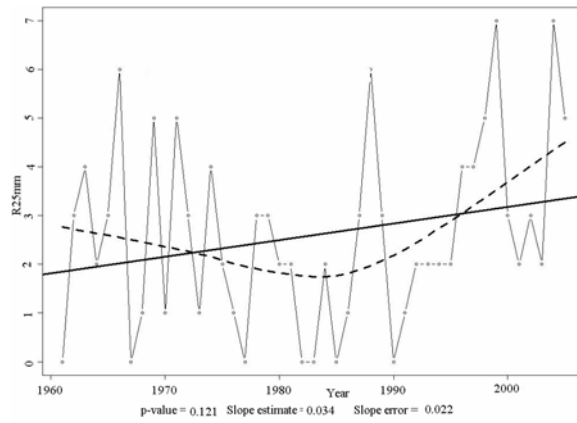


Fig. 7 R25mm evolution for Tulcea series

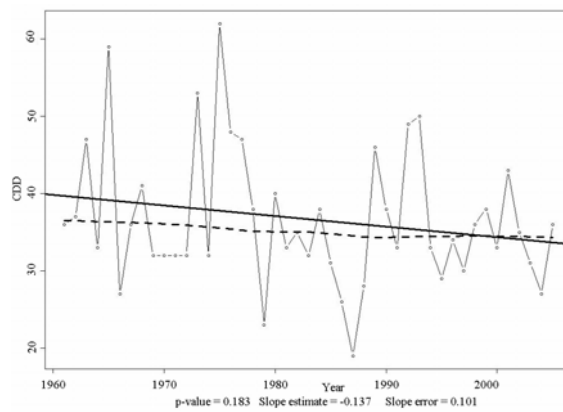


Fig.8 CDD evolution for Tulcea series

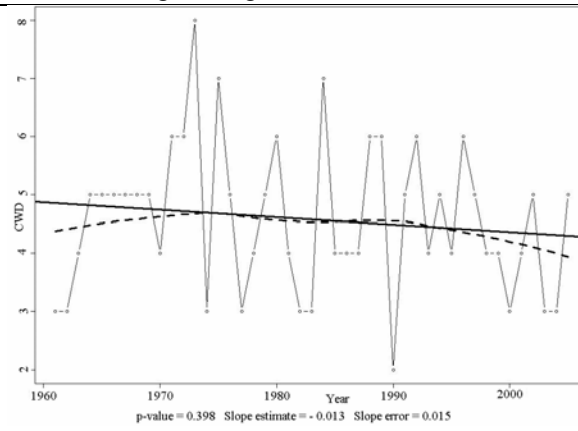


Fig.9 CWD evolution for Tulcea series

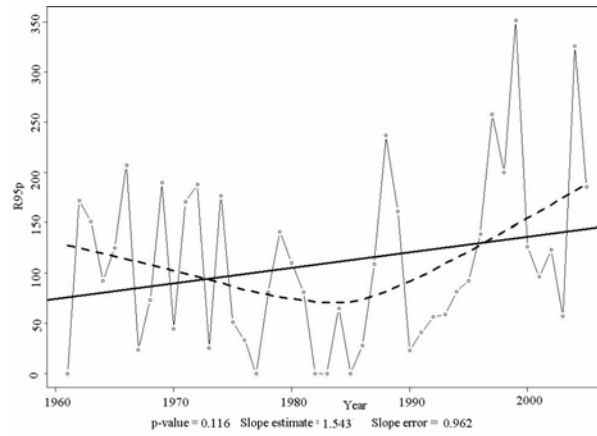


Fig.10 R95p evolution for Tulcea series

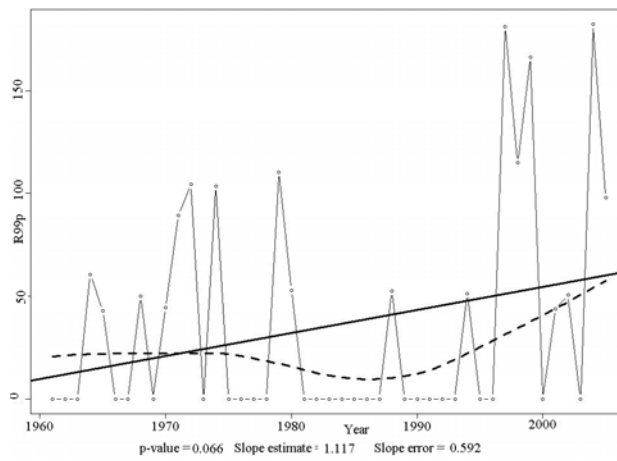


Fig.11 R99p evolution for Tulcea series

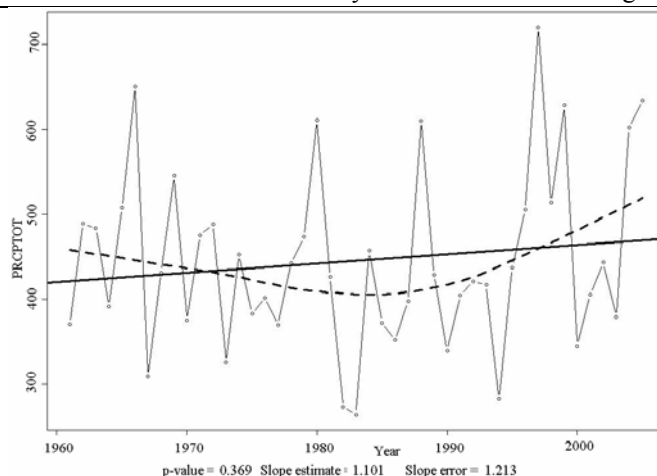


Fig.12 PRCPTOT evolution for Tulcea series

In Table 2 we present the slope and the standard deviation of the slope of the linear trend determined for the evolution of the indices defined in previous section. Kendall's tau based slope estimator has been used to compute the trends since this method doesn't assume a distribution for the residuals and is robust to the effect of outliers in the series.

Table 2. The trend of 11 indices for Sulina and Tulcea precipitation series

Indices	Station					
	Sulina			Tulcea		
	Slope	Stdev.	P - value	Slope	Stdev.	P - value
Rx1day	0.126	0.071	0.083	0.450	0.235	0.062
Rx5day	0.107	0.081	0.191	0.173	0.329	0.603
SDII	0.015	0.008	0.077	0.018	0.013	0.164
R10mm	0.033	0.011	0.004	-0.008	0.042	0.846
R20mm	0.007	0.003	0.032	0.037	0.028	0.190
R25mm	0.005	0.002	0.022	0.034	0.022	0.121
CDD	0.759	0.716	0.295	-0.137	0.101	0.183
CWD	0.119	0.078	0.134	-0.013	0.015	0.398
R95p	0.848	0.293	0.006	1.543	0.962	0.116
R99p	0.479	0.165	0.006	1.117	0.592	0.066
PRCPTOT	1.261	0.488	0.013	1.101	1.213	0.369

The P-value has also been calculated. If this value is less than 0.05, the hypothesis that the trend is statistical significant is accepted at 95% level of confidence. This happened only for six indices (R10mm, R20mm, R25mm, R95p, R99p, PRCPTOT) calculated for Sulina station (Table 2, column 4, the grey cells).

If the standard deviation of the slope is greater than the absolute value of slope estimate, we can not trust the slope estimate, as in the case of Rx1day, R10mm, CWD, PRCPTOT calculated for Tulcea series (the highlighted cells in Table 2, column 6).

Analysing Figs. 2 – 12, we remark that the trend obtained by locally weighted regression (the dashed lines) for Tulcea, has a minimum in the period 1980 – 1990, excepting CDD and CWD. Applying the same method for Sulina, an accentuated increasing trend has been emphasised for the period after 2004.

4. CONCLUSIONS

The results show that the variation of precipitation indices was different for the analysed stations. R10mm, R20 mm, R25mm, R95p, R99p, PRCPTOT registered an increasing slope of the trend for Sulina series, explained by the high quantity of precipitation registered there after 2004 with respect to the previous period. (Fig. 12)

The distribution of the precipitation over 1 mm, present an accentuated left - asymmetry for both series (Fig.13).

Even than there is a relatively small distance between the meteorological stations, the precipitation distribution was different, fact explained by the geographical position of Sulina station - in the Danube Delta.

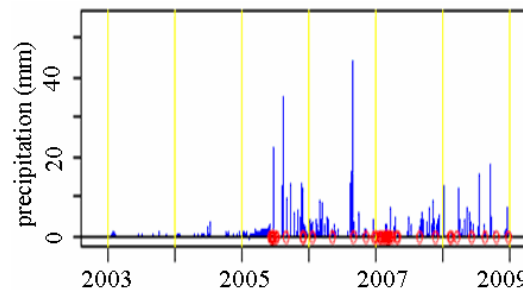


Fig. 12 Daily Precipitation registered at Sulina station

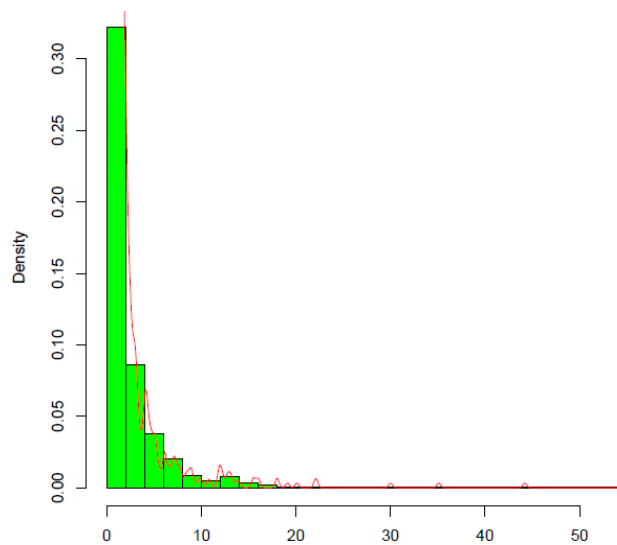


Fig.13 Histogram of precipitation over 1 mm (Sulina station)

5. REFERENCES

- [1] Qian W., Lin X., 2005. *Regional trends in recent precipitation indices in China*, Meteorology and Atmospheric Physics, vol. 90, pp. 193-207.
- [2] European Climate Support Network (ECSN). 1995, *Climate of Europe: Recent Variation, Present State and Future Prospects*. KNMI, De Bilt
- [3] United Nations Message by Secretary-General Kofi Annan on the World Day to Combat Desertification and Drought, 17 June 2004, <http://www.un.org/News/Press/docs/2004/sgsm9329.doc.htm>

- [4] Maftai C., Bărbulescu A., *Statistical analysis of climate evolution in Dobrudja region*. 2008, Lecture Notes in Engineering and Computer Sciences. Proceedings of the World Congress on Engineering, Vol II, pp.1082-1087, http://www.iaeng.org/publication/WCE2008/WCE2008_pp1082-1087.pdf
- [5] Alexander L.V. et al., 2006. *Global observed changes in daily climate extremes of temperature and precipitation*, J. Geophys. Res., 111 (D05109), doi:10.1029/2005JD006290.
- [6] Beniston M. et al., 2007. *Future Extreme Events, In European climate: An exploration of regional climate model projections*, Clim. Change, 81, pp. 71–95.
- [7] Frei C. R., et al, 2005. *Future change of precipitation extremes in Europe: an intercomparison of scenarios from regional climate models*, J Geophys Res 110 (D3), pp. 4124–4137
- [8] Klein Tank A. M. G., Konnen, G.P., 2003. *Trends in indices of daily temperature and precipitation extremes in Europe, 1946–99*, J. Clim., 16, pp. 3665–3680.
- [9] Bărbulescu A., Băutu E., 2009. *ARIMA and GEP models for climate variation*, International Journal of Mathematics and Computation, vol. 3, No J09 pp. 1 – 7
<http://www.ceser.res.in/ceserp/index.php/ijmc/issue/archive>
- [10] Bărbulescu A., Băutu, E., 2010. *Mathematical models of climate evolution in Dobrudja*, Theoretical and Applied Climatology, vol.100, nos.1 – 2/March, pp. 29 - 44, doi: 10.1007/s00704 – 009 – 0160 – 7
- [11] Bărbulescu A., Maftai C., Băutu, E., 2010. *Modeling the hydro-meteorological time series. Applications to Dobrudja region*, Lambert Academic Publishing GmbH & Co. KG, Germany.
- [12] Deguenon J., Bărbulescu A., 2011. *Study of Extreme Daily Rainfall Using GPD Model*, International Journal of Mathematics and Computation, vol.11, no. J11, pp. 28 – 37
- [13] Zhang X., Yang F., 2004. *RClimDex (1.0) User Manual*, 22p.
- [14] Peterson T.C., et al., 2001. *Report on the Activities of the Working Group on Climate Change Detection and Related Rapporteurs 1998-2001*. WMO, Rep. WCDMP - 47, WMO - TD 1071, Geneva, Switzerland, 143pp.
- [15] <http://cccma.seos.uvic.ca/ETCCDMI/software.shtml>
- [16] Wang X. L., 2003. *Comments on "Detection of undocumented change points: A revision of the two-phase regression model."*, J. Climate, 16, pp. 3383 -3385.

Statistical Analysis of Precipitation Variability in Dobrudja Region

Carmen Maftai, Alina Bărbulescu, Cristina Serban (Gherghina), Iulia Ilie

Abstract – In this article we present the results of the statistical analysis of annual precipitation collected for a period of 45 years, at ten meteorological stations situated in Dobrudja region, Romania.

First, some break tests have been performed to determine the discontinuities in the precipitation series. After that, the characteristics of the evolution of precipitation have been studied, and the periods with an increasing or decreasing trend have been emphasized. The analysis indicates an inhomogeneous behaviour of precipitation over Dobrudja. The values of precipitation registered after 1995 reveal an increment of 82.8mm, a value in agreement with existing estimations for the whole Europe.

Keywords – break test, precipitation, statistical analysis, time series.

1. INTRODUCTION

Climatic change has an enormous impact on economic and social activities. Therefore there is an increasing interest for research in the area. Climate warming could severely affect precipitation in different ways, including changes in frequency, intensity, and timing of occurrence [16], [20], [25], [40]. A 2001 assessment of the IPCC-Intergovernmental Panel on Climate Change [18] concluded that as effect of the increase of greenhouse gas concentrations “...over many Northern Hemisphere mid- to high-latitude land areas, more intense precipitation events are very likely”. Annual zonal average precipitation increased by 7% to 12% for the zones 300N to 850N in emerged landmasses in the Northern hemisphere, except in the Far East [18]. At the planetary scale, the models consistently simulate an intensification of the hydrological cycle in a future climate, warmer than the present-day one [3]. This simulation highlights the annual impact of climatic change on precipitation in Europe [11]. In winter, the precipitation increase is more significant in Northern Europe [33].

A downward pluvial trend was observed in Western Africa, starting from the end of the 1960s or the beginning of the 1970s, to the beginning of the 1990s [7], [14], [23], [33]. Gong and Wang [13] and Qian and Zhu [38] indicated a significant negative precipitation trend in eastern China for 1954 – 1976 and a subsequent positive trend for 1977 – 1998.

Figure 1 is based on the scenario of the Special Report on Emission Scenarios (SRES) of the IPCC [17], [18], [19]. The effects of the climate change in Europe were estimated for the period 2071 – 2100 in comparison with the period 1961 – 1990. The map is based on the data of DMI/PRUDENCE [27], processed by the Joint Research Centre (JRC) during the PESETA study [28]. The figure depicts a considerable increase of the precipitation quantities Northern Europe (+20 - +80 % of the total annual quantity of precipitation), while in the

Manuscript received October 1st, 2011 and accepted November 10, 2011.

C. Maftai is with Ovidius University of Constantza, Faculty of Civil Engineering, ROMANIA (e-mail: cmaftai@univ-ovidius.ro)

A. Bărbulescu is with Ovidius University of Constantza, Faculty of Mathematics and Computers Sciences, ROMANIA (corresponding author; phone: 0040 744 284444; e-mail: alinadumitriu@yahoo.com).

C. Serban (Gherghina) is with Ovidius University of Constantza, Faculty of Civil Engineering, ROMANIA (e-mail: serban.cristina@univ-ovidius.ro).

I. Ilie is a master student at Ovidius University of Constantza, Faculty of Mathematics and Computers Sciences, ROMANIA (e-mail: iulia_ilie1988@yahoo.com)

south of the continent the periods of drought are increasingly frequent (-20-60% of the total quantity of precipitation). From this figure, we observe a decrease between 5 and 20% of the total annual quantity of precipitation, in Romania, excepting its northern the north-eastern part, where an increase between 5 and 10% of the total annual quantity of precipitation is predicted. In the Dobrudja region, we observe a variation between -5 and +5% of the total precipitation.

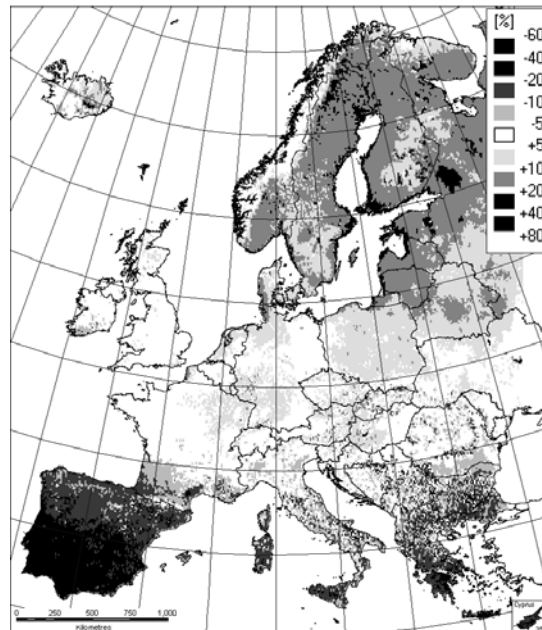


Fig. 1 Estimated evolution of annual mean precipitation for the period 2071-2100 (PRUDENCE Project: reference interval: 1961-1990)

At the country level, Busuioc's study [10] shows a general decrease in precipitation, with some increase in the extremes North - East and South - East (Fig. 2).

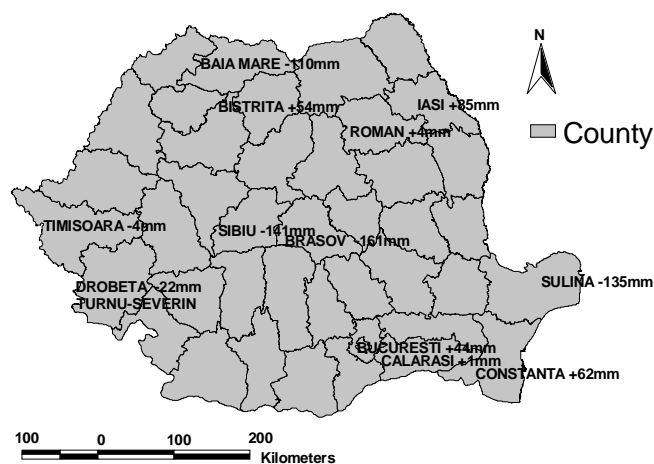


Fig.2 General evolution of precipitation (adapted from [6])

In the attempt of analysing the climate hazards generated by precipitation in Câmpia de Vest (Western Plains), situated in the north of the Mureş River, Şerban [32] concludes that the hazard generated by the excess of precipitation is more intense than that generated by the precipitation deficit, which is due to the oceanic climate influence in this area. The hazard generated by abundant rainfall cumulated over short periods of time (2, 3, 4, 5 days) have increased in the past few years.

Such a situation cannot be ignored, because its effects could be tragic. There is a risk to jeopardize the projects of the agricultural development program, and to perturb the efficiency of the structures built in previous years (such as irrigation works that sometimes stopped working in summer, as a result of the dramatic decrease of the Danube water level). In this context, this paper attempts to identify discontinuities in precipitation time series, using statistical analysis, in order to determine the existence of significant changes in the precipitation regime in Dobrudja.

This paper describes the methodology used for the detection of break points in the precipitation series and presents the results.

2. STUDY AREA

Dobrudja (Dobrogea, in Romanian) is a region situated in the South – East of Romania, between the Black Sea and the lower Danube River (Fig. 3).

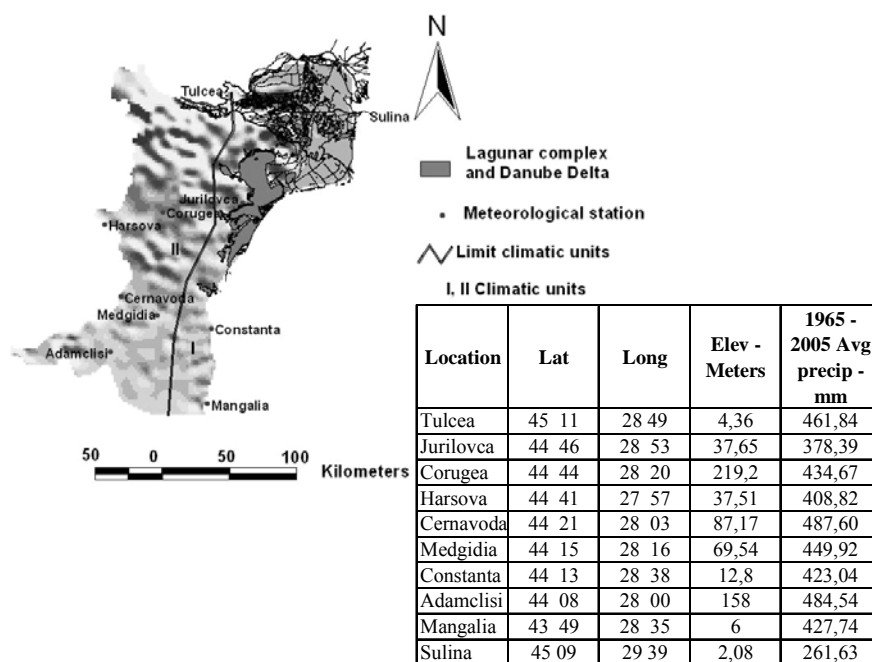


Fig. 3 Dobrudja region and the ten meteorological stations

Dobrudja (without the Danube Delta) is a plateau with hilly aspect. In the North, remnants of Hercinian and Caledonian mountains are present, with an altitude up to some 400m (Greci Peak 467 m). The altitude decreases towards the South, where the average altitude is between 100 and 180m [26]. Generally, Dobrudja's climate is temperate-continent and is divided in two units (Fig. 3): (I), which contains the Danube Delta, the lagoons (Razim Lake and Sinoe Lake) and the Eastern part of the region and (II), which contains the rest of territory, where the climate is influenced by the moderate continental belt. The average air temperature is slightly over 11°C towards the littoral area and the Danube floodplain, and no more than 10 - 11°C in its Northern and central part [24].

3. METHODS

The ten time series used in this study, obtained from the archives of the National Agency of Meteorology, contain the annual average precipitation spanning the period 1965 - 2005 for Dobrudja region. The stations names, their locations, elevations and multi-annual means of precipitation are presented in Fig. 3. We observe that 5 of the 10 meteorological stations are situated in the first climatic unit and the other 5 in the second climatic unit. We have to point out that Sulina station is situated 13 km offshore, on Sulina horn dam.

The methodology presented in this paper, and applied to Dobrudja region, consists of an analysis of the temporal characteristics, and the identification of the discontinuities in precipitation time series. The steps that were followed are: estimation of the annual mean precipitation for each station, estimation of the multi-annual mean precipitation for each station, determination of the anomaly chart, and detection of the discontinuities in data series.

In order to determine the discontinuities in the precipitation regime over the period 1965–2005, some homogeneity and break tests are performed.

We define a break as a change of the probability distribution function of a process variable at a certain moment [22]. The break tests allow the detection of a change in a time series mean.

The methods used to detect a break are: Pettitt test [27], Buishand test [8], [9], Lee and Heghinian test [23] and the segmentation procedure of Hubert [14], [15]. The null hypothesis that is tested is that there is no break in the precipitation series $(X_i)_{i \in \overline{1, N}}$.

The *Pettitt test* is a non-parametric test. To perform it, the steps are [6]: (i) the studied series is divided into two sub-samples of sizes m and n respectively; (ii) the values of the two samples are grouped and arranged by increasing order; (iii) the sum of the ranks of the components of each sub-sample in the total sample is then calculated; (iv) a statistic, U_t , is defined using the two sums thus obtained in order to assess whether the two samples belong to the same population.

Let us define:

$$\text{sgn}(x) = \begin{cases} 1, & x > 0 \\ 0, & x = 0 \\ -1, & x < 0 \end{cases}, \quad (1)$$

$$D_{i,j} = \text{sgn}(x_i - x_j), \quad (2)$$

$$U_{t,N} = \sum_{i=1}^t \sum_{j=t+1}^N D_{i,j}, \quad (3)$$

$$K_N = \max_{t=1, N-1} |U_{t,N}|. \quad (4)$$

If k is the value of K_N taken on the studied series, under the null hypothesis, then:

$$\text{Prob}(K_N > k) \approx 2 \exp(-6 \cdot k^2 / (N^3 + N^2)) \quad (5)$$

If $\text{Prob}(K_N > k) < \alpha$, for a significance level α , then the null hypothesis is rejected.

The *Buishand* and *Lee & Heghinian tests* are Bayesian procedures applied under the assumption that the

studied series is normally distributed. The tests are based on the following model, which supposes a change in the series mean:

$$X_i = \begin{cases} \mu + \varepsilon_i & , \quad i = 1, \dots, m \\ \mu + \varepsilon_i + \delta, & i = m + 1, \dots, N \end{cases} \quad (6)$$

where ε_i are random variables, independent and normally distributed, with null expectation and a constant variance. The break point m and the parameters μ and δ are unknown.

The *Lee & Heghinian method* works in the hypothesis that $(X_i)_{i=1, \dots, N}$ is a series of independent variables, with a constant variance. The method determines the a posteriori probability distribution function of the parameters μ and δ , considering their a priori distributions and supposing that the break time follows a uniform distribution. The range of the break time corresponds to the values of the modes of the a posteriori distributions of m and δ respectively.

Hubert's segmentation procedure detects the multiple breaks in time series. The principle is to cut the series into m segments ($m > 1$) such that the calculated means of the neighbouring sub-series significantly differ. To limit the segmentation, the means of two contiguous segments must be different to the point of satisfying Scheffe's test. The procedure gives the timing of the breaks.

CUSUM charts are constructed by calculating and plotting a cumulative sum based on the data. CUSUM charts show the cumulative sum of differences between the values and the average. Since the average is subtracted from each value, the cumulative sum also ends at zero [37].

If x_i , $i = \overline{1, n}$ represent the registered data, the cumulative sums S_i are calculated by:

$$S_0 = 0, S_i = S_{i-1} + (x_i - \bar{x}), i = \overline{1, n}, \quad (7)$$

where $\bar{x} = \sum_{i=1}^n x_i$ is the average.

The anomaly chart procedure calculates the overall average precipitation for the base period specified. The procedure then calculates the annual differences between each yearly mean precipitation and the base period mean precipitation. To facilitate the understanding of anomaly charting, negative anomalies are represented below the abscissa, positive anomalies above.

In order to facilitate the trend computation in the precipitation patterns in Israel, Steinberger and Gazit-Yaari [30] introduced the concept of "normalized variable", calculated by dividing the actual precipitation by the average rainfall at one station and multiplying by 100%. The same index (named "Percent of Normal") is used by Willeke [34] in the drought analysis. A disadvantage of the use of this index is that the mean precipitation is often not the same as the median, which is the value exceeded by 50% of the precipitation occurrences in a long-term climate record [34].

We use this concept, with one modification: the annual precipitation is normalized by the regional multi-annual mean precipitation (considered to be a 41 year mean calculated by Thiessen method). This index will be called "Normal Precipitation".

4. RESULTS AND DISCUSSION

A. Analysis of Precipitation Variation

Figure 4 represents the spatial evolution of the multi-annual mean precipitation in Dobrudja. The isohyets are automatically generated in GIS ArcView®, by spline interpolation on the base of the annual mean precipitation calculated at each station.

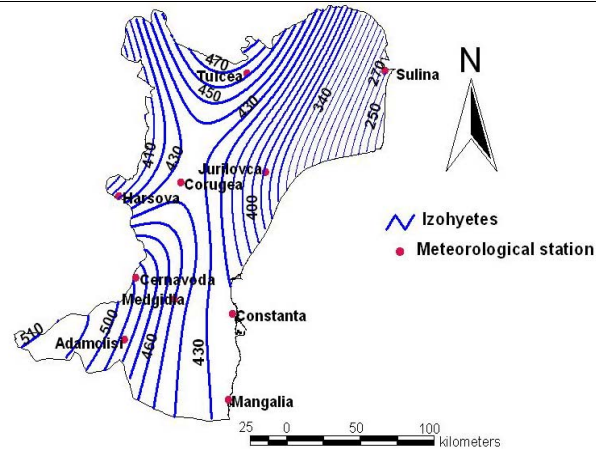


Fig. 4 Multi-annual mean precipitation

The multi-annual mean precipitation varies within large limits (260–500 mm approximately), the highest values being registered in the North and centre of the region. The precipitation values increase with altitude. The lowest precipitation was registered at Sulina (262 mm at 2 m), Constantza (423 mm at 12 m) and Mangalia (427 mm at 6 m) – on the coast, respectively at Harsova (408 mm at 37.31m), on the Danube, and the largest at Tulcea (462 mm at the North).

The variation of the annual mean precipitation for each station (Fig. 5) reveals the succession of the humid and dry years during the study period.

It can be remarked that the same evolution pattern is present at all the stations, i.e. starting in 1995 the mean annual precipitation at each station is higher than the multi-annual mean precipitation (but 2000 and 2001, which are the driest years). This remark suggests that the mean precipitation of the sample 1965 - 1995 and that of the sample 1996 - 2005 are different. In order to demonstrate the values of the annual mean precipitation and the multi-annual mean precipitation are represented for Mangalia station (Fig. 6).

The precipitation anomaly chart (Fig.7) shows the difference between the annual precipitation and the average precipitation during a base period.

The positive anomaly shows those years when the annual mean precipitation exceeded the 1965-2005 baseline average; the negative anomaly shows those years when the mean precipitation was less than the baseline average.

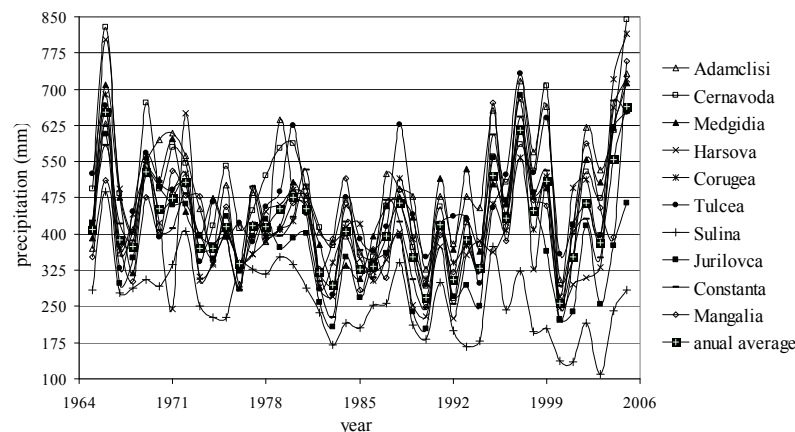


Fig. 5 The mean multi-annual precipitation at the study stations during the period 1965-2005

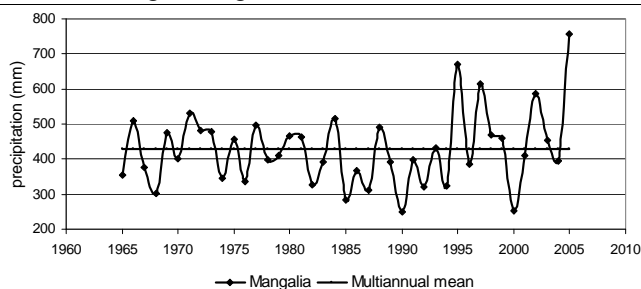


Fig. 6 The evolution of the mean precipitation –Mangalia station

The analysis of the anomaly chart reveals: (i) a negative anomaly, for the period 1981 – 1995 (approx.), excepting Sulina series, where the period with negative anomaly started in 1982; (ii) a positive anomaly for the period 1965 – 1973 and 1995 (1997) – 2005.

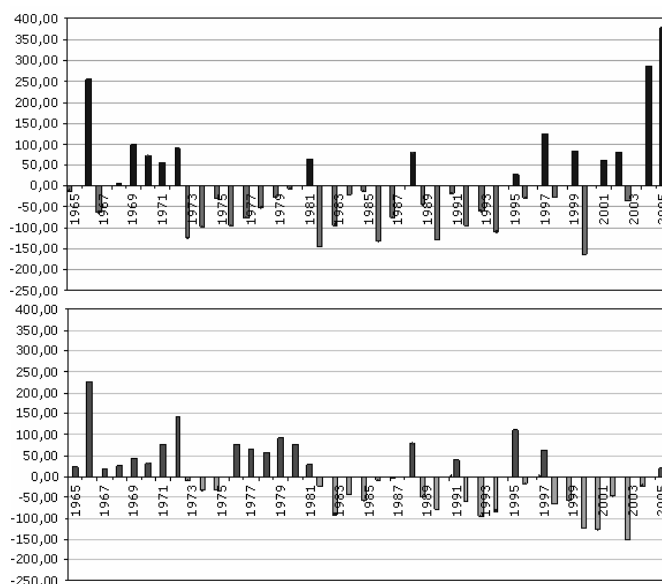


Fig. 7 Example of annual precipitation anomaly chart for Corugea and Sulina series

B. Break analysis

Firstly, the normality, correlation and homoscedasticity hypotheses were tested [2] – [5]. Since some series are not normally distributed, they were normalized by Box – Cox transformations, in order to allow the application of certain break tests. The results of these tests are (Table 1): two tests (Pettitt and Buishand) give the same result, i.e. there is a break in the mean annual precipitation series only for Sulina station. The tests Lee & Heghinian test and Hubert procedure detect a break point, which appears in 2003 or 2004.

Since the results of the procedures are inconclusive, a test of homogeneity (Wilcoxon procedure) was also performed (Table 2).

The choice of the year 2003 (or 2004) as moment of separation into two sub-samples is not conclusive, since there is not enough data. Therefore, other points have been chosen to apply this test.

Interpreting a CUSUM chart requires some practice. The CUSUM chart trend shows the way in which the individual values compare to the overall average. Each time the measurements are below the overall average, the CUSUM decreases. Each time the values are above the overall average, the CUSUM increases. A slope change

in the CUSUM graph indicates a sudden change in the average. Periods where the CUSUM chart follows a relatively straight path indicate a period where the average did not change.

Two CUSUM charts are plotted in Figs. 8 and 9, where a sudden change in direction can be seen around 1995. The results of the CUSUM charts of the series are presented in Table 3, where it can be seen that around 1995 the average shifted. The conclusion of the analysis is that the precipitation regime is changing in Dobrudja area.

Table 1. Results of break tests

Station	Test							Lee & Heghinian	Hubert
	Buishard			Pettitt					
	99%	95%	90%	99%	95%	90%	Year		
Adamclisi	no	no	no	no	no	no	-	2003	2003
Cernavoda	no	no	no	no	no	no	-	2004	2004
Medgidia	no	no	no	no	no	no	-	2003	2003
Harsova	no	no	no	no	no	no		2003	2003
Corugea	no	no	no	no	no	no		2003	2003
Tulcea	no	no	no	no	no	no		no	2003
Sulina	yes	yes	yes	yes	yes	yes	1981	1981	1981
Jurilovca	no	no	no	no	no	no	-	1972	no
Constantza	no	no	no	no	no	no	-	2003	2003
Mangalia	no	no	no	no	no	no	-	2004	2004

Table 2. The result of the Wilcoxon test

Hypothesis: H ₀ The average for the two samples are equal H ₁ The average for the two samples are not equal				
Adamclisi	Cernavoda	Medgidia	Harsova	Corugea
Result -1995 W = 2.40 p = 0.0165 H ₀ rejected at 5%, accepted at 1%	Result -1995 W = 2. p = 0.0329 H ₀ rejected at 5%, accepted at 1%.	Result -2000 W = 1.97 p = 0.0486 H ₀ rejected at 5%, accepted at 1%	Result -1973; 2003 W = 1.99; 2.21 p = 0.046; 0.027 H ₀ rejected at 5 %, accepted at 1%	Result -1973; 2000 W = 2.29; 2.25 p = 0.022; 0.024 H ₀ rejected at 5%, accepted at 1%
Tulcea	Sulina	Jurilovca	Constantza	Mangalia
Result -2003 W = 1.97 p = 0.0492 H ₀ rejected at 5%, accepted at 1%	Result -1981 W = 3.72 p = 0.000202 H ₀ rejected at 5%, accepted at 1 %	Result -1982; W = 2.26 p = 0.0237 H ₀ rejected at 5%, accepted at 1 %	Result -1995 W = 2.43 p = 0.0152 H ₀ rejected at 5%, accepted at 1%	Result W = 1.73 p = 0.0832 H ₀ accepted at 5%,

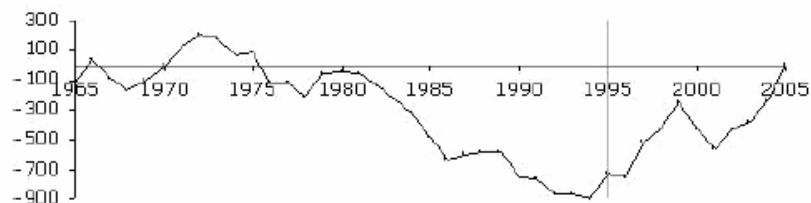


Fig. 8 CUSUM chart for Adamclisi station

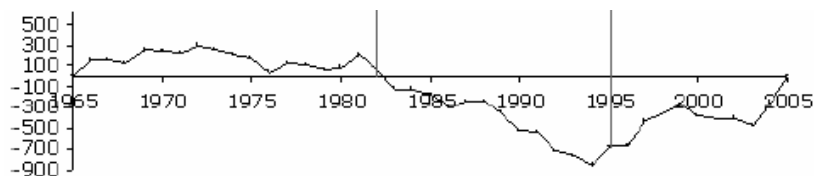


Fig. 9 CUSUM chart for Constantza station

Table 3. Results of CUSUM

	Adamclisi	Cernavoda	Medgidia	Corugea	Harsova	Tulcea	Sulina	Jurilovca	Constantza	Mangalia
Mean	484.54	487.6	449.92	408.82	434.67	461.84	261.63	378.39	423.04	427.74
Conf. level	93%	91%	93%	96%	95%		100%	98%	94%	
Break pts.	1995	1995	2002	1973	1973		1982	1982	1982	
Average 1	454.5	465.3	433.8	497.5	497.2		314.6	418.8	434.8	
Average 2	0.0	0.0	0.0	392.9	367.8		224.1	300.3	341.8	
Change pt				2002	2004			1995	1995	
Average 1				392.9	367.8			300.3	341.8	
Average 2				611.9	691.8			491.5	500.8	
Change pt								1999		
Average 1								491.5		
Average 2								353.1		

We observe that the Wilcoxon test and CUSUM procedure gives the same results concerning the break point year.

Analysing the results of “Normal Precipitation” index we observe that the Dobrudja region can be dividing in 3 zones:

- on the Littoral (without Danube Delta and Laguna complex), the index decreases in the period 1965 – 1995 and is constant or slightly increasing after 1995 (Fig. 10- Mangalia series);
- on the Danube Delta and Lagunar Complex, the trend of normalized precipitation is decreasing, but the slope of linear regression is bigger for the period 1995-2005 than for 1965 - 1995 (Fig. 11- Jurilovca Series);
- in the central and western zone, the index decreases in the period 1965-1995 and increases for 1995-2005 (Fig. 12- Harsova series).

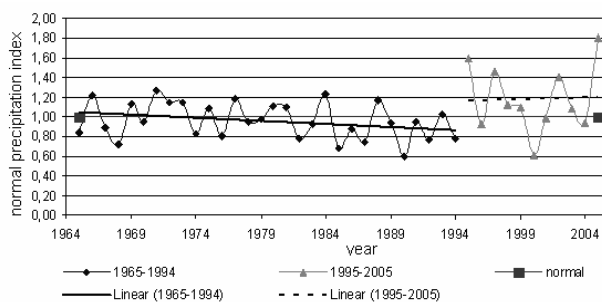


Fig.10 Evolution of the normal precipitation index for Mangalia series

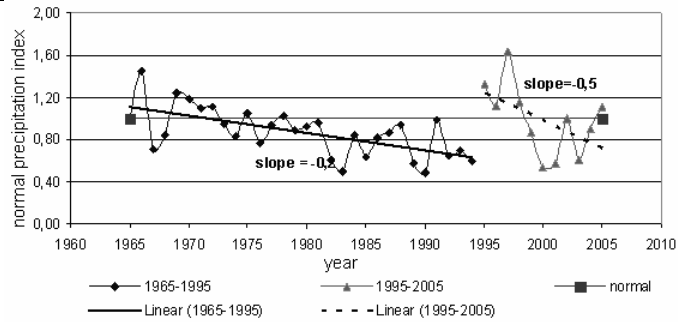


Fig.11 Evolution of the normal precipitation index for Jurilovca series

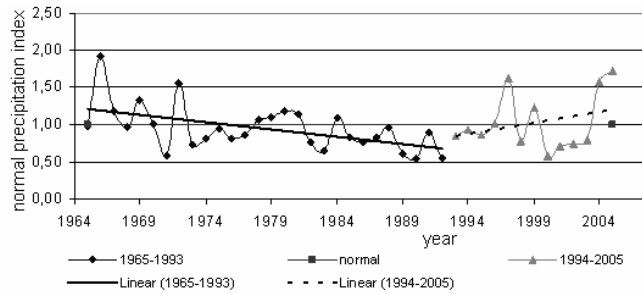


Fig.12 Evolution of the normal precipitation index for Harsova series

The conclusions of CUSUM analysis are:

- 1995 is the break point year,
- In the climatic unit II, the mean annual precipitation increased with 82.8 mm after 1995, fact that is in concordance with the estimations made for Romania and Europe.
- In the climatic unit I (without Jurilovca and Sulina station) the mean annual precipitation increased with 98 mm. Unfortunately the precipitation distribution is not uniform in time. For example, at the Constantza station, a precipitation value of 259 mm was recorded in August 2004, representing one third of the annual mean precipitation at this station.

The isohyet's maps (Figs. 13) depict a general increase of the mean multi-annual precipitations after 1995, compared to the period 1965-1995.

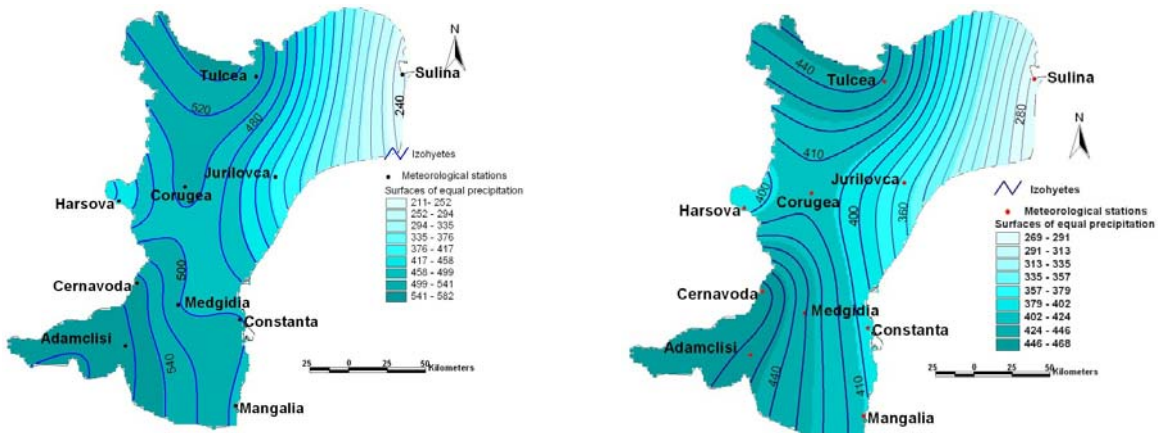


Fig. 13 The isohyets corresponding to the periods 1965 – 1995 and 1995 – 2005

5. CONCLUSION

Statistical tools were used to study the precipitation variation in a region of Romania. They indicate different trends of the precipitation evolution, function of the position of the meteorological station in the Dobruđja region.

Since the break point analysis provided contradictory results, the CUSUM was also performed, leading to the conclusion that generally, starting to 1995, an important movement of the isohyets to the North-West, in the Danube floodplain and the lagoon region, where the precipitation rates decrease, concomitant with the increase of the precipitation rate over the littoral area was registered.

The results obtained are in concordance to those predicted for the Europe.

6. REFERENCES

- [3] A. Bărbulescu, *Time series with applications*. Iasi: Junimea, 2002, Ch.3.
- [4] A. Bărbulescu and E. Băutu, "Meteorological Time Series Modelling Based on Gene Expression Programming", *Recent Advances in Evolutionary Computing*, 2009, pp. 17 – 23. Available: <http://www.wseas.us/e-library/conferences/2009/prague/EVOLUTIONARY/EC02.pdf>
- [5] A. Bărbulescu and E. Băutu, "ARIMA Models versus Gene Expression Programming In Precipitation Modeling", *Recent Advances in Evolutionary Computing*, 2009, pp.112 – 117. Available: <http://www.wseas.us/e-library/conferences/2009/prague/EVOLUTIONARY/EC16.pdf>
- [6] A. Bărbulescu and E. Pelican, "ARIMA models for the analysis of the precipitation evolution" in, *Recent Advances in Computers*, 2009, pp. 221-226. Available: <http://www.wseas.us/e-library/conferences/2009/rodos/COMPUTERS/COMPUTERS32.pdf>
- [7] A. Bărbulescu, C. Șerban (Gherghina) and C. Maftai, "Evaluation of Hurst exponent for precipitation time series", in *Latest Trends on Computers*, Vol.II, 2010, pp. 590 – 595. Available: www.wseas.us/e-library/conferences/2010/Corfu/COMPUTERS/COMPUTERS2-31.pdf
- [8] J. F.Boyer, Logiciel Khronostat d'analyse statistique de séries chronologique, IRD UR2, Programme 21 FRIEND AOC, Equipe Hydrologie UMRGBE, Université de Montpellier II, Ecole des Mines de Paris, 2002. Available: <http://www.hydrosociences.org/mytech/khronostat.html>
- [9] J. P. Bricquet, F. Bamba, G. Mahe, M. Toure and J.C. Olivry, "Variabilité des ressources en eau de l'Afrique Atlantique", *PHI - V*, 6, 1997, pp. 83-95.
- [10] T. A. Buishand, "Some methods for testing the homogeneity of rainfall records", *Journal of Hydrology*, 58, 1982, pp.11-27.
- [11] T. A. Buishand, "Tests for detecting a shift in the mean of hydrological time series", *Journal of Hydrology*, 58, 1984, pp.51-69.
- [12] A. Busuioc, C. Boroneant, M. Baciuc and A. Dumitrescu, *Observed temperature and precipitation variability in Romania*, 1995.
- [13] H. Douville, F. Chauvin, S. Planton, J. - F. Royer, D. Salas-Mélia, S. Tyteca, "Sensitivity of the hydrological cycle to increasing amounts of greenhouse gases and aerosols", *Clim. Dyn.*, 20, 2002, pp. 45 - 68,
- [14] European Climate Support Network (ECSN), *Climate of Europe: Recent Variation, Present State and Future Prospects*, KNMI, De Bilt, 1995
- [15] D. Y. Gong and S.W. Wang, "Severe summer rainfall in China associated with aggravated global warming", 2000, *Climate Research*, 16, pp. 51–59
- [16] P. Hubert, J. P. Carbonnel and A. Chauuche, "Segmentation des séries hydrométéorologiques. Application à des séries de précipitations et de débits de l'Afrique de l'Ouest", *Journal of Hydrology*, 110, , 1989, pp. 349-367.
- [17] P. Hubert and J. P. Carbonnel, "Segmentation des séries annuelles de débits de grands fleuves africains", *Bulletin de liaison du CIEH*, 92, 1993, pp. 3-10.

- [18] C. Huntingford, R.G. Jones, C. Prudhomme, R. Lamb, J.H.C. Gash, and D.A. Jones, "Regional climate - model predictions of extreme rainfall for a changing climate", *Q. J. R. Meteorol. Soc.*, 129, 2003, pp. 1607–1621.
- [19] IPCC, *Climate changes 1995: Contribution of Working Group I to the Second Report of the Intergovernmental Panel on Climate Change*, 1995, pp. 141–193.
- [20] IPCC, *Climate Change 2001: The Scientific Basis*. Cambridge: Cambridge University Press, 2001
- [21] IPCC, *Climate Change 2007: The Scientific Basis*. Cambridge: Cambridge University Press, 2007
- [22] V. Kharin and F. Zwiers, "Changes in the extremes in the ensemble of transient climate simulations with a coupled atmosphere–ocean", *GCM J. Climate*, 13, 2000, pp. 3760–3788.
- [23] A. F. S. Lee and M.S. Heghinian, "A Shift of the Mean Level in a Sequence of Independent Normal Random Variables - A Bayesian Approach", *Technometrics*, 19(4), 1977, pp. 503-506.
- [24] H. Lubes, M. Masson, E. Servat, J.-E. Paturel, B. Kouame and J.F. Boyer, *Caractérisation de fluctuations dans une série chronologique par applications de tests statistique*, Programme ICCARE, Rapport no 3, 1994, 21 pp.
- [25] G. Mahe, J.C. Olivry, "Variations des précipitations et des écoulements en Afrique de l'ouest et centrale de 1951 à 1989", *Sécheresse*, 6 (1), 1995, pp. 109 – 117.
- [26] C. Maftai and A. Bărbulescu, "Statistical analysis of climate evolution in Dobrudja region", *Lecture Notes in Engineering and Computer Sciences*, WCE 2008, vol. II, pp. 1082 -1087.
- [27] W. May, R. Voss and E. Roeckner, "Changes in the mean and extremes of the hydrological cycle in Europe under enhanced greenhouse gas conditions in a global time-slice experiment", *Advances in Global Change Research*, 10, 2002, pp. 1 – 29.
- [28] C.R. Păltineanu, I.F.L. Mihăilescu and I. Seceleanu, *Dobogea. Conditii climatice, consumul si necesarul apei de irigatie pentru principalele culturi agricole*. Constanta: ExPonto, 2000.
- [29] A. N. Pettitt, "A non - parametric approach to the change-point problem", *Applied Statistics*, 28(2), 1979, pp. 126 – 135.
- [30] PESETA project. Available: <http://peseta.jrc.es>
- [31] S. Planton, M. Déqué, H. Douville, B. Spagnoli, "Impact du réchauffement climatique sur le cycle hydrologique", *Geoscience*, 337, 2005, pp.193–202.
- [32] G. Posea, O. Bogdan and I. Zăvoianu, *Geografia Romaniei*, vol. 5. Bucuresti: Ed. Academiei Române, 2005, pp. 47 – 65.
- [33] PRUDENCE project. Available: <http://prudence.dmi.dk>.
- [34] E. Serban, *Climatical risc phenomena generated by precipitations in Câmpia de Vest, situated at the North of Mureş*, PhD. Thesis, Oradea University, 2008. (in Romanian)
- [35] E. Servat, J. - E. Paturel, H. Lubes–Niel, B. Kouame, J.M. Masson, M.Travaglio and B. Marieu, "De différents aspects de la variabilité de la pluviométrie en Afrique de l'ouest et centrale non sahélienne", *Revue des sciences de l'eau*, 12(2), 1999, pp. 363 - 387.
- [36] A. Steinemann, M. Hayes and L. Cavalcanti, *Drought Indicators and Triggers*, 2005. Available: www.water.washington.edu/research/
- [37] E.H. Steinberger and N. Gazit-Yaari, "Recent changes in the spatial distribution of annual precipitation in Israel", *J. Climate*, 9, 1996, pp.3328–3336.
- [38] N. Topor, *Ani ploiosi si secetosii în R.P. Romană*, C.S.A., I.N.M.H., 1964
- [39] W.Taylor, *Change-Point Analyzer*, ASA, 2002. Available: <http://www.variation.com/library.html>.
- [40] W. H. Qian and Y. Zhu, "Climate change in China from 1880 to 1998 and its impact on the environmental condition", *Climate Change*, 50, 2001, pp. 419 – 444.
- [41] G. Willeke, J. R. M. Hosking, J. R. Wallis and N. B. Guttman, *The National Drought Atlas*, Institute for Water Resources Report 94-NDS-4, U.S. Army Corps of Engineers, 1994
- [42] F. Zwiers and V. Kharin, "Changes in the extremes of climate simulated by CCC GCM2 under CO₂ doubling", *J. Climate*, 11, 1998, pp. 2200–2222.

Mathematical Models for Extreme Monthly Precipitation

Alina Bărbulescu, Judicaël Deguenon

Abstract – In this article we present the results of modelling the extreme monthly precipitation series collected in the period January 1965 – December 2005, at ten hydro-meteorological stations situated in Dobrudja, a region from the South - Eastern part of Romania. The main model used was the Generalised Pareto Distribution. For the non-stationary series, determined after performing KPSS test, the existence of a cyclical (harmonic) trend has also been studied and a GPD re - parameterisation by the orthogonal method has been done, using the scale as Poisson parameter, in the case of cyclical trend existence. The comparison between the models, by the likelihood – ratio test, proved that only in two cases (Medgidia and Corugea series) the reparameterized model was better.

Keywords – extreme values, Generalized Pareto Distribution, maximum Likelihood, ratio Likelihood.

1. INTRODUCTION

The study of extremes is of major importance in technique [11][23][29] as well as in the nature sciences, where the extreme events, as rainfall, storms, earthquakes, very low temperature etc. could have disastrous effects. Establishing a probability distribution that provides a good fit to daily rainfall depth has long been a topic interest in the fields of hydrology, meteorology, and others. The investigations into the daily rainfall distribution are primarily spread over three main research areas, namely, (1) stochastic precipitation models, (2) frequency analysis of precipitation, and (3) precipitation trends related to global climate change [14][15][20][27].

Different distributions have been used to study the extreme precipitations. For example: the GEV has been chosen [22] for a study of rainfall extremes in Louisiana and to model some daily and hourly rainfall data in USA [8]. Other authors [24] used the Kappa distribution to generate extreme precipitation quantile maps in Korea, respectively Generalized Pareto Distribution for left-censored records in Sardinia [12].

Annual flood series were found to be often skewed, which led to the development and use of many skewed distributions, the most commonly applied distributions now being the Gumbel (EV1), the Generalized Extreme Value (GEV), the Log Pearson Type III (LP3), and the 3 parameters Lognormal (LN3) [1], [26].

Analyzing the literature we remark that several methods of modelling the extreme values can be applied:

(i) Generalized Extreme Value Distributions (Frechet, Gumbel or Weibull), whose parameters can be estimated either by maximum likelihood or by probability weighted moments. But, for the use of these models, the hypotheses required are not always verified. Also, excepting for the Weibull distribution, the estimation of return levels above 50 years gives unexploitable confidence intervals.

(ii) Peak Over Threshold method and Generalized Pareto Distribution [16], for which the threshold determination is not very facile and the hypotheses of application are restrictive [19], [21].

Manuscript received October 1st, 2011 and accepted November 10, 2011.

Alina Bărbulescu is with Ovidius University of Constanta, faculty of Mathematics and Computers Science, 124, Mamaia Bd., 900527, Constantaa, ROMANIA (corresponding author: phone: 0040 - 744 - 284444; e-mail: alinadumitriu@yahoo.com).

Judicaël Deguenon is with Université d'Abomey – Calavi, École Polytechnique d'Abomey - Calavi, 01 BP 2009 Cotonou, BENIN (e-mail: tjudy73@yahoo.fr).

In spite of the threshold selection difficulties, the GPD model presents some advantages, like: the flexibility in the description of several types of tail behavior.

Since a systematic study of the extreme rainfall values in Dobrudja region has not been done, the article comes to complete our studies [2] – [7] of climate change in this region.

2. STUDY AREA

Dobrudja (Fig.1) is a region situated in the South – Eastern part of Romania, between the Danube and The Black Sea. Excepting the Danube Delta, a marshy region located in its North - Eastern corner, Dobrudja is hilly, with an average altitude of about 200–300 meters. The Dobrudja Plateau covers most of this region.

Dobrudja lies in the temperate continental climatic area. The relatively level terrain and its bare location facilitate the influx of humid, warm air in the spring, summer and autumn from the northwest, as well as that of northern and North - Eastern polar air in the winter. The Black Sea also exerts an influence over the region's climate, particularly within 40 - 60 km from the coast.

In this article we present the results of the study of extreme rainfall performed using a database formed by the monthly precipitation series collected at ten meteorological stations situated in Dobrudja (Fig.1) in the period 1961 – 2005.

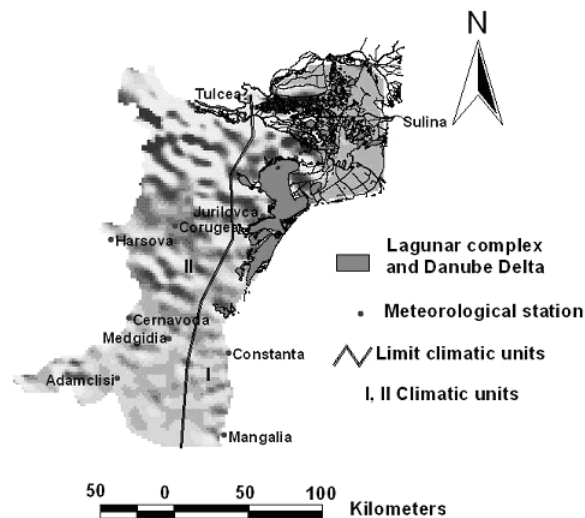


Fig. 1 Dobrudja region and the ten meteorological stations

The structure of this paper is the following: the next chapter contains the methods used to model our data. In chapter 4 we present the modelling results and their discussions. The last chapter contains the conclusions.

3. METHODS

Let X_1, X_2, \dots, X_n be a series of identically distributed random variables (in our case, monthly rainfall) with an unknown underlying distribution $F(x)$. Our interest lies in estimating the behavior of rainfall over a given high threshold u . This can be approached by estimating the excess distribution, $F_u(y)$, which represents the probability that a heavy rainfall event that has a value of X_i exceeds the threshold u by at most an amount of y , given the information that it exceeds the threshold u [19]. In our case, the problem is solved using the General Pareto Distribution (GPD), which has the following distribution form:

$$G_{\xi,\beta}(x) = \begin{cases} 1 - (1 + \xi x/\beta)^{-1/\xi}, & \xi \neq 0 \\ 1 - \exp(-x/\beta) & , \xi = 0 \end{cases} \quad (1)$$

where β is the scaling parameter and ξ , the shape, with: $\beta > 0$ and $0 \leq x < \infty$, if $\xi \geq 0$, and $0 < x \leq -\beta/\xi$, if $\xi < 0$.

Giving a threshold, u , we define the number of exceedences, N_u to be the number of data out of the total number of points, that exceed u , and for which the GPD was fitted by MLE method.

The following steps were followed to carry out the work:

1. Assuming that for a certain threshold u , $F_u(x) = G_{\xi,\beta}(x)$ [21], the parameters estimation is performed by maximum likelihood, the threshold, u , being determined as the lowest value of u for which the estimates $\hat{\xi}$ and $\hat{\beta}_u$ of ξ and $\beta_u = \beta - u\xi$ (the re-parameterizing scale parameter) remain near constant in the charts obtained by plotting $\hat{\xi}$ and $\hat{\beta}_u$ together with their confidence intervals.

2. The Pettit test [25] is used to identify the change point years in each of maximum monthly rainfall series.

3. The Kwiatkowski – Phillips – Schmidt – Shin (KPSS) [18] test is applied to test the null hypothesis that the series is stationary around a deterministic trend. For all the non-stationary series, the orthogonal approach is used [28], that, is the annual cycle in Poisson rate parameter which is fitted by:

$$\log(\lambda(t)) = \lambda_0 + \lambda_1 \sin(2\pi t/T) + \lambda_2 \cos(2\pi t/T), T = 12. \quad (2)$$

And a new GPD is built with the cycle in scale parameter:

$$\log(\beta(t)) = \beta_0 + \beta_1 \sin(2\pi t/T) + \beta_2 \cos(2\pi t/T), T = 12. \quad (3)$$

4. The new models with cycle in scale parameters are compared to the initial ones, using the likelihood ratio [9].

5. Finally, the effective 100 - years-return levels for each value of the harmonics used in the fit for the change point year are found.

4. RESULTS AND DISCUSSION

To model our data the R – packages ismev, extremes and evir were used [9], [10], [13], [30].

In Table 1, the possible threshold to fit GPD models for data (called Model_1), together with the chosen ones are presented for the monthly series. The inferior limit of the interval has been set as the value of chosen threshold, u , in the GPD models. For example, for Adamclisi, the chosen threshold was 55. Knowing the threshold, the number of exceedences, the parameter estimates, together with the corresponding standard errors (Std. err. scale, Std. err. shape) are provided in Table 2.

Table 1. Threshold choice

Station	Interval of possible threshold (mm)	u (mm)
Adamclisi	[55, 58]	55
Cernavoda	[22, 25]	22
Medgidia	[35, 35.5]	35
Harsova	[41, 43]	41
Corugea	[35, 45]	35
Tulcea	[57, 61]	57
Constanta	[21.5, 23.5]	21.5
Mangalia	[32, 45]	32
Jurilovca	[50, 60]	50
Sulina	[10, 30]	10

Table 2. Parameters estimation by maximum likelihood method for GPD models

Series	N_u	Scale ($\hat{\beta}$)	Shape ($\hat{\xi}$)	Std. err. scale	Std.err. shape
Adamclisi	121	28.9754	0.0237	4.0446	0.10590
Cernavoda	342	34.0176	-0.0782	2.4624	0.04829
Medgidia	212	18.4137	0.0173	3.2084	0.08960
Harsova	145	26.3848	0.0673	3.0962	0.08310
Corugea	198	28.6174	-0.0067	2.9185	0.07312
Tulcea	99	34.2407	-0.1149	4.8809	0.10176
Constanta	307	27.2967	0.0284	2.1766	0.05569
Mangalia	217	25.1059	0.0891	2.3935	0.06722
Jurilovca	83	34.5237	-0.1559	4.8449	0.08915
Sulina	334	20.5661	-0.0405	1.5523	0.05202

We remark that the standard errors are in the intervals [1.5523, 4.8829] for the scale and [0.04829, 0.10590], for the shape. In Figs. 2 – 6 the residual probability plots and the quantile residual plots are drawn. The line represents the theoretical residual value in the convergence case, in the part a. of each figure, respectively the theoretical residual quantiles in the convergence case, in the part b (in exponential scale). Since the plots are situated along the first bisectrix, we accept the hypothesis that the model is well fitted.

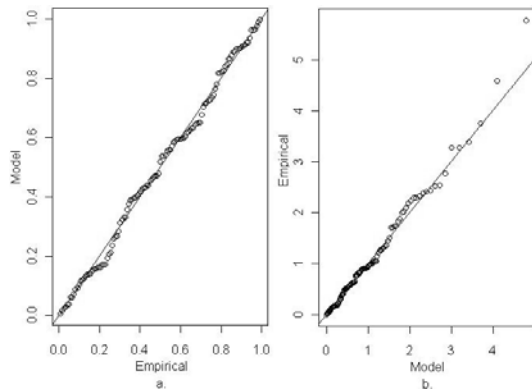


Fig.2 Diagnostics plots – Model_1 Adamclisi.
a. Residual probability plot; b. Residual quantile plot

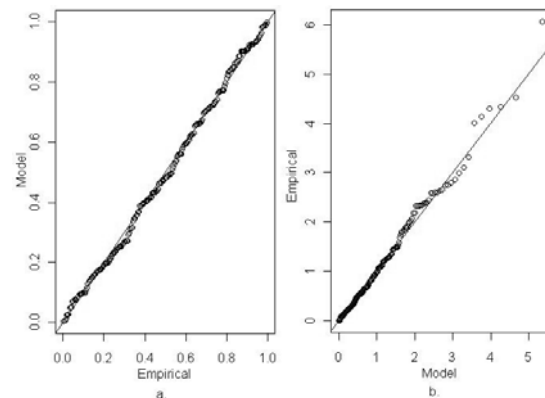


Fig.3 Diagnostics plots - Model_1 Medgidia.
a. Residual probability plot; b. Residual quantile plot

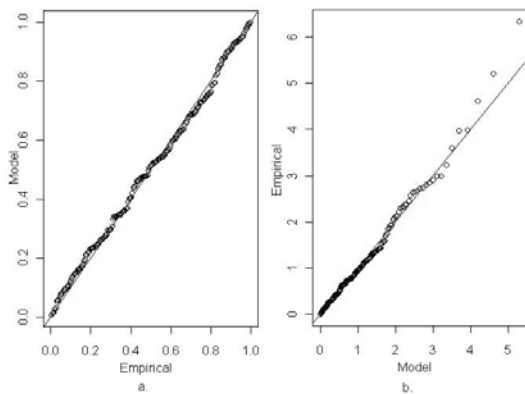


Fig.4 Diagnostics plots - Model_1 Corugea.
Residual probability plot; b. Residual quantile plot

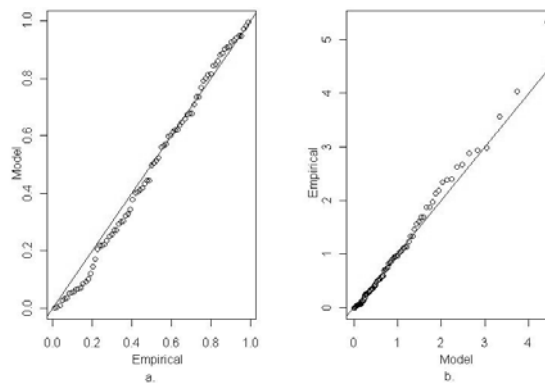


Fig.5 Diagnostics plots - Model_1 Jurilovca.
a. Residual probability plot; b. Residual quantile plot

The models quality is revealed analysing Figs. 2 – 11.

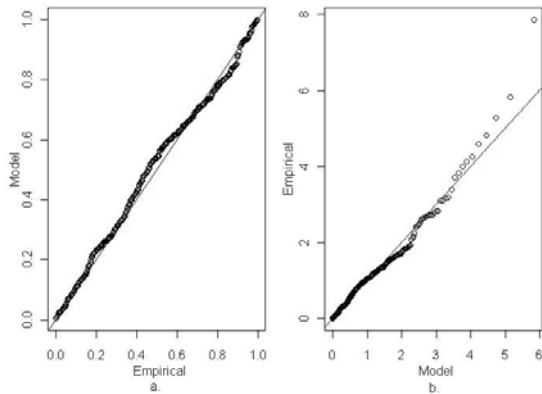


Fig.6 Diagnostics plots - Model_1 Cernavoda.
 a. Residual probability plot;
 b. Residual quantile plot (exponential scale)

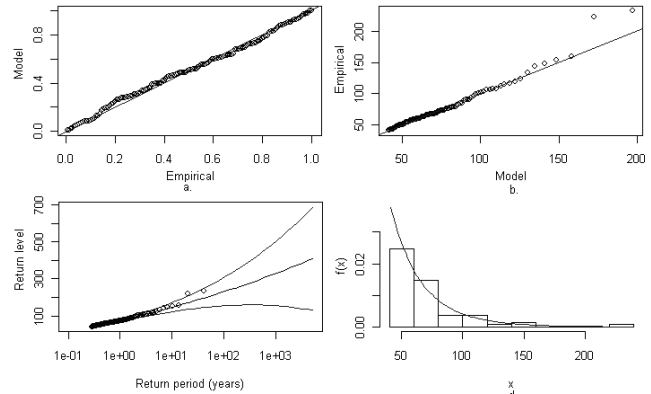


Fig.7 Diagnostics plots: Model_1 Harsova.
 a. Probability plot, b. Quantile plot, c. Return level plot,
 d. Density plot.

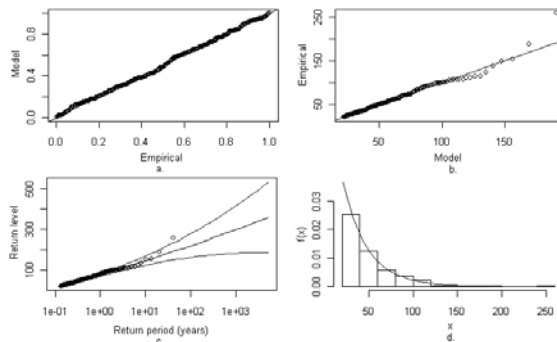


Fig.8 Diagnostics plots: Model_1 Constanta.
 a. Probability plot, b. Quantile plot,
 c. Return level plot, d. Density plot

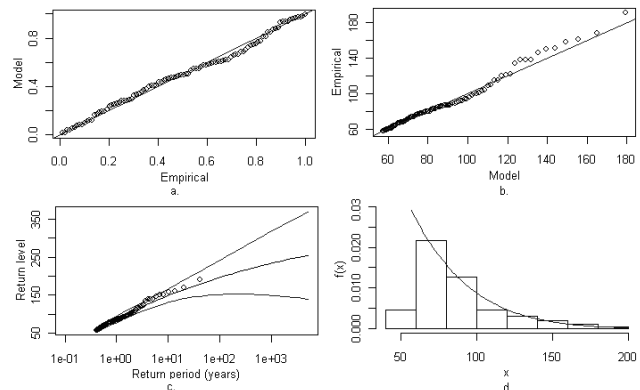


Fig.9 Diagnostics plots: Model_1 Tulcea. a. Probability plot, b. Quantile plot, c. Return level plot, d. Density plot.

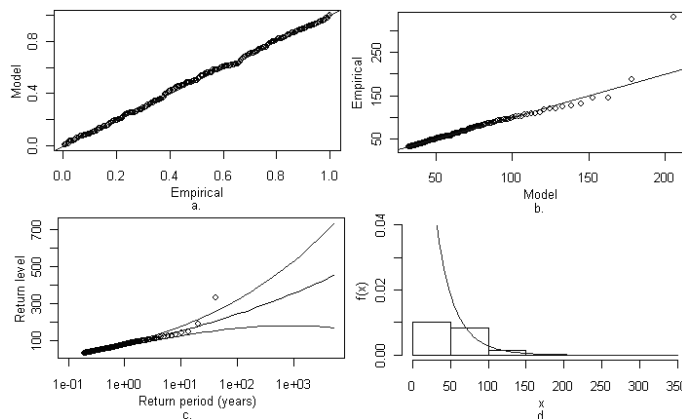


Fig.10 Diagnostics plots: Model_1 Mangalia.
 a. Probability plot, b. Quantile plot, c. Return level plot, d. Density plot

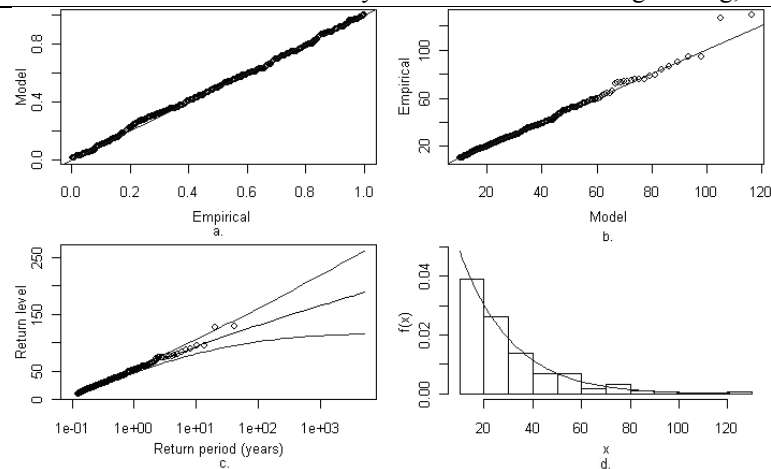


Fig.11 Diagnostics plots: Model_1 Sulina.

a. Probability plot, b. Quantile plot, c. Return level plot, d. Density plot

From the analysis of diagnostic plot it is evident that the GPD Model_1 fit well the excesses over threshold for all the series. In Fig.7-11, the probability plots (a) and the quantile plots (b) are presented together with the return level plot (c) and the histogram of data with the fitted density (d).

In Fig. 7 – 11 (a) and (b) the theoretical curves are represented by solid lines and the empirical ones, by points. In (c), the solid central curve is the return period estimate, the other two being the 95% confidence interval. The empirical return period of extreme rainfalls observed in the studied period is shown as points.

Defining the MLE Poisson rate parameter to be the number of exceedances per year, the following values have been obtained in Model_1, for some stations: 2.4146 – for Tulcea, 5.2927 – for Mangalia, and 8.1463 – for Sulina.

The results of KPSS stationarity test, together with the p – values associated are given in Table 3. For the series for which the p – value is less than 0.05, the stationarity hypothesis was rejected. Therefore, only Tulcea, Mangalia and Sulina series are stationary.

Table 3. Results of KPSS test

Station	Stationarity (significance level of 5%)	p-value
Adamclisi	Rejected	0.03277
Cernavoda	Rejected	< 0.01
Medgidia	Rejected	0.01572
Harsova	Rejected	< 0.01
Corugea	Rejected	< 0.01
Tulcea	Accepted	0.0902
Constanta	Rejected	< 0.01
Mangalia	Accepted	0.0948
Jurilovca	Rejected	0.02422
Sulina	Accepted	> 0.1

For the seven non – stationary series, the annual cycle in Poisson rate parameter was fitted. They are given in Table 4, together with the corresponding standard deviations.

The significance tests lead us to the conclusions that some coefficients are not significant. They are accompanied by a * in Table 4. Therefore:

- Adamclisi, Medgidia, Corugea and Jurilovca series have harmonic trends,
- Cernavoda and Harsova series present a cosine component,
- Constanta series doesn't present a cyclic component.

For the series that present a harmonic cyclic trend, GPD models with annual cycle in parameter scale has been fitted.

Table 4. Parameters in the Poisson model

	λ_0 (std. dev.)	λ_1 (std. dev.)	λ_2 (std. dev.)
Adamclisi	-1.4676942 (0.09691)	-0.3588978 (0.13275)	-0.3680451 (0.13285)
Cernavoda	-0.37008 (0.05442)	-0.01681* (0.07660)	-0.15934 (0.07684)
Medgidia	-0.88004 (0.07132)	-0.25950 (0.09888)	-0.29444 (0.09912)
Harsova	-1.29883 (0.08957)	-0.22873* (0.12049)	-0.51183 (0.12361)
Corugea	-1.02012 (0.07909)	-0.30231 (0.10444)	-0.60033 (0.10788)
Constanta	-0.47340 (0.05717)	-0.06823* (0.08080)	-0.04914* (0.08077)
Jurilovca	-1.8364 (0.1161)	-0.3361 (0.1597)	-0.3428 (0.1597)

* means that the coefficient is not significant

The determined parameters and the corresponding standard deviations (in the brackets) are given in Table 5. The new model is called Model_2.

Table 5. Orthogonal approach: fitting GPD with annual cycle in scale parameter

Series	β_0	β_1	β_2	ξ
Adamclisi	3.294 (0.142)	-0.093 (0.144)	-0.250 (0.132)	0.020 (0.098)
Medgidia	3.223 (0.111)	-0.276 (0.108)	-0.354 (0.098)	0.009 (0.080)
Corugea	3.229 (0.112)	-0.288 (0.119)	-0.189 (0.100)	0.001 (0.072)
Jurilovca	3.747 (0.173)	-0.036 (0.120)	0.292 (0.095)	-0.354 (0.126)

To compare Model_1 to the Model_2 the Likelihood ratio test was performed. The test results are presented in Table 6, where the χ^2 - values are accompanied by the test conclusions: Significant means that better performance have been registered by Model_2 than by Model_1. In this case, the Model_2 explains better the data at the given stations than the Model_1.

Table 6. Results of Likelihood ratio test

	χ^2 -value	Conclusions
Adamclisi	0.1525109	Not Significant
Medgidia	0.0000512	Significant
Corugea	0.0139127	Significant
Jurilovca	0.0705064	Not Significant

The extreme change point years have been determined by the application of Pettitt test, confirmed by CUSUM charts (Fig.12) and the results are presented in Table 7, from which it results that there is no change

point in Sulina series.

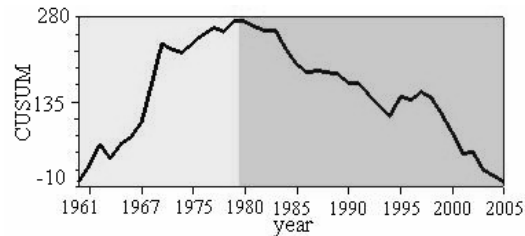


Fig.12 CUSUM chart of Sulina series. The periods before and after the change point are represented by different colors (grey light and grey dark).

Table 7. Extreme change point years

Station	Change point (year)	p-value
Adamclisi	1973	0.41
Cernavodă	1972	0.15
Medgidia	1990	0.34
Harșova	1978	0.26
Corugea	1972	0.12
Tulcea	1995	0.23
Constanta	1975 and 1981	0.16
Mangalia	1994	0.09
Jurilovca	1978	0.08
Sulina	1980	0.20

The year 1975 is an artificial change point for Constanta series, being due to the change of the emplacement of this meteorological station, so we will consider only 1981 as a change point.

Testing the existence of a trend in the extreme series, after the change point, the conclusion was that only Adamclisi (Fig.13), Corugea, Jurilovca, Cernavoda, Mangalia, Sulina extreme series presents increasing trends after the change points.

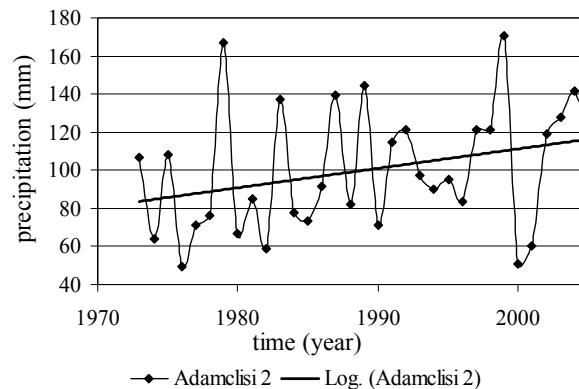


Fig.13 Increasing (logarithmic trend) for Adamclisi extreme series, after the change point (1973)

The 100 - effective return levels have also been determined and are presented in Figs. 14 and 15, for comparison, for the non - stationary series.

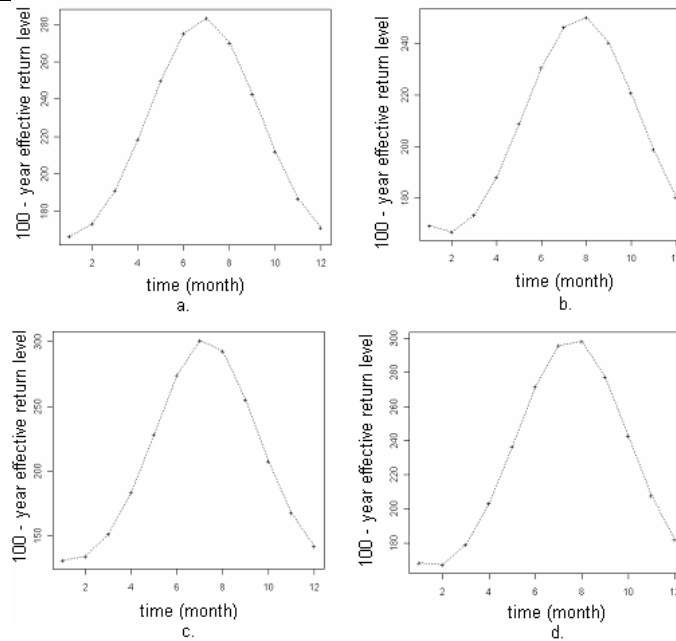


Fig.14 Effective return level:
 a. Adamclisi, b. Cernavodă, c. Medgidia, d. Harsova series

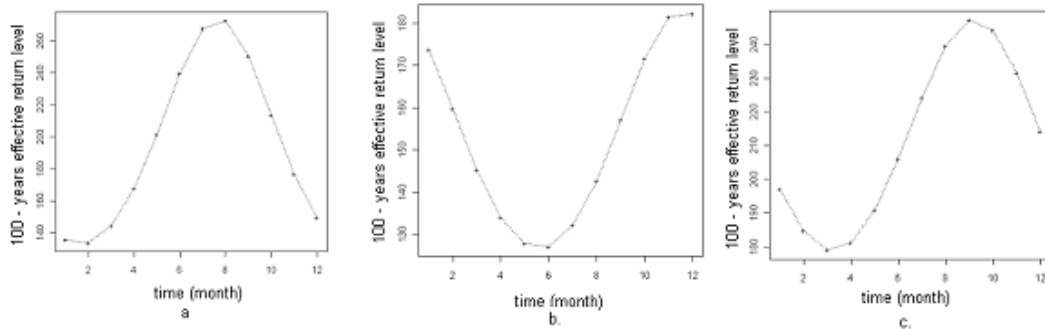


Fig.15 Effective return level: a. Corugea, b. Jurilovca, c. Constanta series.

The values of the return levels and the confidence intervals are given in Table 8.

The return levels are influenced by the geographical situation of each station, the smallest being for Sulina (situated in 8 km off shore) and Corugea (which has the highest altitude). The highest return levels correspond to Mangalia station, which is situated in the southern part of Dobrudja, on the Black Sea Littoral.

5. CONCLUSION

In this article GPD models have been built for monthly precipitation series in Dobrudja region and a selection procedure of the series that present a cyclic harmonic trend was used. The analysis indicated that Mangalia, Tulcea and Sulina are stationary and between those that are non-stationary, Constanta doesn't present a significant cyclic trend, Cernavoda and Harsova present a cosine cyclical trend, Adamclisi, Medgidia, Corugea and Jurilovca presents a significant harmonic trend.

For Medgidia and Corugea, the likelihood ratio test relieves that taking into account the harmonic trend, there a significant improvement in the re-parameterization of GPD model via orthogonal techniques.

For Constanta, Cernavoda and Harsova series it is probable that the climate change is influenced by the latitude and longitude of the meteorological stations.

Table 8. Return levels for extreme rainfalls

Series	return level (mm)	return period (year)	confidence limits (95%)		Series	return level (mm)	return period (year)	confidence limits (95%)	
			lower	upper				lower	upper
Adamclisi	157.12	10	132.39	181.85	Jurilovca	132.53	10	117.07	147.99
	179.06	20	142.68	215.44		146.57	20	127.33	165.80
	208.63	50	151.19	266.06		162.91	50	136.88	188.93
	231.42	100	153.75	309.10		173.78	100	141.53	206.02
	309.90	1000	137.33	482.47		202.37	1000	146.06	258.68
Cernavoda	149.22	10	131.94	166.50	Mangalia	151.55	10	125.70	177.39
	165.46	20	142.93	187.98		177.12	20	139.98	214.25
	185.62	50	154.96	216.28		213.44	50	156.27	270.61
	199.94	100	162.35	237.52		242.95	100	166.30	319.60
	242.30	1000	178.18	306.41		355.18	1000	181.48	528.88
Constanta	146.84	10	124.55	169.12	Medgidia	151.04	10	124.93	177.16
	168.44	20	137.71	199.16		172.26	20	134.33	210.20
	197.65	50	152.83	242.47		200.71	50	142.66	258.76
	220.26	100	162.49	278.04		222.53	100	145.87	299.20
	298.65	1000	182.84	414.46		296.94	1000	136.79	457.10
Corugea	144.52	10	123.33	165.70	Sulina	92.87	10	80.28	105.47
	163.80	20	134.24	193.35		104.63	20	87.83	121.43
	189.14	50	145.47	232.81		119.67	50	96.20	143.15
	208.21	100	151.61	264.81		130.69	100	101.38	159.99
	270.92	1000	158.06	383.79		165.13	1000	112.27	217.99
Harsova	147.33	10	122.48	172.19	Tulcea	148.30	10	130.42	166.18
	171.13	20	135.16	207.11		164.12	20	140.03	188.22
	204.35	50	148.28	260.42		183.20	50	148.16	218.23
	230.87	100	155.16	306.59		196.35	100	151.43	241.26
	328.42	1000	155.75	501.08		233.22	1000	149.33	317.10

Since the likelihood ratio test didn't reveal a significant improvement in the GPD model for Adamclisi and Jurilovca series (even if a harmonic trend has been found), we could try to built Bayesian hierarchical models (in latitude/ longitude or in climate space) to determine the covariate that improve our initial GPD model.

It was also emphasized the unhomogeneity of the extreme rainfalls return level and the correlation with the geographical position of the meteorological stations.

The results presented in this article are important because a systematic study of this type had not been done for this region.

For the perspective we are thinking about the spatial interpolation of return levels and downscaling the heavy rainfalls in the non-stationary extreme cases, as well as the assessment of spatial dependences among maxima.

6. REFERENCES

- [1] H. Abida and M. Ellouze, *Probability distribution of flood flows in Tunisia*, Hydrol. Earth Syst. Sci., 12, 2008, pp. 703–714.
- [2] A. Bărbulescu and E. Băutu, *Alternative Models for Time Series*, An. St. Univ. Ovidius, Mat., vol.3, 2009, pp. 45 – 68.

- [3] A. Bărbulescu and E. Băutu, "Meteorological Time Series Modelling Based on Gene Expression Programming", Recent Advances in Evolutionary Computing, 2009, pp. 17-23.
- [4] A. Bărbulescu and E. Băutu, "ARIMA Models versus Gene Expression Programming In Precipitation Modeling", Recent Advances in Evolutionary Computing, 2009, pp. 112-117.
- [5] A. Bărbulescu, E. Băutu, *Mathematical models of climate evolution in Dobrudja*, Theoretical and Applied Climatology, vol.100, nos.1 – 2/March, 2010, pp. 29 – 44.
- [6] A. Bărbulescu, J. Deguenon and D. Teodorescu, Study on water resources in the Black Sea region, Nova Publishing, USA, 2011
- [7] A. Bărbulescu and E. Pelican, "ARIMA models for the analysis of the precipitation evolution", Recent Advances in Computers, 2009, pp. 221 – 226.
- [8] G.M. Bonnin, D. Martin, B. Lin, T. Parzyok, M. Yekta and D. Riley, Precipitation-Frequency Atlas of the United States, Vol.1, Version 4.0: Semiarid Southwest (Arizona, Southeast California, Nevada, New Mexico), NOAA Atlas 14, 2006
- [9] S. G. Coles, An Introduction to Statistical Modeling of Extreme Values. Springer, 2001
- [10] S.G. Coles and A. Stephenson, ismev: An Introduction to Statistical Modeling of Extreme Values, 2010. Available: <http://www.ral.ucar.edu/~ericg/softextreme.php>
- [11] A. Constantin, M. Stănescu, and C. S. Nănescu, "Transient Movement in a Single Looped Water Distribution Network. Pressure Simulation and Experimental Measurement", Recent Researches in Computational Techniques, Non-Linear Systems & Control, 2011, pp.238 - 242.
- [12] R. Deidda and M. Puliga, *Sensitivity of goodness-of-fit statistics to rainfall data rounding off*, Physics and Chemistry of the Earth, 31, 2006, pp. 1240 – 1251.
- [13] E. Gilleland, R. Katz and G. Young, extRemes: Extreme value toolkit, R package, 2009. Available: <http://www.assessment.ucar.edu/toolkit/>
- [14] C. Gherghina, *A Web Services Composition with BPEL and Satellite Image Processing for urban and river bed changes assessment*, An. St. Ovidius Univ., Series Mathematics, Vol. 17(3), 2009, pp. 131–148.
- [15] L.S. Hanson and R. Vogel, The Probability Distribution of Daily Rainfall in the United States, 2008. Available: <http://engineering.tufts.edu/cee/people/vogel/publications/DailyRainfall.pdf>
- [16] J. R. Hosking and J. R. Wallis, *Parameter and quantile estimation for the generalized Pareto distribution*, Technometrics, 29, 1987, pp. 339 – 349.
- [17] IPCC, In: Climate Change, The Scientific Basis, J. T.Houghton, Y. Ding, D. J. Griggs, M. Noguer, P.J. van der Linden, X. Dai, K. Maskell, C.A. Johnson (Eds.), Cambridge University Press, 2001, pp. 34 – 44.
- [18] D. Kwiatkowski, P. C. B. Phillips, P. Schmidt and Y. Shin, *Testing the Null Hypothesis of Stationarity against the Alternative of a Unit Root*, Journal of Econometrics, 54, 1992, pp. 159 – 178.
- [19] I. Li, W. Cai and E.P. Campbell, *Statistical Modeling of Extreme Rainfall in Southwest Western Australia*. Journal of Climate, 18, 2005, pp. 852 – 863.
- [20] C. Maftai, C. Gherghina, S. Gelmambet and C. Buta, *ETREF un logiciel qui calcule l'évapotranspiration de référence*, Annals of Oradea University, Fascicle of Management and Technological Engineering, 2007, pp. 86-93.
- [21] A. J. McNeil, Extreme value theory for risk managers; in Extreme and Integrated Risk Management, Embrechts P, Ed., UBS Warbug, 2005, pp. 1–35.
- [22] B. Naghavi and F.X. Yu, *Regional frequency analysis of extreme precipitation in Louisiana*. Journal of Hydraulic Engineering, 121, 1995, pp. 819–827.
- [23] C. S. Nănescu, A. Constantin and M Stănescu, "Hydraulic Study on Pumping Stations Equipped with Air Chamber", *Recent Researches in Computational Techniques*, 2011, pp.228 – 231.
- [24] J.S. Park and H.S Jung, *Modelling Korean extreme rainfall using a Kappa distribution and maximum likelihood estimate*, Theoretical and Applied Climatology, 72, pp. 55 – 64, 2002.
- [25] A. N. Pettitt, *A nonparametric approach to the change point problem*, Appl. Stat., 28, 1979, pp. 126–135.
- [26] P.J. Pilon and J. D. Harvey, Consolidated frequency analysis, Reference manual, Environment Canada, Ottawa, Canada, 1994

-
- [27] C. Serban and C. Maftai, *Thermal analysis of climate regions using remote sensing and grid computing*, International Journal of Computer Networks & Communications, vol. 3 (1), 2011, pp 35-50.
- [28] J. Soyoung, "Data Analysis in Extreme Value Theory: Non-stationary Case", 2008. Available: www.unc.edu/~rls/s890/SoyoungWriteup.pdf
- [29] M. Stănescu, A. Constantin, C. Nițescu, L. Roșu and A.M. Dobre, "Research on the Steady Motion in Water Distribution Looped Pipe Networks", Recent Researches in Computational Techniques, Non-Linear Systems & Control, Iasi, Romania, 1-3 July, 2011, WSEAS Press, pp.243 – 246.
- [30] A. Stephenson and E. Gilleland, *Software for the analysis of extreme events: The current state and future directions*, *Extremes*, 8, 2006, pp. 87-109.

Preparation of Papers for The Scientific Annals of Ovidius University of Constanta, Series of Civil Engineering

First A. Author, Second B. Author, and Third C. Author

Abstract – (no more than 10 lines) These instructions give you guidelines for preparing papers for The Scientific Annals of Ovidius University of Constanta, Series of Civil Engineering. Use this document as a template if you are using Microsoft Word 6.0 or later. Otherwise, use this document as an instruction set. The electronic file of your paper will be formatted further at THE SCIENTIFIC ANNALS OF OVIDIUS UNIVERSITY OF CONSTANTA, SERIES OF CIVIL ENGINEERING. We accept papers in the following formats: .doc, .docx and .pdf. Do not delete the blank line immediately above the abstract; it sets the footnote at the bottom of this page. Do not insert page numbers. Define abbreviations and acronyms in the abstract.

Keywords – About four key words or phrases in alphabetical order, separated by commas.

1. INTRODUCTION

An author may submit maximum two papers. Each paper should have an even number of pages and a maximum of 8 pages.

The paper size should be A4 with the margins top: 4.4 cm, bottom: 4.4 cm, left: 2.5 cm, and right: 2.5 cm. The article will be written on a single column, using the font Times New Roman. Please use the following table for Font and Paragraph styles:

	Case	Font size	Font style	Alignment	Line spacing	Spacing before text	Left indent first line
Title	Title case	16	Bold	Centred	Single	8 pt	-
Authors	Sentence case	10	Roman	Centred	Single	-	-
Abstract	Sentence case	10	Bold	Justified	Single	-	0.8 cm
Keywords	Sentence case	10	Bold	Justified	Single	-	0.8 cm
Section titles	Uppercase, small caps	10	Bold	Centred	Single	8 pt	-
Captions and legends	Sentence case	10	Regular	Centred	Single	-	-
Body text	Sentence case	10	Regular	Justified	Single	-	0.8 cm
Footnote (only on the 1 st page)	Sentence case	8	Regular	Justified	Single	-	0.8 cm

Manuscript received February 15, 2010. (Write the date on which you submitted your paper for review.) Avoid writing long formulas with subscripts in the title; short formulas are fine. Full names of authors are preferred in the author field, but are not required. Put a space between authors' initials. This work was supported in part by the Romanian Government under Grant nr. 1222/2010 (sponsor and financial support acknowledgment go here).

F. A. Author is with Ovidius University of Constanta, Bd. Mamaia nr. 124, 900356-Constanta, Romania (corresponding author to provide phone: +40-241-619040; fax: +40-241-618372; e-mail: author@univ-ovidius.ro).

S. B. Author is with the University of Architecture, Civil Engineering and Geodesy, 1, Hristo Smirnesky Boulevard, 1046-Sofia, Bulgaria (e-mail: author@uacg.bg).

T. C. Author is with Ovidius University of Constanta, Bd. Mamaia nr. 124, 900356-Constanta, Romania (e-mail: author@univ-ovidius.ro).

Reference	Sentence case	10	Regular	Justified	Single	-	-
-----------	---------------	----	---------	-----------	--------	---	---

For Microsoft Word users, Highlight a section that you want to designate with a certain style, then select the appropriate name on the style menu. The style will adjust your fonts and line spacing. **Do not change the font sizes or line spacing to squeeze more text into a limited number of pages.** Use italics for emphasis; do not underline.

Before the abstract and after the keywords a horizontal line should be drawn.

A paper usually contains five sections: (1) introduction, (2) description of the theoretical model or method / description of the experiment, experimental materials and equipments, (3) results and their significance, (4) conclusions and (5) references. Synthesis papers are an exception from this recommendation.

2. EXPERIMENT DESCRIPTION

Tables and figures should be inserted in the text, preferably where they are referred to. Each of them must have a reference number and a title (tables) or a caption (figures). Place figure captions below the figures and table titles above the tables. If your figure has two parts, include the labels “(a)” and “(b)” as part of the artwork. Please verify that the figures and tables you mention in the text actually exist. **Do not put borders around the outside of your figures.** Tables and figures are separated from the above/under text by a single spaced line.

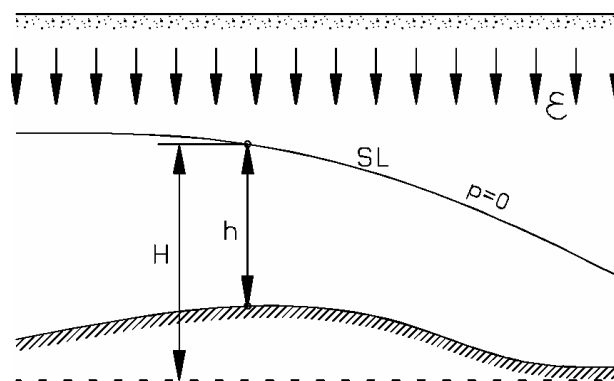


Fig. 1. Unsteady infiltration scheme (example)

Taking into account that the proceedings will be printed in black and white, coloured illustrations must have a proper contrast.

Tables and figures that exceed the width of the page may be rotated to the left, at 90°.

Tables and figures should be cited as follows: **Table 1, Fig. 1.**

The abbreviation **Fig. 1** is not allowed at the beginning of a statement. In this case it should be written **Figure 1.**

Table 1. Underground water level variation in time (example).

Year	x (m)	Month in the irrigation season:					
		IV	V	VI	VII	VIII	IX
1	26	0,03	0,17	0,29	0,47	0,63	0,67
5	26	0,12	0,62	1,00	1,63	2,13	2,21
10	26	0,29	0,97	1,56	2,54	3,33	3,43
1	620	0,02	0,11	0,17	0,28	0,36	0,38
5	620	0,09	0,46	0,73	1,19	1,56	1,61
10	620	0,16	0,78	1,25	2,03	2,66	2,74

3. RESULTS AND SIGNIFICANCES

Define abbreviations and acronyms the first time they are used in the text, even after they have already been defined in the abstract. Abbreviations such as SI, ac, and dc do not have to be defined. Abbreviations that incorporate periods should not have spaces: write “U.O.C.,” not “U. O. C.” Do not use abbreviations in the title unless they are unavoidable (for example, “DSA 2009” in the title of this article).

If you are using *Word*, use the Microsoft Equation Editor. Equations should be separated from the text by a single spaced line.

Equations should be numbered with Arabic numerals within brackets, aligned to the right on the last line of the equation (default tab stops at 15 cm), as in the following examples:

$$\varepsilon(k) = \varepsilon_0 - 2t_0 \cos(ka) \quad (1)$$

and also,

$$c_\alpha = \left(\frac{E_w}{\rho_w} \right) \cdot \left[\left(1 - \frac{\gamma_\alpha \cdot R \cdot T}{p} \right) \cdot \left(1 + \frac{\gamma_\alpha \cdot R \cdot T}{p^2} \cdot E_w + \frac{E_w}{E_c} \cdot \frac{D}{e} \right) \right] \quad (2)$$

Be sure that the symbols in your equation have been defined before the equation appears or immediately following. Italicize symbols (*T* might refer to temperature, but *T* is the unit tesla). Refer to “(1),” not “Eq. (1)” or “equation (1),” except at the beginning of a sentence: “Equation (1) is”

4. CONCLUSIONS

References should be written at the end of the paper, after the text. When the text ends at the bottom of a page, references should be written on a new page.

Number citations consecutively in square brackets [1]. The sentence punctuation follows the brackets [2]. Multiple references [2], [3] are each numbered with separate brackets [1]–[3]. When citing a section in a book, please give the relevant page numbers [2]. In sentences, refer simply to the reference number, as in [3]. Do not use “Ref. [3]” or “reference [3]” except at the beginning of a sentence: “Reference [3] shows”

Please do not use footnotes (except for the footnote on the first page). When necessary, a Notes section can be added at the end of the document.

Please note that the references at the end of this document are in the preferred referencing style. Give all authors’ names; do not use “*et al.*” unless there are six authors or more. Use a space after authors’ initials. Papers that have not been published should be cited as “unpublished” [4]. Papers that have been submitted for publication should be cited as “submitted for publication” [5]. Papers that have been accepted for publication, but not yet specified for an issue should be cited as “to be published” [6]. Please give affiliations and addresses for private communications [7].

Capitalize only the first word in a paper title, except for proper nouns and element symbols. For papers published in translation journals, please give the English citation first, followed by the original foreign-language citation [8].

APPENDIX

Appendixes, if needed, appear before the acknowledgment.

5. ACKNOWLEDGMENTS

This section is optional. Use the singular heading even if you have many acknowledgments. Avoid expressions such as “One of us (S.B.A.) would like to thank” Instead, write “F. A. Author thanks” **Sponsor and financial support acknowledgments are placed in the unnumbered footnote on the first page.**

6. REFERENCES

- [1] Boieru P., *Asupra unor rezultate privind curgerea bifazică apă-aer în conducte*. 1972, Hidrotehnica Nr.1, vol. XVIII, pag 23-29.
- [2] Wylie E.B. Free air in liquid transient flow. Third International Conference on Pressure Surges. BHRA Fluid Engineering, Conterburz, England.
- [3] H. Poor, An Introduction to Signal Detection and Estimation. New York: Springer-Verlag, 1985, ch. 4.
- [4] B. Smith, "An approach to graphs of linear forms (Unpublished work style)," unpublished.
- [5] E. H. Miller, "A note on reflector arrays (Periodical style—Accepted for publication)," IEEE Trans. Antennas Propagat., to be published.
- [6] J. Wang, "Fundamentals of erbium-doped fiber amplifiers arrays (Periodical style—Submitted for publication)," IEEE J. Quantum Electron., submitted for publication.
- [7] C. J. Kaufman, Rocky Mountain Research Lab., Boulder, CO, private communication, May 1995.
- [8] Y. Yorozu, M. Hirano, K. Oka, and Y. Tagawa, "Electron spectroscopy studies on magneto-optical media and plastic substrate interfaces(Translation Journals style)," IEEE Transl. J. Magn.Jpn., vol. 2, Aug. 1987, pp. 740–741 [Dig. 9th Annu. Conf. Magnetism Japan, 1982, p. 301].
- [9] J. Jones. (1991, May 10). Networks (2nd ed.) [Online]. Available: <http://www.atm.com>

OUR SPONSORS

R.A.T.C. CONSTANTA



OIL DEPOL SERVICE S.R.L.



TOP GEOCART



AKDEMIR PROD S.R.L.

S.C. CEPLINSCHI COM S.R.L.

S.C. CLEAN CONTROL I.T.C. S.R.L.

S.C. DOBROGEA GRUP S.A.

S.C. GTF PROSPECT S.R.L.

SINDICATUL LIBER AL S.C. RAJA S.A. CONSTANTA

S.C. VMB LUX CONSTRUCT S.R.L.

ISSN 1584 - 5990